ISSN 2410-3993

Volume 12, Issue 30 — e20251230 January — December 2025

# Journal of Technology and Innovation

ECORFAN®

**Journal of Technology and Innovation,** Volume 12, Issue 30: e20251230 - January - December 2025, is a Continuous publication – ECORFAN-Bolivia. Santa Lucia N-21, Barrio Libertadores, Cd. Sucre. Chuquisaca, Bolivia, http://www.ecorfan.org/bolivia/rj_tecnologia_innovacion.php, revista@ecorfan.org. Editor in Chief: Bujari - Alli, Ali. PhD. ISSN: 2410- 3993. Responsible for the last update of this issue ECORFAN Computer Unit. Imelda Escamilla Bouchán, PhD. Vladimir Luna Soto, PhD. Updated as of December 30, 2025.

# Journal of Technology and Innovation

## Definition of Journal Scientific Objectives

Support the international scientific community in its written production Science, Technology and Innovation in the Field of Engineering and Technology, in Subdisciplines of technology and technology in telecommunications, food technology, computer technology, technology in transport systems, technology in motor vehicles, energy technology, naval technology, nuclear technology, textile technology, systems engineering, electronics engineering, energy engineering, innovation.

ECORFAN-Mexico, S.C. is a Scientific and Technological Company in contribution to the Human Resource training focused on the continuity in the critical analysis of International Research and is attached to SECIHTI-RENIECYT number 1702902, its commitment is to disseminate research and contributions of the International Scientific Community, academic institutions, agencies and entities of the public and private sectors and contribute to the linking of researchers who carry out scientific activities, technological developments and training of specialized human resources with governments, companies and social organizations.

Encourage the interlocution of the International Scientific Community with other Study Centers in Mexico and abroad and promote a wide incorporation of academics, specialists and researchers to the publication in Science Structures of Autonomous Universities - State Public Universities - Federal IES - Polytechnic Universities - Technological Universities - Federal Technological Institutes - Normal Schools-Decentralized Technological Institutes - Intercultural Universities - S & T Councils - SECIHTI Research Centers.

## Scope, Coverage and Audience

Journal of Technology and Innovation is a Journal edited by ECORFAN-Mexico S.C in its Holding with repository in Bolivia, is a scientific publication arbitrated and indexed with semester periods. It supports a wide range of contents that are evaluated by academic peers by the Double-Blind method, around subjects related to the theory and practice of technology and technology in telecommunications, food technology, computer technology, technology in transport systems, technology in motor vehicles, energy technology, naval technology, nuclear technology, textile technology, systems engineering, electronics engineering, energy engineering, innovation with diverse approaches and perspectives, that contribute to the diffusion of the development of Science Technology and Innovation that allow the arguments related to the decision making and influence in the formulation of international policies in the Field of Engineering and Technology. The editorial horizon of ECORFAN-Mexico® extends beyond the academy and integrates other segments of research and analysis outside the scope, as long as they meet the requirements of rigorous argumentative and scientific, as well as addressing issues of general and current interest of the International Scientific Society.

## Editorial Board

## Arbitration Committee

**Assignment of Rights**

The sending of an Article to Journal of Technology and Innovation emanates the commitment of the author not to submit it simultaneously to the consideration of other series publications for it must complement the Originality Format for its Article.

The authors sign the Authorization Format for their Article to be disseminated by means that ECORFAN- Mexico, S.C. In its Holding Bolivia considers pertinent for disclosure and diffusion of its Article its Rights of Work.

**Declaration of Authorship**

Indicate the Name of Author and Coauthors at most in the participation of the Article and indicate in extensive the Institutional Affiliation indicating the Department.

Identify the Name of Author and Coauthors at most with the CVU Scholarship Number-PNPC or SNI- SECIHTI- Indicating the Researcher Level and their Google Scholar Profile to verify their Citation Level and H index.

Identify the Name of Author and Coauthors at most in the Science and Technology Profiles widely accepted by the International Scientific Community ORC ID - Researcher ID Thomson - arXiv Author ID
- PubMed Author ID - Open ID respectively.

Indicate the contact for correspondence to the Author [Mail and Telephone] and indicate the Researcher who contributes as the first Author of the Article.

**Plagiarism Detection**

All Articles will be tested by plagiarism software PLAGSCAN if a plagiarism level is detected Positive will not be sent to arbitration and will be rescinded of the reception of the Article notifying the Authors responsible, claiming that academic plagiarism is criminalized in the Penal Code.

**Arbitration Process**

All Articles will be evaluated by academic peers by the Double Blind method, the Arbitration Approval is a requirement for the Editorial Board to make a final decision that will be final in all cases. MARVID® is a derivative brand of ECORFAN® specialized in providing the expert evaluators all of them with Doctorate degree and distinction of International Researchers in the respective Councils of Science and Technology the counterpart of SECIHTI for the chapters of America-Europe-Asia-Africa and Oceania. The identification of the authorship should only appear on a first removable page, in order to ensure that the Arbitration process is anonymous and covers the following stages: Identification of the Journal with its author occupation rate - Identification of Authors and Coauthors - Detection of plagiarism PLAGSCAN - Review of Formats of Authorization and Originality- Allocation to the Editorial Board- Allocation of the pair of Expert Arbitrators-Notification of Arbitration -Declaration of observations to the Author-Verification of Article Modified for Editing-Publication.

**Instructions for Scientific, Technological and Innovation Publication Knowledge Area**

The works must be unpublished and refer to topics of technology and technology in telecommunications, food technology, computer technology, technology in transport systems, technology in motor vehicles, energy technology, naval technology, nuclear technology, textile technology, systems engineering, electronics engineering, energy engineering, innovation and other topics related to Engineering and Technology.

## Presentation of content

In the first article we present, *Design and simulation of gas mixing valve*, by Vázquez-Carreón, José Roberto, Cisneros-Sinencio, Luis Fortino, Arvizu-Rodríguez, Liliana Elizabeth and González-Hernández, José Genaro, with adscription in the Tecnológico de Ciudad Madero, in the next article we present, *Implementation of an LVDT sensor to measure the viscoelastic deformation of parts created with additive manufacturing*, by Martínez-Olmos, Sergio, Soto-Mendoza, Gilberto, Hernández-Gómez, Luis Héctor and Mier-Quiroga, Luis Antonio, with adscription in the Tecnológico Nacional de México - Tecnológico de Estudios Superiores de Jocotitlán and Instituto Politécnico Nacional - Escuela Superior de Ingeniería Mecánica y Eléctrica, in the next article we present, *Intelligent algorithm using convolutional neural networks for facial recognition of people with Autism Spectrum Disorder [ASD]*, by Paredes-Xochihua, Maria Petra, Sánchez-Juárez, Ivan Rafael and Pedroza-Méndez, Blanca Estela, with adscription in the Tecnológico Nacional de México/ITS de San Martín Texmelucan, Universidad Da Vinci and Tecnológico Nacional de México/ ITApizaco, in the next article we present, *Design of an experimental reactor for the selective and efficient recovery of lithium from waste battery cathode leaching processes* by Herrera-Gutiérrez, Hugo, Cisneros-Villalobos, Luis, Torres-Islas, Álvaro and Saldarriaga-Noreña, Hugo Albeiro, with adscription in the Universidad Autónoma del Estado de Morelos, in the next article we present, *Drone-based Multi sensor System for Air Quality Monitoring* by Sánchez-Reyes, Javier Ángel, Sánchez-Medel, Luis Humberto, Sánchez-Sosol, Silvia and Piña-Martínez, Ana Laura, with adscription in the Tecnológico Nacional de México - Instituto Tecnológico Superior de Huatusco, in the next article we present, *Analysis and methodological design for the implementation of a home electrical energy loss detection system* by Duran-Belman, Israel, García-Guzmán, José Miguel, Perez, Gerardo Daniel and Gallardo-Alvarez, Dennise Ivonne, with adscription in the Tecnológico Nacional de México/ITS de Irapuato, in the last article we present, *Evaluation of LED Systems for controlled spectral lighting in indoor hydroponic cultivation* by Juárez-Balderas, Mario Alberto, Daniel-Eufracio, América Abigail, Araiz-Aguilar, Gustavo Rafael and Villaseñor-Aguilar, Marcos Jesús, with adscription in the Tecnológico Nacional de México/Campus Irapuato.

## Content

**Journal of Technology and Innovation** 12[30]1-7: e11230107
Article

# Design and simulation of gas mixing valve

# Diseño y simulación de una válvula mezcladora de gas

Vázquez-Carreón, José Roberto [a], Cisneros-Sinencio, Luis Fortino * [b], Arvizu-Rodríguez, Liliana Elizabeth [c] and González-Hernández, José Genaro [d]

[a] Tecnológico de Ciudad Madero • 1324562
[b] Tecnológico de Ciudad Madero • 102695
[c] Tecnológico de Ciudad Madero • 0000-0002-0527-150X • 444517
[d] Tecnológico de Ciudad Madero • 0000-0002-2126-2304 • 321142

**Classification:**

Area: Engineering
Field: Engineering
Discipline: Mechanical Engineering
Subdiscipline: Fluids

https://doi.org/10.35429/JTI.2025.12.30.1.1.7
**History of the article:**
Received: July 01, 2025
Accepted: September 30, 2025

* ✉ [fortino.cs@cdmadero.tecnm.mx]

**Abstract**

This study presents a design methodology for a mixing valve for two gases. The first of the gases have an ultra-low pressure and velocity, while the second have a fastest mobility. Taking advantage of the Bernoulli effect, a Venturi-type mixer is implemented to take advantage of the fast speed primary gas to create a slightly suction to move the secondary gas. To validate this methodology, simulation results of the designed valve are shown. According to the results, the suction present in the low pressure line is enough to dislodge the secondary gas without cause vacuum.

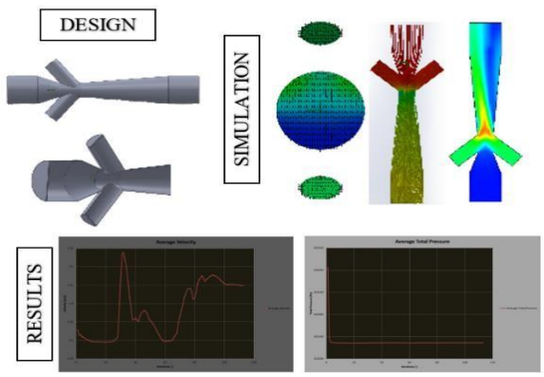


**Bernoulli effect; Venturi; gas mixing valve**

**Resumen**

En el presente estudio se aborda la metodología de diseño de una válvula mezcladora de gases, uno de los cuales posee características de presión y velocidad muy bajas, mientras que el otro presenta una velocidad mayor. Aprovechando el efecto Bernoulli, se empleó un mezclador tipo Venturi con el fin de aprovechar la velocidad del fluido principal para provocar una ligera succión que moviera al gas secundario. Para validar la metodología presentada, se simuló la válvula mezcladora. Los resultados mostraron que la succión en la línea de baja presión es suficiente para desalojar el gas secundario sin crear un vacío.

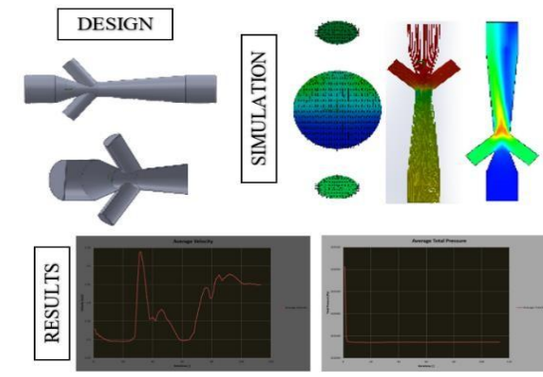


**Efecto Bernoulli; Venturi; Válvula mezcladora de gases**

**Area**: Development of strategic leading-edge technologies and open innovation for social transformation

**Citation:** Vázquez-Carreón, José Roberto, Cisneros-Sinencio, Luis Fortino, Arvizu-Rodríguez, Liliana Elizabeth and González-Hernández, José Genaro. [2025]. Design and simulation of gas mixing valve. Journal of Technology and Innovation. 12[30]1-7: e11230107.

## Introduction

Gas mixing is a practice that has been used in recent years in different contexts, providing a homogeneous gas mixture of different gaseous sources. Applications for this valve range from the pharmaceutical industry to mix and package medicines, to automotive to mix fuel with oxidants.

As a case of study, a valve to be used in the oil refining industry is proposed. The valve will take residual gas from different stages of the refining process to be mixed with a like with gaseous fuel. This fuel can be propane or natural gas used for heating in the same process. This way, user can take advantage of the energetic potential of harmful gases that otherwise would be thrown to the environment. As the source of the secondary residual gas is not constant and its availability depends on the process, the valve should be designed assuming a very small amount of gas present in the line.

A slight suction should be applied to the line in order to transport the secondary gas to the valve. However, this suction should not be strong enough to pull the raw materials for the corresponding process stage.

As the purpose of this valve is to burn the residual gas together with the fuel in the primary line, there is no need for the gas to be homogeneously mixed. Instead, the efforts of this methodology are oriented in order to effectively dislodge the residual gas from the corresponding line without creating a vacuum that negatively affect the process.

## Venturi Effect

To take advantage or the venturi effect, a venturi tube is constructed. The structure of the venturi tube is a short pipe with a narrow and restricted inner surface, commonly used to accelerate the fluid working as a functional pump. This device, designed by Giovanni Battista Venturi, has a constricted throat in the center. When fluid enters this throat, the flow through it accelerates and the pressure decreases.

This device is meticulously designed to take advantage of the effects of narrow channels and restricted fluid movement. This way, the Venturi tube is a configuration used to modify the speed of a fluid. Venturi tubes are a popular option for a wide variety of processes: from high precision measurement of fluid behavior to the modification of the dynamics of a fluid.

## Characteristics of the Venturi tube

As shown in Figure 1, the venturi tube is constructed with three fundamental parts. Each of these parts guarantee the characteristics and behavior of the device. The sections on the venturi tube are:

- Convergent inlet section
- Throat section
- Divergent outlet section/coning section

**Box 1**

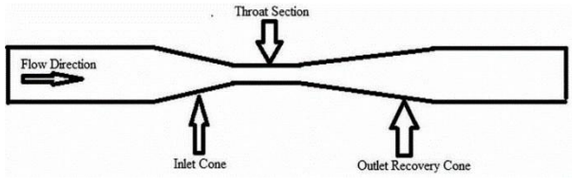


**Figure 1**
Basic model of a Venturi meter

**The convergent inlet cone** is the region where the cross-section of the inlet pipe is conically reduced for its connection to the throat, resulting in a progressive decrease in cross-section from one end to the other.

This component is attached to both the inlet pipe and the cylindrical neck. According to the ASME manual [ASME MFC-3M-2004, 2004], the angle of convergence is set at a range of 20 to 22°, while the flow length is 2.7[Dd], where D represents the diameter of the inlet section and d corresponds to the diameter of the throat. The convergent region is connected to the throat region of the inlet pipe at the lower end. Due to the reduction of the cross-sectional area, the fluid experiences an acceleration and the static pressure decreases.

The maximum angle of the cone of the convergent area is limited to avoid the vena contract, so that the flow area will be minimal in the throat. The convergent angle is considered to be a function of the β ratio, as well as the Reynolds number. The ratio between the diameter of the throat and the diameter of the inlet pipe is often referred to as the β ratio. The β ratio acts as a physical parameter of utmost importance in the design of a Venturi meter. Any modification in the Reynolds number or in the β ratio affects the most efficient convergent angle for that specific Venturi.

ISSN: 2410-3993.
RENIECYT: 1702902


Vázquez-Carreón, José Roberto, Cisneros-Sinencio, Luis Fortino, Arvizu-Rodríguez, Liliana Elizabeth and González-Hernández, José Genaro. [2025]. Design and simulation of gas mixing valve. Journal of Technology and Innovation. 12[30]1-7: e11230107
https://doi.org/10.35429/JTI.2025.12.30.1.1.7

**The throat section** is the central part of the Venturi tube and has the smallest cross-sectional area. In general, the length of the throat is proportional to its diameter. As a rule of thumb, the diameter of the throat varies between 0.25 and 0.75 times the diameter of the inlet pipe, although, in most cases it is close to 0.5 times that diameter.

It is important to emphatize that the diameter of the throat remains constant throughout its length.

**The divergent outlet section/coning section** is the last part of the instrument, connected to both the throat cylinder and the pipe outlet. The diameter of this section increases gradually; according to the ASME manual, the divergent section should have an angle of 5-13°.

This diverging angle, which is smaller than the converging angle, is used to prevent the flow from separating from the walls and to prevent the formation of eddies. In order to find the optimum angle for the Venturi recovery cone, Sharp et al. [2018] found the optimum angle to minimize pressure drop.

Design of Gas Mixing Valve

The design of the gas mixing valve has been developed strictly in accordance with the parameters established by the ASME, respecting the fundamental principles of Venturi design.

For the simulation, three basic models have been used: the conventional Venturi model [a], the modified model of the suction port at 50° [b] and a third model [c] that incorporates modifications in its structure and adds a second suction port at 50°. The design of the gas mixing valve has been meticulously conceived in strict compliance with the parameters established by the ASME.

To this end, three simulation models have been used: the first [a] is based directly on a conventional Venturi model; the second [b] has modified the suction port to 50° taking into account the ASME parameters; and finally, the third model [c] has been designed to be more efficient than the previous two, modifying its structure and adding a second suction port at 50°

**Box 2**

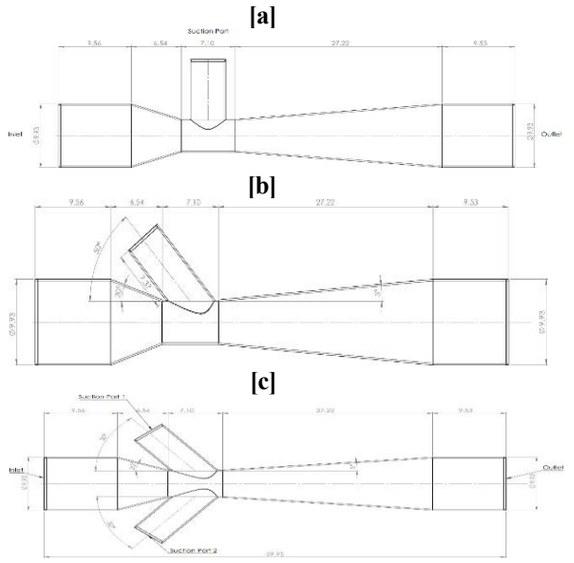


**Figure 2**
Models of gas mixing valve

As we know, the pressure in a pipe in relation to the speed of the flow is described by Bernoulli's equation.

$$P + ½\,\rho\, v^2 + \rho\, g\, h = constante \qquad [1]$$

The present study addresses the analysis of fluid behavior under restricted flow conditions, taking as a reference the principles of Bernoulli and Venturi. In this sense, the reduction of the pressure of a fluid when subjected to a narrow section of a tube is examined, as well as its behavior at the moment of reaching said change of speed. This analysis is based on the aforementioned principles and on the following expression:

$$P_1 + ½\,\rho\, v_1^2 = P_2 + ½\,\rho\, v_2^2 \qquad [2]$$

**Experimental facility**

To proceed with the final design of the valve, the initial value of the Venturi convergence angle was taken as the range established by the ASME, which ranges between 20° and 22° as optimal values. Consequently, the minimum value of 20° was adopted.

With regard to the valve's diverging angle, the minimum optimum value according to ASME was taken, set at 5°. Finally, for the suction ports, 50° was assigned for both ports. The dimension values used for the valve are listed below.

ISSN: 2410-3993.
RENIECYT: 1702902


Vázquez-Carreón, José Roberto, Cisneros-Sinencio, Luis Fortino, Arvizu-Rodríguez, Liliana Elizabeth and González-Hernández, José Genaro. [2025]. Design and simulation of gas mixing valve. Journal of Technology and Innovation. 12[30]1-7: e11230107
https://doi.org/10.35429/JTI.2025.12.30.1.1.7

### Simulation of Gas Mixing Valve

The simulation was carried out using SolidWorks, a program recognized for its efficiency in the design of Venturi mechanisms. The simulation was carried out for each of the models represented in Fig 2. Subsequently, the pressure and velocity of each of them were compared with each other. As can be seen in Fig. 2, model [a] has a suction port and an angle of 90°. In model [b], there is a suction port and an angle of 50°. Finally, the most effective model is characterized by the addition of a second suction port with an angle of 50°.

### Parameters of the Simulation

In order to estimate the simulation parameters, values close to a real case have been used, in which the combination of two gases is required: one of low pressure and speed, and another of high pressure and speed, with the aim of achieving stability during the gas mixing process

**Box 3**

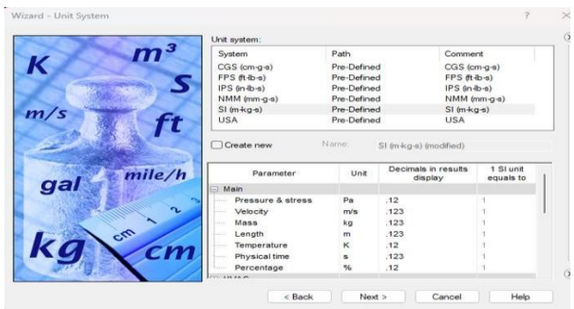


**Figure 3**

The International System of Units has been selected as the main parameter to be used in the simulator as the main measurement system for the model [although it could be any other measurement system]

*Source: Own elaboration*

**Box 4**

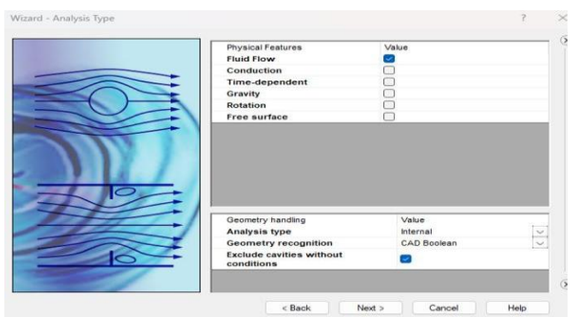


**Figure 4**

Subsequently, the type of analysis to be carried out is selected. In this case, it is of interest to know the behavior of the flow of a fluid, be it gas or liquid or any other fluid.

*Source: Own elaboration*

**Box 5**


**Figure 5**

Subsequently, the type of fluid that will be channeled through the valve is selected. On this occasion, two gases, propane and butane, have been used in order to carry out a preliminary evaluation and observe their behavior.

*Source: Own elaboration*

**Box 6**

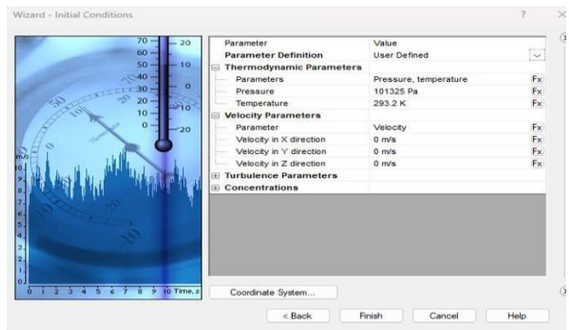


**Figure 6**

Finally, atmospheric pressure and temperature were determined as initial parameters, since in this case no conditions other than atmospheric conditions are observed.

*Source: Own elaboration*

### Comparison of initial and optimized structure

To carry out the simulation, the same input and output values were used for each of the models, obtaining the speed and pressure parameters for each of them. The gas entering the valve, classified as a low-consumption gas, will have an almost zero speed. For the simulation, it was assigned an initial value of 0.2 m/s. On the other hand, the gas in the suction port will act as our main gas inside the Venturi chamber. In this case, it was assigned an initial value of 5 m/s.

With regard to the variations, taking into consideration the recommendations of the ASME, a comparison can be seen between each of them, which are shown in Fig.7 and Fig.8.

ISSN: 2410-3993.
RENIECYT: 1702902


Vázquez-Carreón, José Roberto, Cisneros-Sinencio, Luis Fortino, Arvizu-Rodríguez, Liliana Elizabeth and González-Hernández, José Genaro. [2025]. Design and simulation of gas mixing valve. Journal of Technology and Innovation. 12[30]1-7: e11230107
https://doi.org/10.35429/JTI.2025.12.30.1.1.7

**Box 7**

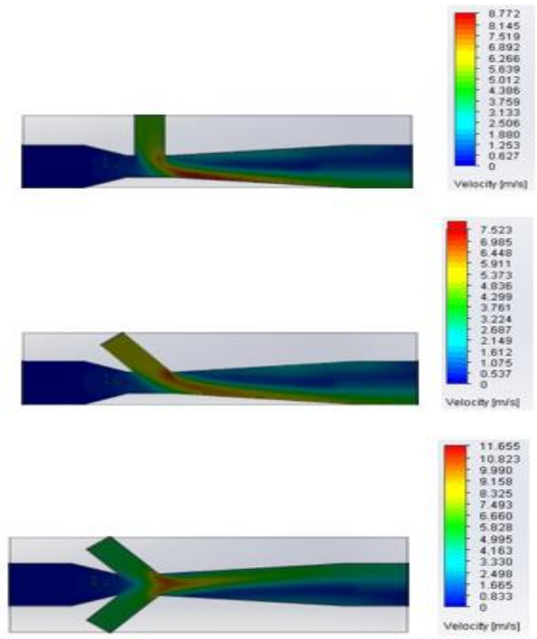


**Figure 7**

Comparison of the maximum and minimum speeds of the models.

*Source: Own elaboration*

**Box 8**

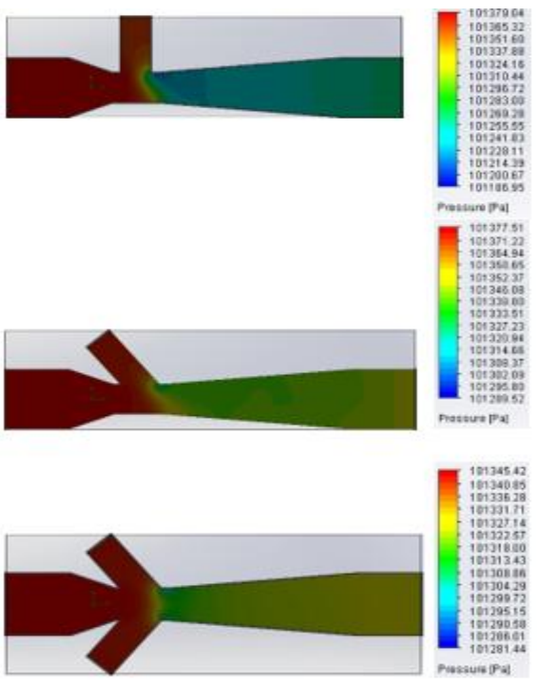


**Figure 8**

Comparison of the maximum and minimum pressure of the models.

*Source: Own elaboration*

As can be seen, model [c] exhibits a marked optimization in speed, both at its maximum and minimum and average points, while maintaining a more uniform pressure. The combination of both gases in this case results in significantly higher quality.

As is evident from the comparison, model [c] with an additional suction port distributes the fluid more evenly during the mixing phase. For additional clarity, see Figure 6, which illustrates the efficiency of the model.

**Box 9**

**Table 1**

Model [a] with a 90° suction port.

| Parameters | Averaged Value | Minimum Value | Maximum Value |
|---|---|---|---|
| Minimum Total Pressure | 101281.934 | 101281.442 | 101283.290 |
| Average Total Pressure | 101338.054 | 101337.658 | 101338.533 |
| Maximum Total Pressure | 101376.244 | 101375.404 | 101377.616 |
| Minimum Velocity | 0 | 0 | 0 |
| Average Velocity | 1.94358335 | 1.91805349 | 1.95912524 |
| Maximum Velocity | 7.7919682 | 7.76503024 | 7.828078233 |

*Source: Own elaboration*

**Box 10**

**Table 2**

Model [b] with a 50° suction port.

| Parameters | Averaged Value | Minimum Value | Maximum Value |
|---|---|---|---|
| Minimum Total Pressure | 101291.562 | 101289.519 | 101293.447 |
| Average Total Pressure | 101350.301 | 101349.762 | 101350.727 |
| Maximum Total Pressure | 101410.9798 | 101409.138 | 101412.888 |
| Minimum Velocity | 0 | 0 | 0 |
| Average Velocity | 2.04578818 | 1.96138923 | 2.11772532 |
| Maximum Velocity | 8.80264006 | 8.77666325 | 8.847917719 |

*Source: Own elaboration*

**Box 11**

**Table 3**

Model [c] with two suction ports at 50.

| Parameters | Averaged Value | Minimum Value | Maximum Value |
|---|---|---|---|
| Minimum Total Pressure | 101186.871 | 101186.652 | 101187.019 |
| Average Total Pressure | 101357.641 | 101357.495 | 101357.817 |
| Maximum Total Pressure | 101416.068 | 101415.5629 | 101416.5983 |
| Minimum Velocity | 0 | 0 | 0 |
| Average Velocity | 2.93038806 | 2.92422760 | 2.94466428 |
| Maximum Velocity | 11.5634218 | 11.5438487 | 11.5793544 |

*Source: Own elaboration*

## Reynolds Number

The Reynolds number is a key measurement in fluid analysis, as it determines its behavior. In this particular case, it is crucial that the flow is stable to minimize energy losses and guarantee an optimal mixture between the gases. This is essential to create a more orderly environment conducive to chemical reaction.

ISSN: 2410-3993.
RENIECYT: 1702902


Vázquez-Carreón, José Roberto, Cisneros-Sinencio, Luis Fortino, Arvizu-Rodríguez, Liliana Elizabeth and González-Hernández, José Genaro. [2025]. Design and simulation of gas mixing valve. Journal of Technology and Innovation. 12[30]1-7: e11230107
https://doi.org/10.35429/JTI.2025.12.30.1.1.7

To do this, the optimized model was evaluated to determine how it compared with the other two models. The following formula was used for the Reynolds calculation:

$$\boldsymbol{Re} = D * v * p / \mu \qquad [3]$$

According to the established parameters, for values of Re lower than 2300, the flow will be laminar. On the other hand, for values of Re higher than 4000, the flow will behave in a turbulent manner.

According to the measurements obtained, the diameter of the pipe is 9.93 mm. Taking this into account, the average speed of the gas is 1450.3 m/s. Likewise, the average density of the gas is 2084.2 kg/m³. Finally, considering the viscosity of the fluid, in this case propane gas, which is 0.00011, the Reynolds number is calculated.

**Box 12**

**Table 4**

Speed and density parameters of the model [c]

| | Unit | Averaged Value | Minimum Value | Maximum Value |
|---|---|---|---|---|
| Average Velocity | [m/s] | 1.4503944 | 1.4471230 | 1.4601850 |
| Average Density [Fluid] | [kg/m^3] | 2.08422 | 2.084223 | 2.084224 |

*Source: Own elaboration*

After carrying out the relevant measurements and analyses, it has been determined that the value obtained is 272.889 m/s, which is below the 2300 m/s required for the flow to be laminar.

**Box 13**

**Table 5**

Reynolds results of the model [c]

| | Unit | Averaged Value | Minimum Value | Maximum Value |
|---|---|---|---|---|
| Reynolds | [m/s] | 46.22821 | 46.06452 | 46.586711 |

*Source: Own elaboration*

## Comparative speed test

In this section, we proceed to compare the results of the speed behavior of the three models. In this way, the effectiveness of model [c] is evident in relation to the other two models, reaching a maximum speed of 11.5469 m/s.

**Box 14**

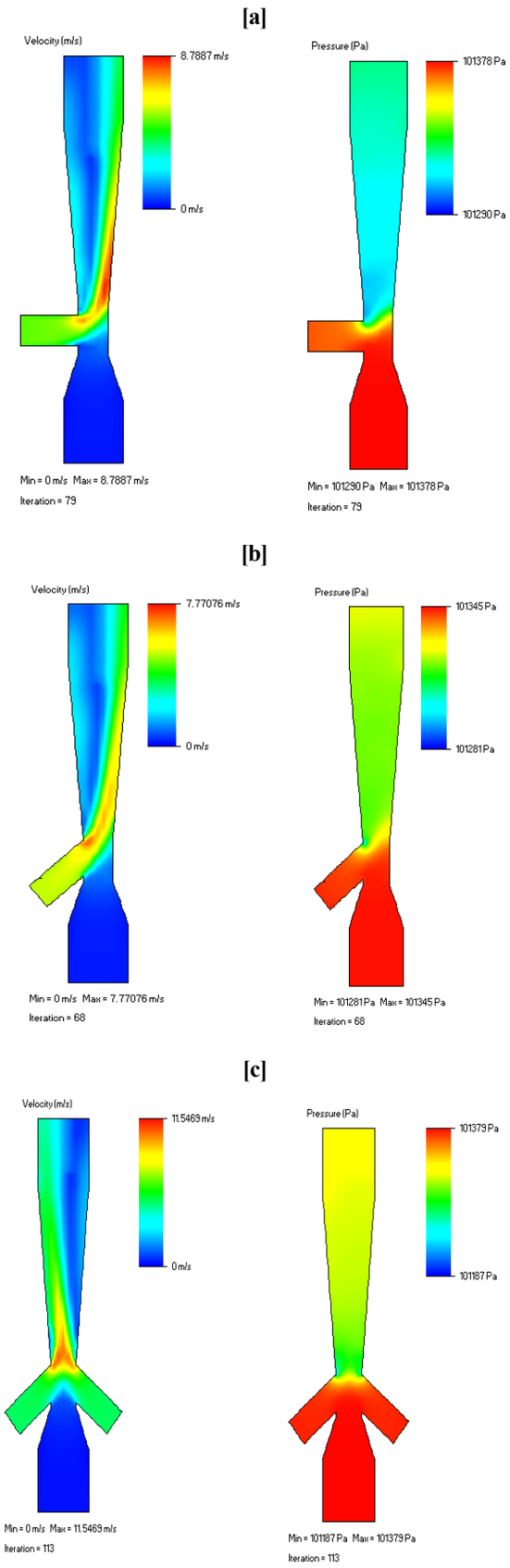


**Figure 9**

Comparison of results from different Venturi-type gas mixer models.

*Source: Own elaboration*

ISSN: 2410-3993.
RENIECYT: 1702902


Vázquez-Carreón, José Roberto, Cisneros-Sinencio, Luis Fortino, Arvizu-Rodríguez, Liliana Elizabeth and González-Hernández, José Genaro. [2025]. Design and simulation of gas mixing valve. Journal of Technology and Innovation. 12[30]1-7: e11230107
https://doi.org/10.35429/JTI.2025.12.30.1.1.7

## Conclusions

In the present study, the model of three types of venturis for the mixing of two gases, one at low pressure and the other at higher pressure, was implemented in order to efficiently simulate the mixing of the two gases.

This allowed for the evaluation of their laminar behavior and the maximum velocity they reach at their critical point. Using this procedure, a comparison was made that demonstrated the effectiveness of model [c], which incorporates a second suction port that allows for a more stable and efficient flow.

## References

Lyu, Q. and Ji, B. [2017] Experimental Investigation of the Global Cavitation Dynamic Behavior in a Venturi Tube with Special Emphasis on the Cavity Length Variation. International Journal of Multiphase Flow, 89, 290-298.

Khan, Z. A., & Jain, N. [2022]. Optimization of Convergent Angle of the Venturi Meter for Best Coefficient of Discharge. Water Supply, 22[12].

Reader-Harris, M. J., Brunton, W. C., Gibson, J. J., Hodges, D., & Nicholson, I. G. [2001]. Discharge coefficients of Venturi tubes with standard and non-standard convergent angles. Flow Measurement and Instrumentation, 12[2], 135–145
.
Zhang, L., Wei, Z., & Zhang, Q. [2024]. Structural optimization of the low-pressure Venturi injector with double suction ports based on computational fluid dynamics and orthogonal test. Desalination and Water Treatment, 214, 347–354.

Xiao, J., Liang, Z., Liu, X., Zhao, Z., & Xie, X. [2021]. Design Optimization Analysis of Venturi Tube for Medium Conveying in Strengthen Grinding Process. Engineering, 13[08], 431–447.

Hou, L., Feng, D., Wang, J., Zhang, Y., & Hou, X. [2024]. Analysis of the influence of venturi structural parameters on the performance of hydraulic impactors. Journal of Physics: Conference Series, 2707[1], 012128.

García-Saldaña, A., María D. R. Castañeda-Chávez, Pérez-Vázquez, A., Martínez-Dávila, J. P., & Carrillo-Ávila, E. [2023]. Design of Venturi-Type Fertilizer Injectors to Low-Pressure Irrigation Systems. Journal of Agricultural Science, 15[2], 25–25.

ISSN: 2410-3993.
RENIECYT: 1702902


Vázquez-Carreón, José Roberto, Cisneros-Sinencio, Luis Fortino, Arvizu-Rodríguez, Liliana Elizabeth and González-Hernández, José Genaro. [2025]. Design and simulation of gas mixing valve. Journal of Technology and Innovation. 12[30]1-7: e11230107
https://doi.org/10.35429/JTI.2025.12.30.1.1.7

**Journal of Technology and Innovation** 12[30]1-10: e21230110
Article

# Implementation of an LVDT sensor to measure the viscoelastic deformation of parts created with additive manufacturing

# Implementación de un sensor LVDT para medir la deformación viscoelástica de piezas fabricadas con manufactura aditiva

Martínez-Olmos, Sergio [a], Soto-Mendoza, Gilberto * [b], Hernández-Gómez, Luis Héctor [c] and Mier-Quiroga, Luis Antonio [d]

[a] Tecnológico Nacional de México - Tecnológico de Estudios Superiores de Jocotitlán
[b] Tecnológico Nacional de México - Tecnológico de Estudios Superiores de Jocotitlán • B-7472-2019 • 0000-0001-7357-9445 • 635154
[c] Instituto Politécnico Nacional - Escuela Superior de Ingeniería Mecánica y Eléctrica • Q-8053-2019 • 0000-0003-2573-9672 • 5107
[d] Tecnológico Nacional de México - Tecnológico de Estudios Superiores de Jocotitlán • 0000-0001-8290-4115

**Classification:**

Area: Engineering
Field: Engineering
Discipline: Mechanical Engineering
Subdiscipline: Automation

https://doi.org/10.35429/JTI.2025.12.30.2.1.10
**History of the article:**
Received: July 30, 2025
Accepted: October 30, 2025

* ✉ [gilberto.soto@tesjo.edu.mx]

**Abstract**

Additive manufacturing has experienced rapid growth due to significantly reduced manufacturing times. Besides, it is versatility, and its costs are low, among other aspects. Fused Deposition Modeling [FDM] is widely used in various sectors including healthcare, construction and aerospace. The most used materials are polymers. These exhibit viscoelastic behavior. In the present work, an LVDT [Linear Variable Differential Transformer] sensor was implemented to measure the viscoelastic deformation of parts manufactured with additive manufacturing. For this purpose, an electronic circuit with its hardware was developed. The LVDT sensor was characterized and calibrated, an interface was developed, and finally, a functional test was carried out. The minimum measurement that the system can perform is hundreds of a millimeter. A comparison was made between the LVDT readings and a dial indicator. The maximum difference between the readings was 0.46 %. The graphical interface allows viewing and saving the readings generated during the tests.

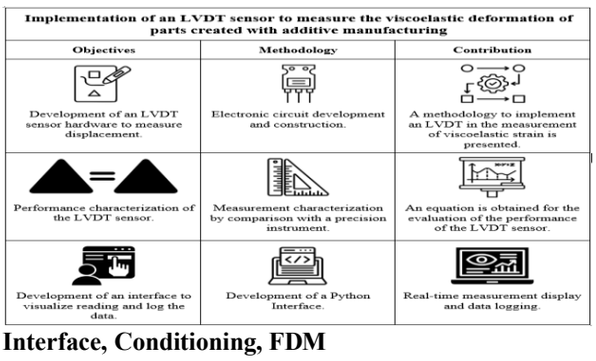


**Interface, Conditioning, FDM**

**Resumen**

La manufactura aditiva ha tenido un rápido crecimiento debido a que permite reducir significativamente los tiempos de fabricación. Además, es versátil y de bajo costo, entre otros aspectos. El proceso más utilizado es el Modelado por Deposición Fundida [FDM, por sus siglas en inglés]. Se usa en sectores como salud, construcción e industria aeroespacial. Los materiales más utilizados son polímeros. Estos presentan un comportamiento viscoelástico. En el presente trabajo, se implementó un sensor LVDT [Transformador Diferencial de Variación Lineal, por sus siglas en inglés] para medir la deformación viscoelástica de piezas fabricadas con manufactura aditiva. Para este fin se desarrolló un circuito electrónico, se creó un hardware, se caracterizó y calibró el sensor LVDT, se desarrolló una interfaz y finalmente se hizo una prueba de funcionamiento. El sistema permite medir centésimas de milímetro. Se realizó una comparación entre las lecturas del LVDT y un comparador de carátula. La diferencia máxima entre las lecturas fue de 0.46 %. La interfaz gráfica permite visualizar y guardar las lecturas generadas durante las pruebas.


**Interfaz, Acondicionamiento, FDM**

**Area**: Development of strategic leading-edge technologies and open innovation for social transformation

**Citation:** Martínez-Olmos, Sergio, Soto-Mendoza, Gilberto, Hernández-Gómez, Luis Héctor and Mier-Quiroga, Luis Antonio. [2025]. Implementation of an LVDT sensor to measure the viscoelastic deformation of parts created with additive manufacturing. Journal of Technology and Innovation. 12[30]1-10: e21230110.

## 1. Introduction

In recent years, additive manufacturing [AM], and particularly fused deposition modelling [FDM] technology, has experienced rapid growth due to its potential to transform traditional production processes.

According to Mohsen Attaran [Attaran, 2017], this production process allows for the large-scale manufacture of customised parts, while significantly reducing manufacturing times and accelerating time to market. For their part, Cano et al. [Cano-Vicent et al., 2021] highlight the versatility, low cost and ease of operation of the FDM printing technique and its adoption in strategic sectors such as healthcare, construction and aerospace. In particular, they mention that during the Coronavirus pandemic, this technique was extremely helpful in the manufacture of masks, ventilators, respirators, and nasopharyngeal swabs.

On the other hand, various studies have shown that printing parameters directly influence the mechanical properties of the parts. Gao et al. [Gao et al., 2022] present a summary, based on several articles, of the variables that affect mechanical properties, as well as dimensional properties, such as filament direction, layer thickness, fill density, nozzle temperature, printing speed, etc. This highlights the importance of being able to measure the mechanical behaviour of parts manufactured using AM.

One of the key components for achieving accurate measurement of minimal linear displacements is the Linear Variable Differential Transformer [LVDT].

As Nyce [Nyce, 2003] states, an LVDT is a non-contact position transducer that operates by means of an alternating excitation signal applied to a primary coil, which induces voltages in two secondary coils depending on the position of a moving core. The design and implementation of signal conditioning is one of the main challenges when integrating LVDT sensors into measurement systems.

The literature shows various technical approaches to overcoming the limitations associated with LVDT signal conditioning.

According to Rerkratn [Rerkratn et al., 2020], an effective strategy is to use an RMS-to-DC converter together with an XOR-type phase detector, which allows a continuous output proportional to displacement and direction to be obtained without requiring low-pass filters.

In addition, he proposes a technique based on the hyperbolic sine function to compensate for non-linearity and extend the useful range of the sensor without increasing energy consumption [Rerkratn et al., 2022]. Petchmaneelumka et al. [Petchmaneelumka et al., 2017] propose the use of a circuit based on transconductance amplifiers and a sample-and-hold module, improving thermal stability without adding complexity to the system.

The proposed circuit does not require a low-pass filter. Therefore, fast responses are obtained. They also use a sample-and-hold approach, combined with a direct sum of the secondary signals, achieving accuracy without the need for additional filtering or digital processing [Petchmaneelumka et al., 2018].

Bengtsson [Bengtsson, 2018] presents a low-cost, high-resolution signal conditioning solution for LVDT.

Other works focus on integrated circuit-based solutions. Liu and Bu [Liu & Bu, 2013] describe a design using the AD598 integrated circuit. It integrates excitation, demodulation and continuous output functions, achieving a compact and accurate design with few external components. In their work, Zhang et al. [Zhang et al., 2022] propose a measurement system with an LVDT and a self-holding circuit to measure micro-displacements in satellites.

From a more innovative approach, Songsuwankit et al. [Songsuwankit et al., 2024] present a circuit that eliminates the need for an external oscillator. It takes advantage of the self-oscillation of the primary winding and uses a phase-locked loop [PLL] control system to obtain a signal proportional to the displacement. Similarly, Raghunath et al. [Raghunath et al., 2019] propose a digital system implemented using a specific integrated circuit [ASIC].

The linearity and dynamic response of the sensor are improved through closed-loop control and synchronous demodulation techniques.

ISSN: 2410-3993.
RENIECYT: 1702902


Martínez-Olmos, Sergio, Soto-Mendoza, Gilberto, Hernández-Gómez, Luis Héctor and Mier-Quiroga, Luis Antonio. [2025]. Implementation of an LVDT sensor to measure the viscoelastic deformation of parts created with additive manufacturing. Journal of Technology and Innovation. 12[30]1-10: e21230110.
https://doi.org/10.35429/JTI.2025.12.30.2.1.10

Finally, Fan et al. [Fan et al., 2025] introduce an advanced non-linear compensation technique using artificial intelligence, employing a neural network with optimisation algorithms. This significantly reduces measurement error and extends the useful range of the sensor.

Although there are studies related to various parameters of the AM manufacturing process and the effect on its mechanical properties, it is necessary to measure its behaviour as a final product. To this end, the use of LVDT sensors, which are widely recognised in metrological applications, is proposed. One of the challenges they present is signal design and conditioning.

The aim of this work is to implement an LVDT sensor to measure the viscoelastic deformation of parts manufactured using additive manufacturing. A graphical interface is required to visualise and save the readings generated during the tests. This system must be low cost.

## 2. Problem statement

Additive manufacturing has a major impact on the way new products are created. This sector is expected to continue growing. The most commonly used materials are PLA, ABS and PETG. These are polymers, which have viscoelastic behaviour, meaning that when a load is applied, they will continue to deform over time. Currently, data has been reported on the printing parameters that affect mechanical properties.

In general, they report information on tensile strength and fatigue. Information on their viscoelastic behaviour is lacking. On the other hand, there are LVDT displacement sensors with data acquisition systems that can be purchased commercially. However, their cost is high. There are also reports with proposals for low-cost circuit designs and others with higher costs with integrated circuits that allow for more compact designs. In general, they focus on obtaining more accurate readings, but do not discuss their implementation in the phenomenon of viscoelasticity.

It is relevant for the design of products manufactured with additive manufacturing to know the viscoelastic behaviour.

For this purpose, devices that measure displacement can be used. However, it would be uneconomical to take readings and record them at all times.

One solution is to create a system that measures the displacement of AM-produced components over time and stores this data. For the reasons outlined above, it is important to develop a low-cost system that allows real-time visualisation and acquisition of displacement data over time in atomic form for parts created with additive manufacturing.

This allows products to be designed taking into account the phenomenon of viscoelasticity.

## 3. Methodology

To develop the project, the following steps were taken after the documentary research:

1. Electronic circuit design
2. Hardware
3. Characterisation and calibration of the LVDT sensor
4. Interface development
5. Functional testing

## 4. Development

### 4.1 Electronic circuit design

The electronic system developed allows for the excitation, conditioning and reading of the signal from an LVD sensor. The main stages of the circuit are:

- Symmetrical source circuit
- Excitation circuit for the LVDT sensor
- Full-wave precision rectifier
- Low-pass filter
- Offset and amplification adjustment

**Symmetrical source circuit**

A symmetrical source was designed to power the circuit from a simple 15 V DC source. A symmetrical power supply was chosen in order to obtain both positive and negative signals.

This decision facilitated the interpretation of the sensor's behaviour, as it allowed for a more intuitive visualisation of the core's displacement around a reference position. **Figure 1** shows the design of the symmetrical source circuit.

ISSN: 2410-3993.
RENIECYT: 1702902


Martínez-Olmos, Sergio, Soto-Mendoza, Gilberto, Hernández-Gómez, Luis Héctor and Mier-Quiroga, Luis Antonio. [2025]. Implementation of an LVDT sensor to measure the viscoelastic deformation of parts created with additive manufacturing. Journal of Technology and Innovation. 12[30]1-10: e21230110.
https://doi.org/10.35429/JTI.2025.12.30.2.1.10

## Box 1

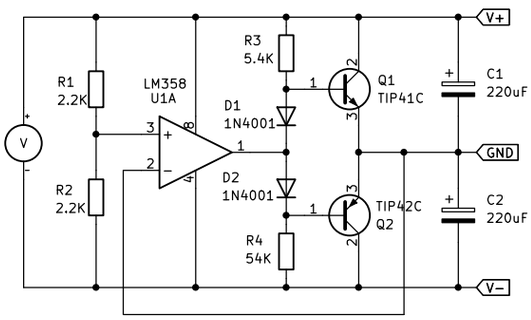


**Figure 1**

Symmetrical source circuit.

*Own source*

### Excitation circuit for the LVDT sensor

The excitation signal was generated using the ICL8038 integrated circuit as shown in **Figure 2,** configured according to the datasheet recommendations to obtain a sine wave with minimum distortion [Intersil, 2001]. Because the LVDT sensor used has a recommended optimum operating frequency of 5 Hz, this frequency set the values of the associated passive components in the generator circuit.

The resulting sinewave signal was applied to the primary winding of the LVDT via a voltage follower, in order to maintain a stable signal delivery.

## Box 2

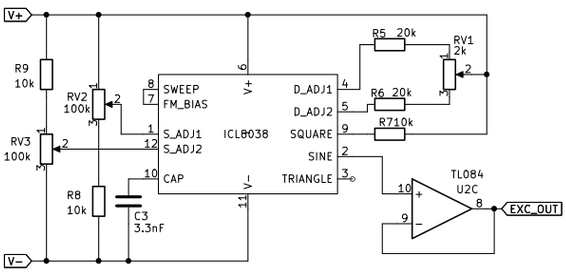


**Figure 2**

Excitation circuit for the LVDT sensor.

*Own source*

### Full wave precision rectifier

For the conditioning of the signals coming from the secondary windings, two full-wave precision rectifiers were used [see Figure 3].

This was based on operational amplifiers and diodes, following a widely used connection for analogue processing of weak signals. For more information see reference [Franco, 2015].

## Box 3

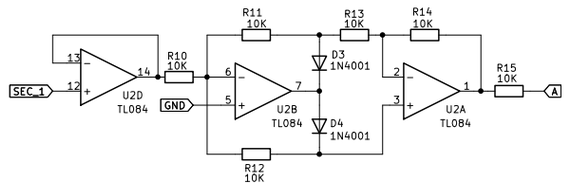


**Figure 3**

Full-wave precision rectifier.

*Own source*

One of the rectified signals was inverted [see Figure 4] by means of an additional stage to obtain the difference between the outputs of the secondaries. In this way it was possible to obtain an incremental signal proportional to the displacement of the core with respect to its initial position. The use of two rectifiers, one with an inverting stage, allows the direct addition of both signals.

## Box 4

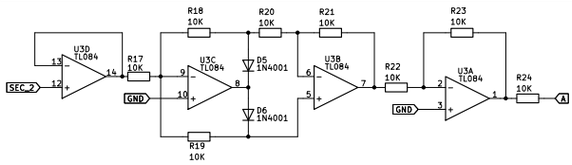


**Figure 4**

Precision rectifier with output inverter stage.

*Own source*

### Low-pass filter

Subsequently, the signal was filtered using a first-order low-pass filter [**see Figure** 5] with a cut-off frequency of 9 kHz. The value of the filter components was calculated using Equation [1] that relates the ripple factor to the capacitor, which facilitates the choice of suitable values without compromising filter performance and response time. For more information see references [Horowitz & Hill, 2015] and [Sánchez Almeida, 2013].

$$C = \frac{1}{4\sqrt{3}f_r(FR)R} \quad [1]$$

$$= \frac{1}{4\sqrt{3}(9000)(0.005)(10000)}$$

$$= 0.3207\mu F$$

Where:
$C$ is the value of the capacitor [μF]
$f_r$ is the cut-off frequency [Hz]
$FR$ is the ripple factor [dimensionless]
$R$ is the resistance value [Ω]

ISSN: 2410-3993.
RENIECYT: 1702902


Martínez-Olmos, Sergio, Soto-Mendoza, Gilberto, Hernández-Gómez, Luis Héctor and Mier-Quiroga, Luis Antonio. [2025]. Implementation of an LVDT sensor to measure the viscoelastic deformation of parts created with additive manufacturing. Journal of Technology and Innovation. 12[30]1-10: e21230110.
https://doi.org/10.35429/JTI.2025.12.30.2.1.10

## Box 5

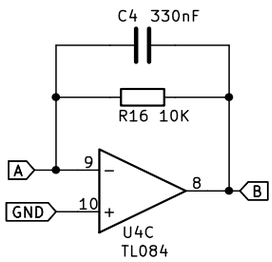


**Figure 5**
Low-pass filter.
*Own source*

### Offset and amplification adjustment

Since the filtered signal had a negative offset, an adjustment stage was incorporated using a subtractor amplifier with an adjustable reference generated by a potentiometer.

This stage made it possible to compensate the offset so that the output is zero at the initial position of the core. To adapt the signal level to the input range of the microcontroller [0-5 V], an amplification stage with a variable gain of up to 10 times was added, followed by a passive low-pass filter that attenuates the noise introduced by the amplification [see **Figure 6**].

## Box 6

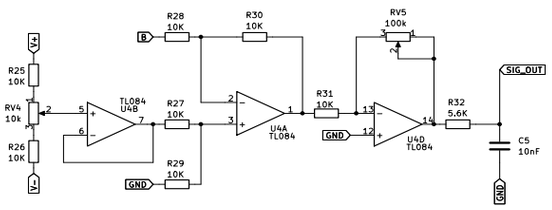


**Figure 6**
Offset and amplification adjustment.

### 4.2 Hardware

### PCB

The circuit design was created using KiCAD software. A single-layer board was designed and jumpers were incorporated. Figure 7 shows the copper traces in blue and the jumpers in red.

The components were organised into five functional modules: symmetrical power supply, signal generator, precision rectifiers, and the filtering and amplification stage. The board was manufactured using LPKF ProtoMat S104 equipment [CNC equipment for PCB machining].

The final dimensions of the PCB were 125 mm × 105 mm.

## Box 7

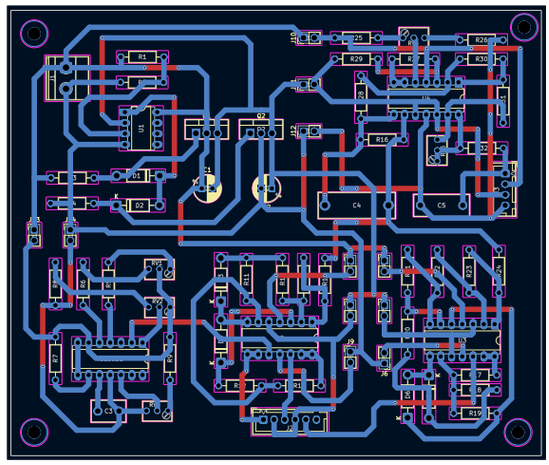

**Figure 7**
Printed circuit board [PCB] design.
*Own source*

### Data acquisition system with microcontroller

An Arduino Nano board, which incorporates the ATmega328P microcontroller, was used to acquire data from the LVDT sensor. This was due to its ease of programming, low cost, and sufficient resolution for the purpose of this work.

This microcontroller incorporates a 10-bit analogue-to-digital converter [ADC], which allows signals in the range of 0 to 5 V to be discretised with a resolution of approximately 4.88 mV per unit.

The analogue signal from the conditioning circuit is connected to pin A0 of the Arduino. To reduce noise, the implemented code averages 30 consecutive readings from that pin, thus obtaining a more stable signal measurement. A button connected to digital pin D2 was also implemented, configured with the microcontroller's internal pull-up resistor.

When this button is pressed, the system records the current position as a new reference point or ‘zero’, allowing the user to reset the displacement reference.

The acquisition frequency was set at one reading per second [1 Hz]. The data obtained is transmitted via the serial port to a graphical interface developed in Python, from which it can be viewed in real time and stored for later analysis.

ISSN: 2410-3993.
RENIECYT: 1702902


Martínez-Olmos, Sergio, Soto-Mendoza, Gilberto, Hernández-Gómez, Luis Héctor and Mier-Quiroga, Luis Antonio. [2025]. Implementation of an LVDT sensor to measure the viscoelastic deformation of parts created with additive manufacturing. Journal of Technology and Innovation. 12[30]1-10: e21230110.
https://doi.org/10.35429/JTI.2025.12.30.2.1.10

**Housing and layout of the electronic system**

To protect the system's electronic components, a housing was designed to contain the PCB manufactured with the components and the microcontroller during use, thus ensuring safe handling of the device. In addition, the connection to the LVDT sensor is improved [see **Figure 8**].

**Box 8**

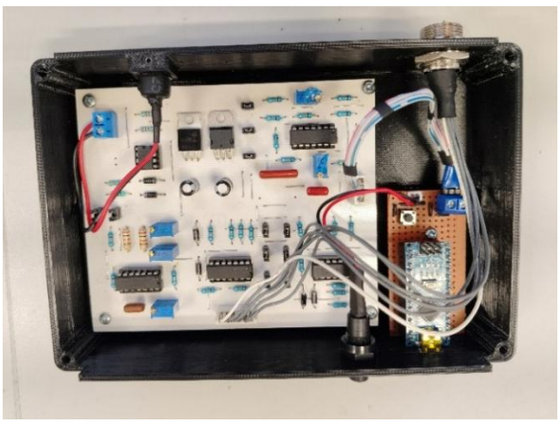

**Figure 8**
Housing and electronics layout.
*Own source*

### 4.3 LVDT sensor characterisation and calibration

The LVDT sensor was characterised under controlled conditions. This was done following the guidelines established by ISO/IEC 17025 and ISO 9513. The former establishes general requirements for the competence of testing and calibration laboratories [ISO, 2017]; while the latter specifies a method for the static calibration of extensometer systems used in uniaxial testing, including axial and diametral extensometer systems [ISO, 2012].

Some environmental factors mentioned by ISO/IEC 17025, such as temperature, vibrations or electromagnetic disturbances, could not be strictly controlled.

Nevertheless, efforts were made to comply with the related essential principles such as methodology, mechanical assembly and traceability of the reference standard.

Figure 9 shows the complete LVDT characterisation device. It allowed to compare the signal delivered by the LVDT with the displacements recorded by a dial indicator. The resolution of the dial indicator is 0.01 mm.

The instruments were mounted horizontally on a rigid base, ensuring that their stems remained parallel, aligned and with a common contact point.

**Box 9**

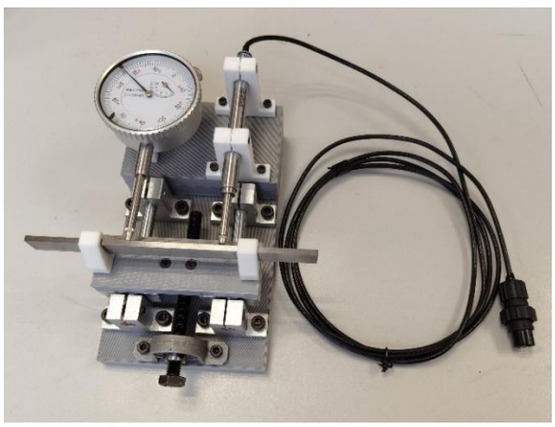

**Figure 9**
Characterisation support device.
*Own source*

The displacement was generated by a screw pushing a sliding table guided by linear bearings. A ground steel parallel was placed on top of this, which serves as a simultaneous contact surface for the two transducers.

This configuration meets the requirements of ISO 9513 for structural rigidity, motion control and mounting stability.

The characterisation process consisted of incremental displacements of 1 mm, starting from the position where the parallel made simultaneous contact with both instruments until a total travel of 22 mm was reached.

At each point, both the reading of the caratula indicator and the signal delivered by the LVDT sensor were recorded. According to ISO 9513, the number of calibration points should be defined based on Eq. [2]:

$$\frac{L_{max}}{L_{min}} = \frac{22mm}{1\ mm} = 22 \qquad [2]$$

Where:
$L_{max}$ is the maximum displacement
$L_{min}$ is the minimum displacement
This places the system in category [b] of that standard, where at least two calibration ranges and five measurements per range are required.

ISSN: 2410-3993.
RENIECYT: 1702902


Martínez-Olmos, Sergio, Soto-Mendoza, Gilberto, Hernández-Gómez, Luis Héctor and Mier-Quiroga, Luis Antonio. [2025]. Implementation of an LVDT sensor to measure the viscoelastic deformation of parts created with additive manufacturing. Journal of Technology and Innovation. 12[30]1-10: e21230110.
https://doi.org/10.35429/JTI.2025.12.30.2.1.10

The applied procedure met this criterion, covering the entire operating range of the sensor without omitting critical regions**. Figure 10** shows the scatter plot of the data and the fit line obtained by linear regression. Equation 3 shows the relationship:

$$y = 0.0221x - 0.5548 \quad [3]$$

Where:
$y$ is the displacement in millimetres
$x$ is the average value read by the ADC

This equation was subsequently implemented in the microcontroller for the conversion of ADC units to mm. As can be seen, the sensor presented a highly consistent linear behaviour.

**Box 10**

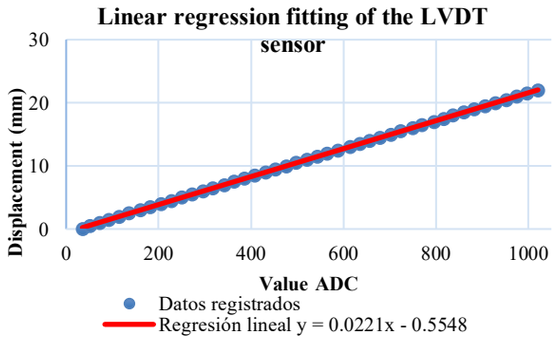


**Figure 10**
Dispersion of the obtained data and the fit line.
*Own source*

### 4.4 Graphical interface of the data acquisition system

The graphical interface developed allows visualisation of the LVDT sensor readings. Also, a file with displacement and time information can be generated. This was done in Python, using the Tkinter libraries to build the GUI, Matplotlib for the graphical visualisation of the data and PySerial to establish serial communication with the Arduino Nano. The **Figure 11** shows the interface. The left side consists of a control panel, which allows selecting the communication port, starting or ending a test and displaying the elapsed time.

The right side includes a graph that plots the displacements as a function of time, showing the last readings for easy visual tracking. During a test, the data received from the microcontroller is dynamically updated on the graph. At the end, the user can save the results in a CSV file.

**Box 11**

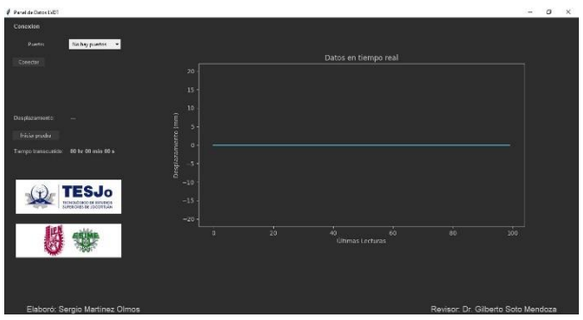


**Figure 11**
Graphical interface of the measurement system.
*Own source*

### 4.5 Functional test

A PLA cantilever beam was tested by applying a constant load of 5.3 kg on the specimen for a total time of 6 hours.

Figure 12. The beam has a length of 210 mm, the restraint is 20 mm, from the left end of the beam the load is located at 10 mm to the right and the sensor at 60 mm to the right. The cross section of the beam is 8 mm wide and 16 mm high.

**Box 12**

**Figure 12**
Test run.
Own source

## 5. Analysis of Results

Once the equation characterising the behaviour of the LVDT was obtained, it was loaded into the code. Subsequently, the readings obtained with this LVDT sensor were compared with those of the dial indicator.

ISSN: 2410-3993.
RENIECYT: 1702902


Martínez-Olmos, Sergio, Soto-Mendoza, Gilberto, Hernández-Gómez, Luis Héctor and Mier-Quiroga, Luis Antonio. [2025]. Implementation of an LVDT sensor to measure the viscoelastic deformation of parts created with additive manufacturing. Journal of Technology and Innovation. 12[30]1-10: e21230110.
https://doi.org/10.35429/JTI.2025.12.30.2.1.10

The latter was used as a reference instrument. Displacements were applied in 1 mm increments from 0 to 22 mm. Table 1 presents the measurements obtained by both devices, as well as the difference in readings between them. The maximum difference was 0.10 mm

**Box 13**

**Table 1**

Comparison of measurements between a Dial Indicator and the LVDT.

| Front cover indicator,mm | LVDT, mm | Difference, mm |
|---|---|---|
| 0.00 | 0.00 | 0.00 |
| 1.00 | 0.99 | 0.01 |
| 2.00 | 2.03 | 0.06 |
| --- | --- | --- |
| 9.00 | 9.10 | 0.10 |
| 10.00 | 9.98 | 0.02 |
| 11.00 | 10.92 | 0.08 |
| --- | --- | --- |
| 20.00 | 20.09 | 0.09 |
| 21.00 | 21.10 | 0.10 |
| 22.00 | 22.10 | 0.10 |

When comparing the maximum percentage error with other works, it was found that Rerkratn et al. [Rerkratn et al., 2020] report a maximum error of 1.1% and later this author presented another with a maximum error of 0.295 % [see Table 2]. The maximum error presented in this work is 0.46 %.

**Box 14**

**Table 2**

Comparison of the percentage of measurement error.

| Autor | Measuring range [mm] | Maximum error [mm] | Maximum error [%] |
|---|---|---|---|
| Olmos et al. | 22.00 | 0.10 | 0.46 |
| Rerkratn et al. [Rerkratn et al., 2020] | 20.00 | 0.220 | 1.10 |
| Fan et al. [Fan et al., 2025] | 16.00 | 0.042 | 0.27 |
| Bengtsson et al.[Bengtsson, 2018] | 12.70 | 0.006 | 0.047 |
| Songsuwankit et al.[Songsuwankit et al., 2024] | 8.00 | 0.034 | 0.42 |
| Rerkratn et al. [Rerkratn et al., 2022] | 6.20 | 0.018 | 0.295 |
| Ran and Hui [Liu & Bu, 2013] | 5.80 | 0.016 | 0.27 |

The result of the function test is shown in Figure 13, where the vertical axis represents the displacement and the horizontal axis corresponds to the time. The sensor was set to zero with no load, when the load was applied it displaced approximately 8 mm [elastic deformation].

Subsequently, the material continued to deform over time. At the end of the test, the total displacement recorded was 11.08 mm, which represents a viscous deformation of 3.08 mm.

**Box 15**

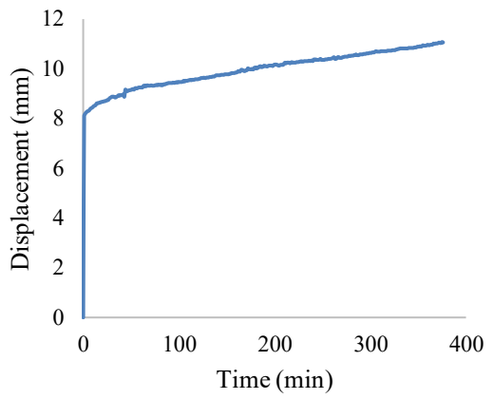


**Figure 13**

Result of the cantilever beam test.

*Own source*

## Conclusions

An LVDT sensor was implemented as a tool to measure the viscoelastic deformation of parts manufactured using additive manufacturing. The graphical interface allows real-time displacement to be visualised. It also has the function of saving displacement information as a function of time in a CSV file. The characterisation of the LVDT sensor allowed an equation to be created with linear regression adjustment.

When directly comparing the LVDT sensor readings with a dial indicator, the maximum variation obtained was 0.1 mm. The sensor's measurement range is 22 mm and it has a maximum error of 0.46%. The application example was a PLA beam in which an elastic deformation of 8 mm and a viscous deformation of 3.08 mm were found in a time of 6 hours. The proposal represents an economical manufacturing version. It was also found that the integrated AD598 can be used, which allows for a more compact circuit, although it has a higher cost.

ISSN: 2410-3993.
RENIECYT: 1702902


Martínez-Olmos, Sergio, Soto-Mendoza, Gilberto, Hernández-Gómez, Luis Héctor and Mier-Quiroga, Luis Antonio. [2025]. Implementation of an LVDT sensor to measure the viscoelastic deformation of parts created with additive manufacturing. Journal of Technology and Innovation. 12[30]1-10: e21230110.
https://doi.org/10.35429/JTI.2025.12.30.2.1.10

**Declarations**

**Conflict of interest**

The authors declare that they have no conflict of interest.

They have no financial interests or personal relationships that could have influenced this article.

**Contribution of the authors**

*Martínez-Olmos, Sergio*: Contributed to the research, methodology, formal analysis, software, and writing.

*Soto-Mendoza, Gilberto*: Contributed to the project idea, project management, supervision, methodology, validation, review, and writing.

*Hernández-Gómez, Luis Héctor*: Contributed to the project idea, review, and editing.

*Mier-Quiroga, Luis Antonio*: Review and editing.

**Availability of data and materials**

The data generated during this study are available from the corresponding author upon reasonable request.

**Funding**

No funding was received to conduct this study.

**References**

**Background**

Attaran, M. [2017]. The rise of 3-D printing: The advantages of additive manufacturing over traditional manufacturing. *Business Horizons*, *60*[5], 677–688.

Bengtsson, L. E. [2018]. Single-chip Implementation of LVDT Signal Conditioning. *American Journal of Sensor Technology*, *5*[1], 7–16.

Cano-Vicent, A., Tambuwala, M. M., Hassan, Sk. S., Barh, D., Aljabali, A. A. A., Birkett, M., Arjunan, A., & Serrano-Aroca, Á. [2021]. Fused deposition modelling: Current status, methodology, applications and future prospects. *Additive Manufacturing*, *47*, 102378.

Fan, Q., Zhang, X., Wen, Z., Xu, L., & Zhang, Q. [2025]. Nonlinear Compensation of the Linear Variable Differential Transducer Using an Advanced Snake Optimization Integrated with Tangential Functional Link Artificial Neural Network. *Sensors*, *25*[4].

Gao, G., Xu, F., Xu, J., Tang, G., & Liu, Z. [2022]. A Survey of the Influence of Process Parameters on Mechanical Properties of Fused Deposition Modeling Parts. *Micromachines*, *13*[4].

Liu, R., & Bu, H. [2013]. Design on LVDT Displacement Sensor Based on AD598. *Sensors & Transducers*, *160*, 68–73.

Nyce, D. S. [2003]. *Linear Position Sensors*. Wiley.

Petchmaneelumka, W., Mano, P., & Riewruja, V. [2018]. LVDT demodulator based on amplitude detector. *2018 3rd International Conference on Control and Robotics Engineering [ICCRE]*, 218–221.

Petchmaneelumka, W., Songsuwankit, K., & Riewruja, V. [2017]. Simple LVDT Signal to DC Converter. *Proceedings of the 9th International Conference on Computer and Automation Engineering*, 193–197.

Raghunath, K. P., Manu Sagar, K. V, Gokulan, T., Kumar, K., & Thakur, C. S. [2019]. ASIC Based LVDT Signal Conditioner for High-Accuracy Measurements. In A. Sengupta, S. Dasgupta, V. Singh, R. Sharma, & S. Kumar Vishvakarma [Eds.], *VLSI Design and Test* [pp. 385–397]. Springer Singapore.

Rerkratn, A., Luangpol, A., Petchmaneelumka, W., & Riewruja, V. [2020]. Position signal detector for linear variable differential transformer. *Energy Reports*, *6*, 603–607.

Rerkratn, A., Tongcharoen, J., Petchmaneelumka, W., & Riewruja, V. [2022]. Linear-Range Extension for Linear Variable Differential Transformer Using Hyperbolic Sine Function. *Sensors*, *22*[10].

Songsuwankit, K., Petchmaneelumka, W., Riewruja, V., & Rerkratn, A. [2024]. Linear Variable Differential Transformer Signal Conditioning Circuit Based on Phase-Locked Loop. *Sensors and Materials*, *36*[4], 1473–1486.

ISSN: 2410-3993.
RENIECYT: 1702902


Martínez-Olmos, Sergio, Soto-Mendoza, Gilberto, Hernández-Gómez, Luis Héctor and Mier-Quiroga, Luis Antonio. [2025]. Implementation of an LVDT sensor to measure the viscoelastic deformation of parts created with additive manufacturing. Journal of Technology and Innovation. 12[30]1-10: e21230110.
https://doi.org/10.35429/JTI.2025.12.30.2.1.10

Zhang, X., Liu, H., Che, M., Geng, Z., & Jiu, Y. [2022]. Research on Displacement Measurement and Self-detecting Circuit Based on LVDT. *Journal of Physics: Conference Series*, *2437*[1].

**Basics**

Intersil. [2001]. *Precision Waveform Generator/Voltage Controlled Oscillator*.

Franco, S. [2015]. *Design with Operational Amplifiers and Analog Integrated Circuits* [4th ed.]. McGraw-Hil.

Horowitz, P., & Hill, W. [2015]. *The Art of Electronics* [3rd ed.]. Cambridge University.

Sánchez Almeida, T. [2013]. *ELECTRÓNICA: Dispositivos y aplicaciones* [T. y R. de Información. Departamento de Electrónica, Ed.; 2nd ed.]. ESCUELA POLITÉCNICA NACIONAL.

ISO. [2012]. *ISO 9513:2012 - Materiales metálicos — Calibración de sistemas de extensómetros utilizados en ensayos uniaxiales*.

ISO. [2017]. *ISO/IEC 17025:2017[es], Requisitos generales para la competencia de los laboratorios de ensayo y calibración*.

**Support**

Bengtsson, L. E. [2018]. Single-chip Implementation of LVDT Signal Conditioning. *American Journal of Sensor Technology*, *5*[1], 7–16.

Liu, R., & Bu, H. [2013]. Design on LVDT Displacement Sensor Based on AD598. *Sensors & Transducers*, *160*, 68–73.

Fan, Q., Zhang, X., Wen, Z., Xu, L., & Zhang, Q. [2025]. Nonlinear Compensation of the Linear Variable Differential Transducer Using an Advanced Snake Optimization Integrated with Tangential Functional Link Artificial Neural Network. *Sensors*, *25*[4].

Songsuwankit, K., Petchmaneelumka, W., Riewruja, V., & Rerkratn, A. [2024]. Linear Variable Differential Transformer Signal Conditioning Circuit Based on Phase-Locked Loop. *Sensors and Materials*, *36*[4], 1473–1486.

Rerkratn, A., Luangpol, A., Petchmaneelumka, W., & Riewruja, V. [2020]. Position signal detector for linear variable differential transformer. *Energy Reports*, *6*, 603–607.

Rerkratn, A., Tongcharoen, J., Petchmaneelumka, W., & Riewruja, V. [2022]. Linear-Range Extension for Linear Variable Differential Transformer Using Hyperbolic Sine Function. *Sensors*, *22*[10].

ISSN: 2410-3993.
RENIECYT: 1702902


Martínez-Olmos, Sergio, Soto-Mendoza, Gilberto, Hernández-Gómez, Luis Héctor and Mier-Quiroga, Luis Antonio. [2025]. Implementation of an LVDT sensor to measure the viscoelastic deformation of parts created with additive manufacturing. Journal of Technology and Innovation. 12[30]1-10: e21230110.
https://doi.org/10.35429/JTI.2025.12.30.2.1.10

**Journal of Technology and Innovation** 12[30]1-8: e31230108
Article

# Intelligent algorithm using convolutional neural networks for facial recognition of people with Autism Spectrum Disorder [ASD]

# Algoritmo inteligente utilizando redes neuronales convolucionales para reconocimiento facial de personas con Trastorno del Espectro Autista [TEA]

Paredes-Xochihua, Maria Petra * [a], Sánchez-Juárez, Ivan Rafael [b] and Pedroza-Méndez, Blanca Estela [c]

[a] Tecnológico Nacional de México/ITS de San Martín Texmelucan • KVA-5814-2024• 0000-0003-1753-2313 • 298117
[b] Universidad Da Vinci • ABW-3403-2022 • 0000-0001-8296-5532 • 493160
[c] Tecnológico Nacional de México/ ITApizaco• HKF-7420-2023 • 0000-0002-9819-635X • 74723

**Classification:**

Area: Engineering
Field: Technological sciences
Discipline: Computer technology
Subdiscipline: Artificial intelligence

https://doi.org/10.35429/JTI.2025.12.30.3.1.8
**History of the article:**
Received: July 30, 2025
Accepted: October 30, 2025

* ✉ [petra.paredes@smartin.tecnm.mx]

**Abstract**

This article describes the implementation of an algorithm for facial recognition in individuals with ASD. Computational technologies have advanced significantly, benefiting various sectors, including healthcare and education. In the case of ASD, computational techniques and intelligent algorithms can contribute to more accurate and earlier diagnosis, representing a key tool for healthcare professionals and society. Intelligent algorithms play a crucial role in automating complex processes, such as analyzing large volumes of data and making decisions in real time. Their ability to identify patterns and trends allows for more informed and accurate decisions. Therefore, implementing an intelligent algorithm for identifying individuals with ASD allows for more efficient, reliable, and accessible diagnosis.

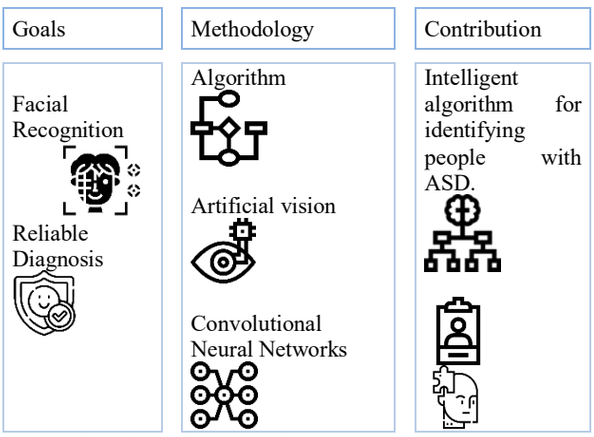


**Autism Spectrum Disorder, facial recognition, computer vision, deep learning**

**Resumen**

El presente artículo describe la implementación de un algoritmo para el reconocimiento facial de personas con TEA. Las tecnologías computacionales han avanzado significativamente, beneficiando diversos sectores, incluidos salud y educación. En el caso del TEA, las técnicas computacionales y algoritmos inteligentes pueden contribuir a un diagnóstico más preciso y temprano, representando una herramienta clave para profesionales de la salud y la sociedad. Los algoritmos inteligentes desempeñan un papel crucial en la automatización de procesos complejos, como el análisis de grandes volúmenes de datos y la toma de decisiones en tiempo real. Su capacidad para identificar patrones y tendencias permite obtener decisiones más informadas y precisas. Por lo que, implementar un algoritmo inteligente para la identificación de personas con TEA permite un diagnóstico más eficiente, confiable y accesible.

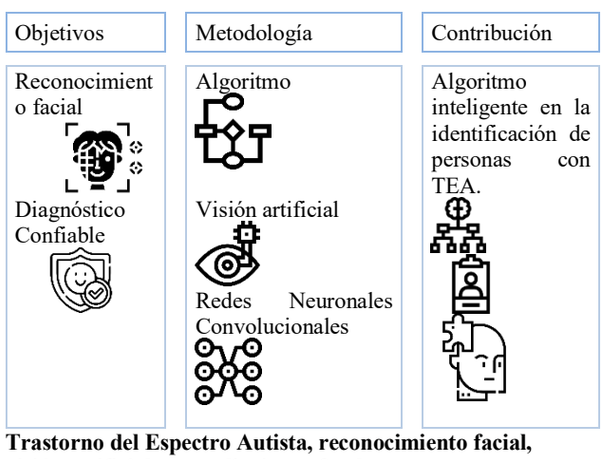


**Trastorno del Espectro Autista, reconocimiento facial, visión artificial, aprendizaje profundo**

**Area**: Development of strategic leading-edge technologies and open innovation for social transformation

**Citation:** Paredes-Xochihua, Maria Petra, Sánchez-Juárez, Ivan Rafael and Pedroza-Méndez, Blanca Estela. [2025]. Intelligent algorithm using convolutional neural networks for facial recognition of people with Autism Spectrum Disorder [ASD]. Journal of Technology and Innovation. 12[30]1-8: e31230108.

## 1. Introduction

In Mexico, a 2016 study conducted by Autism Speaks and the Mexican Autism Clinic [CLIMA] identified that 1 in every 115 children has autism, occurring more frequently in boys than in girls, and identifying that, for every 5 cases of autism, 4 of them are men and 1 is a woman [Teletón México, 2024].

Today, computational techniques have advanced significantly, providing highly useful technologies that support people in various sectors, from healthcare to education, as well as commerce, industry, research, and more. These technologies not only optimize processes but also have the potential to improve people's quality of life by facilitating their daily activities, increasing their productivity, or even assisting in complex decision-making. In this context, it is essential to leverage these tools to address specific challenges affecting groups of people with particular needs, such as those with ASD.

Due to the diversity of their characteristics and the complexity of their diagnosis, identifying individuals with ASD early and accurately represents a significant challenge for healthcare professionals and society at large. This is where computational techniques, such as artificial intelligence and intelligent algorithms, can play a crucial role. It is important to develop and propose an intelligent algorithm capable of identifying individuals with ASD in an efficient, reliable, and accessible manner.

This type of solution would not only support early diagnosis but could also facilitate the personalization of therapeutic interventions, improve social inclusion, and offer families an additional tool to better understand and address the needs of their loved ones.

The objective is to identify and implement an algorithm to recognize facial features associated with individuals with ASD, with the goal of implementing it in a system that helps identify these individuals. For this important task, machine learning and convolutional neural networks were used for the image selection and classification process.

To evaluate the algorithm, we used the Kaggle dataset with images of people with autism, and a dataset of images of Mexican citizens created for this study.

For the training and testing phases, they were combined into a single dataset, which serves as the training and evaluation corpus for the facial recognition algorithm.

The sections covered in the article are: related works, materials, techniques, algorithm for ASD detection, algorithm models and tests, and results with evaluation metrics.

## 2. Related works

To develop the project, it was necessary to conduct research to identify how this issue has been addressed in other studies and by various authors from different regions.

The advancement of Machine Learning [ML] and Deep Learning [DL] techniques has allowed them to be widely applied in various fields, including pattern recognition, disease monitoring, sentiment analysis, gender classification, and the identification of facial expressions, among others [Ahmad et al, 2024].

Ahmad et al. [2024] performed autism spectrum disorder detection using facial images: comparing the performance of pre-trained convolutional neural networks. They used the detection of autism spectrum disorders using facial images [Autism Spectrum Disorder – Detection Facial Image ASD-DFI] at early ages.

The methodology they proposed contains 6 pre-trained models of great recognition, these were ResNet34, ResNet50, VGG16, VGG19, AlexNet and MobileNetv2, all of them implemented in Python.

Juárez et al. [2024] developed a computer vision system that uses facial and text recognition to recommend professional profiles.

They used advanced image processing and machine learning techniques to evaluate facial and handwriting characteristics. The results showed an accuracy of 87.5% in facial analysis and 85.93% in text analysis.

Cadena, J.,'s thesis [2021] presents an efficient technique for global face recognition using wavelet transforms and support vector machines [SVMs] on 3D images.

ISSN: 2410-3993.
RENIECYT: 1702902


Paredes-Xochihua, Maria Petra, Sánchez-Juárez, Ivan Rafael and Pedroza-Méndez, Blanca Estela. [2025]. Intelligent algorithm using convolutional neural networks for facial recognition of people with Autism Spectrum Disorder [ASD]. Journal of Technology and Innovation. 12[30]1-8: e31230108.
https://doi.org/10.35429/JTI.2025.12.30.3.1.8

This work addresses the challenges associated with face recognition in three-dimensional environments, such as variations in facial expression, lighting, and partial occlusions, proposing an innovative approach that improves the accuracy and robustness of the system.

The technique is based on two key components: the wavelet transform, used for extracting relevant features, and SVMs, used for identity classification. The wavelet transform allows the facial surface to be decomposed into multiple scales and frequencies, capturing both global and local information about facial shapes and textures.

These features, represented in the frequency domain, are subsequently classified using SVMs, which separate the different identities by maximizing the margin between classes.

Feng [2023] presents research addressing the early detection of Autism Spectrum Disorder [ASD] in children, using advanced deep learning techniques applied to functional magnetic resonance imaging [fMRI]. Early diagnosis of ASD is crucial for implementing early interventions and improving developmental outcomes in affected children.

The authors developed an algorithm based on a custom Convolutional Neural Network [CNN] specifically designed to analyze resting-state fMRI data. The CNN architecture incorporates convolution, pooling, batch normalization, dropout, and fully connected layers, optimized for interpreting high-dimensional data.

This configuration enables the extraction and learning of hierarchical features from brain images, facilitating the distinction between children with ASD and those with typical development.

## 3. Materials y Techniques

CNNs have established a strong reputation in the field of image data processing, producing superior results compared to traditional methods. However, they require a large amount of data for the training phase, which is sometimes referred to as data-hungry algorithms, especially training from scratch.

However, transfer learning [TL] has largely solved this problem, where a pre-trained model is retrained to perform a specific task with fewer data samples [Pineda, 2021].

Pre-trained deep learning models provide substantial benefits in artificial intelligence and machine learning. These models allow practitioners to save time and computing resources by providing powerful starting points for numerous tasks, leveraging knowledge from extensive training on large and diverse datasets.

The ability to adapt pre-trained models to specific tasks using limited labeled data is an important feature of transfer learning. It reduces the need for large datasets [Pineda, 2021].

Python was used as the programming language due to its simplicity and variety of specialized libraries, such as OpenCV, TensorFlow, Keras, and Scikit-Learn.

## 4. Algorithm for ASD detection

Based on related work and the analysis of deep learning techniques, it is proposed to follow the algorithm consisting of the steps presented in figures 1, 2 and 3. Figure 1 presents the first steps that the algorithm will follow; it has two connectives, A and B, which are related to figures 2 and 3 respectively.The descriptive algorithm for training and prediction with the ResNet50 model is described below.

1. Start
2. Evaluate whether a pre-trained model exists [.h5]:

- If the model exists: Proceed to Section B [Image Prediction].
- If the model does not exist: Proceed to Section A [Model Training].

**Box 1**

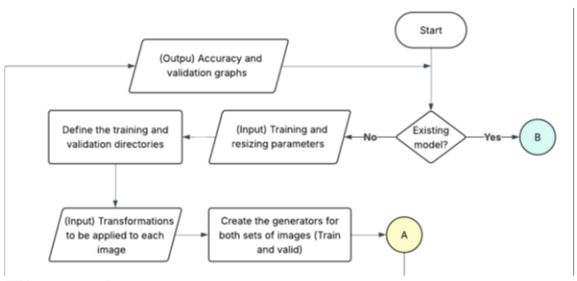


**Figure 1**
Flowchart of the algorithm
*Source: Own elaboration*

ISSN: 2410-3993.
RENIECYT: 1702902


Paredes-Xochihua, Maria Petra, Sánchez-Juárez, Ivan Rafael and Pedroza-Méndez, Blanca Estela. [2025]. Intelligent algorithm using convolutional neural networks for facial recognition of people with Autism Spectrum Disorder [ASD]. Journal of Technology and Innovation. 12[30]1-8: e31230108.
https://doi.org/10.35429/JTI.2025.12.30.3.1.8

**Section A:** Model training [if no model exists]

Step 1. Parameters and training directories. The input parameters for training and image resizing are defined. In addition, the directories for the training and validation sets are specified. Transformations are applied to each image in the training and validation directories.

Step 2. Create the image generators. The training and validation image sets [Train and Valid] are established. The previously defined transformations are implemented, indicating the directory of the sets and the parameter data to apply them.

**Box 2**

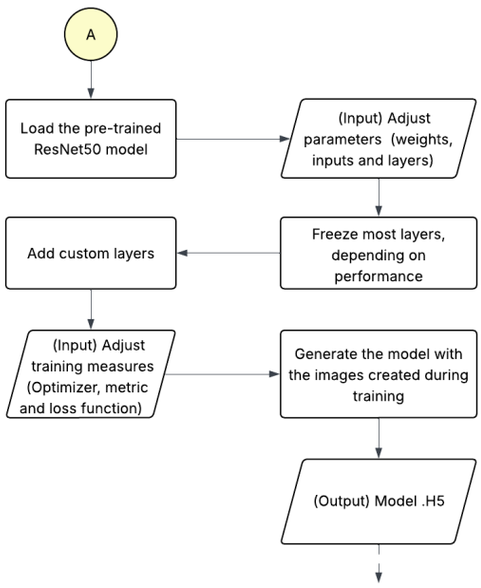


**Figure 2**
Flowchart of section A of the algorithm
*Source: Own elaboration*

Step 3. Load the pre-trained ResNet50 model. Import the pre-trained ResNet50 model, defining the input image with the width and height dimensions, using three RGB color channels. Load the pre-trained ResNet model, and fine-tune the model parameters [omit the last layer of input images].

Step 4. Add custom layers. The specific layers for the classification problem are added and the model output is stored in the variable x. The dimensionality of the 3D convolutional output is reduced to a 1D vector. A fully connected dense layer, with 128 neurons, is added to learn to classify, with a relu function that allows learning non-linear patterns, a Dropout of 0.3 is defined to avoid overfitting.

The dense output layer is appended, creating n neurons, one for each category [2 classes], a sigmoid activation function, and the name of the output. The complete model is created using the custom layers that were built previously, considering the ResNet50 model as a base, but using the custom output layer.

Transfer learning is performed by freezing all the layers prior to those chosen, thus ensuring that the training or knowledge that has already been acquired with another dataset is not lost.

Step 5. Freeze pre-trained model layers. Most pre-trained layers are frozen, that is, all layers in the model except those indicated, the last 3 in this algorithm. This is to avoid processing time, i.e., the ResNet50 convolutional layers that will not be modified, since they have already been trained, and thus allow training only the custom layers.

Step 6. Adjust training measures. The loss function is calculated using the categorical_crossentropy function. The Adam optimizer is used for learning, as it adjusts the model's weights to reduce error. It also calculates the model's accuracy, allowing us to identify how many predictions were correct and how many were incorrect.

Step 7. Generate the trained model with the training data. The model is validated using the validation set, and performance metrics are monitored. The first phase is trained with the generated images, performance is evaluated with the validation images, and the weights for fc1, fc2, and output are adjusted. Five epochs are generated. From step 5 up to this point, the model is repeated in two more phases, with the only difference being the time to unfreeze the training layers. Therefore, the changes in phases 2 and 3 are briefly described below.

Step 8. Generate output from the trained model. The trained model is generated in .h5 format. The accuracy and validation data are evaluated to assess model performance.

**Section B.** Image prediction [if a trained model exists]

Step 1. Check if you only want to classify one image.

ISSN: 2410-3993.
RENIECYT: 1702902


Paredes-Xochihua, Maria Petra, Sánchez-Juárez, Ivan Rafael and Pedroza-Méndez, Blanca Estela. [2025]. Intelligent algorithm using convolutional neural networks for facial recognition of people with Autism Spectrum Disorder [ASD]. Journal of Technology and Innovation. 12[30]1-8: e31230108.
https://doi.org/10.35429/JTI.2025.12.30.3.1.8

Question: Do you only want to analyze one image?

Yes: Select an image from the gallery, go to Step 2.

- Predict which category it belongs to based on the image data and present it.

No: Identify the path to the folder with multiple images, go to Step 3.

**Box 3**

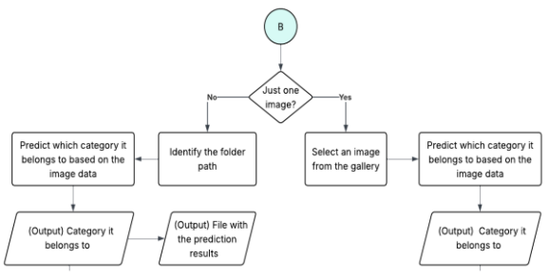


**Figure 3**

Flowchart of section B of the algorithm.

*Source: Own elaboration*

Step 2: Prediction for a single image. The image is selected from the gallery. The model predicts which category the image belongs to. The image category is defined. Go to Step 4.

Step 3: Prediction for an image folder. The path to the image folder is selected. The model performs mass predictions on the images and generates a TXT file with the prediction results. Go to Step 4.

Step 4. Finalize the process.

## 5. Models and tests of the algorithm

This session describes some of the models and parameters that were configured and used for the classification of individuals with ASD. The goal is to test the feasibility of using facial recognition with artificial intelligence techniques, specifically Machine Learning and Convolutional Neural Networks, to identify individuals with ASD and implement it in a system.

To evaluate the proposed model, in pre-training the ResNet model uses the ImageNet dataset [ImageNet, 2020] and in the testing phase the Kaggle dataset is used together with a dataset built for this specific study, the datasets used are freely licensed [Autism dataset, 2024].

The training and testing dataset is composed of four subsets: Consolidate, Test, Training, and Valid. Table 1 presents the detailed data.

**Box 4**

**Table 1**

Dataset

| No. | Subset | Autism | Non-Autism |
|---|---|---|---|
| 1 | Consolidate | 1523 | 1521 |
| 2 | Test | 361 | |
| 3 | Training | 1290 | 1321 |
| 11 | Valid | 70 | 71 |

*Source: Own elaboration*

Table 2 presents the parameters with which the different models with which tests were performed with ResNet were defined.

**Box 5**

**Table 2**

Test results

| Test | Model generation parameters | Classification percentage | |
|---|---|---|---|
| | | Autist | Non-Autist |
| 3 | Flatten<br>BatchSize = 32<br>Epochs = 10<br>Loss = 'categorical_crossentropy'<br>Optimizer = Adam[LearningRate = .0001]<br>Width & Height shapes = 224<br>AdicionalLayers = Si | **74.97%** | **25.03%** |
| | | **24.08%** | **75.92%** |
| 16 | Flatten<br>BatchSize = 64<br>Epochs = 50<br>Loss = 'categorical_crossentropy'<br>Optimizer = Adam[LearningRate = .0001]<br>Width & Height shapes = 124<br>AdicionalLayers = Si | **95.24%** | **4.76%** |
| | | **38.44%** | **61.56%** |
| 23 | GlobalAverage<br>BatchSize = 32<br>Epochs = 5, 7 y 8<br>Loss = 'categorical_crossentropy'<br>Optimizer = Adam[LearningRate = .0001]<br>Width & Height shapes = 224<br>AdicionalLayers = No | **95.03%** | **4.97%** |
| | | **37.62%** | **62.38%** |

*Source: Own elaboration*

ISSN: 2410-3993.
RENIECYT: 1702902


Paredes-Xochihua, Maria Petra, Sánchez-Juárez, Ivan Rafael and Pedroza-Méndez, Blanca Estela. [2025]. Intelligent algorithm using convolutional neural networks for facial recognition of people with Autism Spectrum Disorder [ASD]. Journal of Technology and Innovation. 12[30]1-8: e31230108.
https://doi.org/10.35429/JTI.2025.12.30.3.1.8

According to the results represented in classification percentages shown in Table 2, the models for tests 16 and 23 are shaded, because of the 25 tests developed. The 2 models that obtained the best classification results, the model for test 16 presents 95.24% correct classification of people who DO have ASD and 61.56% of people classified as NOT having ASD correctly. For model 23, 95.03% correct classification of people who DO have ASD and 62.38% of people classified as NOT having ASD was obtained.

Based on the values in Table 2, it can be seen that the BatchSize in test 16 is greater than in test 23, thus consuming more processing time and resources. Regarding Epoch, test 16 is also greater than test 23, although it can be seen that the latter performs three phases in which some changes are also made.

## 6. Results with evaluation metrics

Figure 4 presents the evaluation metrics of time represented in seconds [s] for each step, accuracy and loss applied to all models, however, the results correspond to model 23. It can be seen that, when in phase 1 the time is lower, the accuracy has an average value and the loss exceeds the average.

For phase 2 the time increases, the accuracy value increases and the loss decreases, and the same behavior occurs in phase 3, which indicates that the model is learning, this given that the accuracy increases and the loss decreases. Figures 5, 6 and 7 present the accuracy and loss graphs for the 3 phases correspondingly.

Once the model training process is complete, it can be used to classify images of people. This can be done by individual images or by a set of images of people stored in a folder. To achieve this, a system named after the trained model was implemented, allowing it to predict the class to which the model belongs.

**Box 6**

```
Entrenando Fase 1 [Última capa]...
…
82/82 ━━━━━━━━━━━━━━━━━━━━━━━━━━━━━━━━━━━━ 242s 3s/step - accuracy: 0.5495 - loss: 0.7830 - val_accuracy: 0.6525 - val_loss: 0.6537
Epoch 4/5
82/82 ━━━━━━━━━━━━━━━━━━━━━━━━━━━━━━━━━━━━ 278s 3s/step - accuracy: 0.5701 - loss: 0.7597 - val_accuracy: 0.6454 - val_loss: 0.6436
Epoch 5/5
82/82 ━━━━━━━━━━━━━━━━━━━━━━━━━━━━━━━━━━━━ 271s 3s/step - accuracy: 0.5839 - loss: 0.7245 - val_accuracy: 0.6241 - val_loss: 0.6228

Entrenando Fase 2 [Últimas 2 capas]...
Epoch 1/7
82/82 ━━━━━━━━━━━━━━━━━━━━━━━━━━━━━━━━━━━━ 308s 4s/step - accuracy: 0.6015 - loss: 0.7255 - val_accuracy: 0.6809 - val_loss: 0.6524
Epoch 2/7
82/82 ━━━━━━━━━━━━━━━━━━━━━━━━━━━━━━━━━━━━ 256s 3s/step - accuracy: 0.6431 - loss: 0.6891 - val_accuracy: 0.6809 - val_loss: 0.6345
…
Epoch 7/7
82/82 ━━━━━━━━━━━━━━━━━━━━━━━━━━━━━━━━━━━━ 273s 3s/step - accuracy: 0.6522 - loss: 0.6529 - val_accuracy: 0.5816 - val_loss: 0.6578

Entrenando Fase 3 [Ajuste fino total]...
Epoch 1/8
82/82 ━━━━━━━━━━━━━━━━━━━━━━━━━━━━━━━━━━━━ 1170s 14s/step - accuracy: 0.6587 - loss: 0.6171 - val_accuracy: 0.6950 - val_loss: 0.5655

….
82/82 ━━━━━━━━━━━━━━━━━━━━━━━━━━━━━━━━━━━━ 1050s 13s/step - accuracy: 0.8633 - loss: 0.3213 -
val_accuracy: 0.6667 - val_loss: 0.7558
Epoch 8/8
82/82 ━━━━━━━━━━━━━━━━━━━━━━━━━━━━━━━━━━━━ 998s 12s/step - accuracy: 0.8902 - loss: 0.2823 - val_accuracy: 0.7234 - val_loss: 0.6638
Model: "functional"
```

**Figure 4**

Model training results.

*Source: Own elaboration*

ISSN: 2410-3993.
RENIECYT: 1702902


Paredes-Xochihua, Maria Petra, Sánchez-Juárez, Ivan Rafael and Pedroza-Méndez, Blanca Estela. [2025]. Intelligent algorithm using convolutional neural networks for facial recognition of people with Autism Spectrum Disorder [ASD]. Journal of Technology and Innovation. 12[30]1-8: e31230108.
https://doi.org/10.35429/JTI.2025.12.30.3.1.8

## Box 7

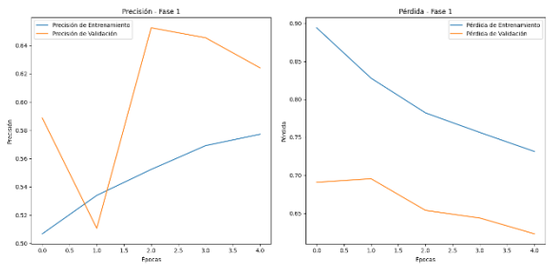


**Figure 5**

Phase 1 Chart.

*Source: Own elaboration*

## Box 8

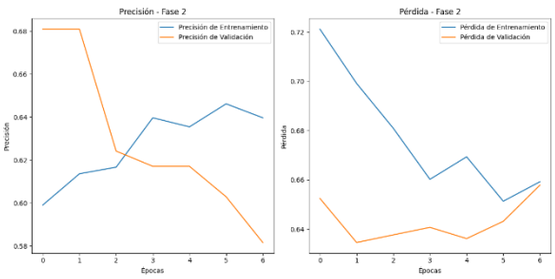


**Figure 6**

Phase 2 Chart.

*Source: Own elaboration*

## Box 9

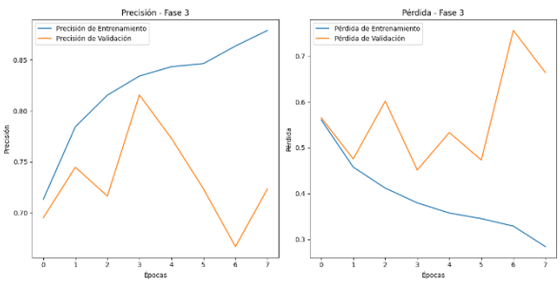


**Figure 7**

Phase 3 Chart.

*Source: Own elaboration*

## Conclusions

The facial recognition algorithm was developed and implemented using artificial vision techniques, in which the face in the image is detected and convolutional neural networks were used for detection, however, prior to using CNNs, transformations are performed on the images such as rotation, horizontal and vertical flipping, displacement, zooming, in order for the classification model to identify patterns regardless of how the person's face is presented.

The accuracy and specificity metrics were evaluated, yielding the results presented above. This improved on the results of other studies that used the Kaggle dataset, which, like the one used in this study, was used, except that in this study images of Mexican nationals were added. Therefore, it is believed that the algorithm detected and/or strengthened characteristic patterns exhibited by individuals with ASD.

Finally, ASD is a neurodevelopmental condition that manifests itself uniquely in each individual. However, it is important to emphasize that ASD is not associated with specific or distinctive facial characteristics that allow a person with this condition to be identified based solely on their physical appearance. ASD is diagnosed primarily through behaviors, communication patterns, and social skills, not facial features, as these are highly varied and therefore difficult to identify.

## Declarations

### Conflict of interest

The authors declare no conflicts of interest. They have no known competing financial interests or personal relationships that could have appeared to influence the article reported in this article.

### Authors' contribution

*Paredes-Xochihua, Maria Petra:* Contributed to the project idea, identification of techniques to be applied, development, elaboration, validation testing, and implementation, as well as the creation of the dataset of Mexican nationals.

*Sánchez-Juárez, Ivan Rafael*: Contributed to the creation of the dataset of Mexican nationals, the development of functional tests, and the evaluation of results.

*Pedroza-Méndez, Blanca Estela:* Contributed with input into the algorithm, techniques used in the development, evaluation and review of results.

### Acknowledgments

We would like to thank the National Institute of Technology of Mexico/ITS of San Martín Texmelucan, Da Vinci University, and the Apizaco Institute of Technology for all the support provided to carry out this research project.

ISSN: 2410-3993.
RENIECYT: 1702902


Paredes-Xochihua, Maria Petra, Sánchez-Juárez, Ivan Rafael and Pedroza-Méndez, Blanca Estela. [2025]. Intelligent algorithm using convolutional neural networks for facial recognition of people with Autism Spectrum Disorder [ASD]. Journal of Technology and Innovation. 12[30]1-8: e31230108.
https://doi.org/10.35429/JTI.2025.12.30.3.1.8

## Abbreviations

| | |
|---|---|
| APP | Software application designed to run on mobile devices |
| CNNs | Convolutional Neural Networks |
| fMRI | Functional Magnetic Resonance Imaging. |
| ITS | Instituto Tecnologico Superior |
| RGB | Red, Green, and Blue. RGB color model |
| TecNM | Tecnológico Nacional de México |
| ASD | Autism Spectrum Disorder |

## References

### Background

Ahmad, I., Rashid, J., Faheem, M., Akram, A., Khan, N., & Amin, R. [2024]. Autism spectrum disorder detection using facial images: A performance comparison of pretrained convolutional neural networks. Healthcare Technology Letters.

Autism dataset. [August 2024, 2024]. Autism_Image_Data. Retrieved from

Cadena, M. J. [2021]. An efficient technique for global face recognition using wavelets and support vector machines in 3D images. CADENA MOREANO J, General Directorate of Postgraduate Studies, Faculty of Systems Engineering and Computer Science, Postgraduate Unit. Retrieved from

Feng, M. y. [2023]. Detection of ASD Children through Deep-Learning Application of fMRI. [S. P. Salerno, Ed.] doi:10.3390/children10101654

ImageNet. [2020]. ImageNet. Retrieved from

Juárez Velázquez, E., Hernández Lara, D., & Trejo Villanueva, C. [2024]. Using machine vision to recommend professional profiles through facial and text recognition. Transdigital.

Teletón México. [2024]. Overview of Autism in Mexico and the World. Retrieved from

### Basics

Pineda, P. C. [2021]. Machine and Deep Learning in Python: A Look at Artificial Intelligence. U. Editions. ISBN 9587923154, 9789587923155. pp. 123-135.

ISSN: 2410-3993.
RENIECYT: 1702902


Paredes-Xochihua, Maria Petra, Sánchez-Juárez, Ivan Rafael and Pedroza-Méndez, Blanca Estela. [2025]. Intelligent algorithm using convolutional neural networks for facial recognition of people with Autism Spectrum Disorder [ASD]. Journal of Technology and Innovation. 12[30]1-8: e31230108.
https://doi.org/10.35429/JTI.2025.12.30.3.1.8

**Journal of Technology and Innovation** 12[30]1-6: e41230106
Article

# Design of an experimental reactor for the selective and efficient recovery of lithium from waste battery cathode leaching processes

# Diseño de un reactor experimental para la recuperación selectiva y eficiente del litio a partir de procesos de lixiviación de cátodos de baterías de desecho

Herrera-Gutiérrez, Hugo [a], Cisneros-Villalobos, Luis * [b], Torres-Islas, Álvaro [c] and Saldarriaga-Noreña, Hugo Albeiro [d]

[a] Universidad Autónoma del Estado de Morelos • OIR-8684-2025 • 0000-0002-4064-6688 • 955626
[b] Universidad Autónoma del Estado de Morelos • ABD-4724-2020 • 0000-0002-9409-1374 • 82259
[c] Universidad Autónoma del Estado de Morelos • OLP-8703-2025 • 0000-0001-7102-0138 • 200758
[d] Universidad Autónoma del Estado de Morelos • E-6038-2019 • 0000-0002-0676-0639 • 225261

**Classification:**

Area: Engineering
Field: Engineering
Discipline: Electronic Engineering
Subdiscipline: Design and systems

https://doi.org/10.35429/JTI.2025.12.30.4.1.6
**History of the article:**
Received: July 30, 2025
Accepted: October 30, 2025

* ✉ [luis.cisneros@uaem.mx]

**Abstract**

This paper presents the design of an experimental reactor based on hardware and software, which monitors the reaction parameters of leaching processes for the recovery of lithium from waste battery cathodes. The hardware consists of a 250 ml double-layer reaction bottle, a magnetic stirring controller, and an Arduino-based system for measuring the temperature and pH of the reaction. The measured data is fed into the software, where it is processed to determine reaction parameter profiles. The experimental reactor will fulfill its purpose by correlating the selective lithium recovery efficiency with the different reaction profiles carried out, which will allow the identification of key variables, the establishment of mathematical models that describe the behavior of the reaction, and the determination of the conditions that improve the efficiency of the process.

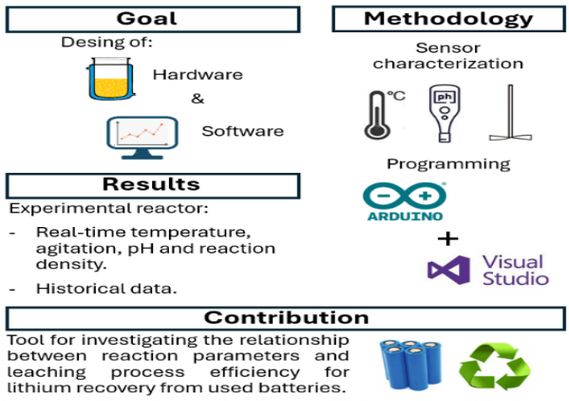


**Reactor, Leaching, Lithium, Efficiency, Hardware, Software**

**Resumen**

En este trabajo se expone el diseño de un reactor experimental basado en hardware y software, el cual monitorea los parámetros de reacción de procesos de lixiviación para la recuperación del litio a partir de cátodos de baterías de desecho. El hardware consiste en una botella de reacción de 250 ml de doble capa, un controlador de agitación magnética y un sistema basado en Arduino para la medición de temperatura y pH del medio en reacción. Los datos medidos son llevados al software, donde son procesados para determinar perfiles de parámetros de reacción. El reactor experimental cumplirá su propósito al relacionar la eficiencia de recuperación selectiva del litio con los distintos perfiles de reacción llevados a cabo, lo cual permitirá identificar las variables clave, establecer modelos matemáticos que describan el comportamiento de la reacción y determinar las condiciones que mejoran la eficiencia del proceso.

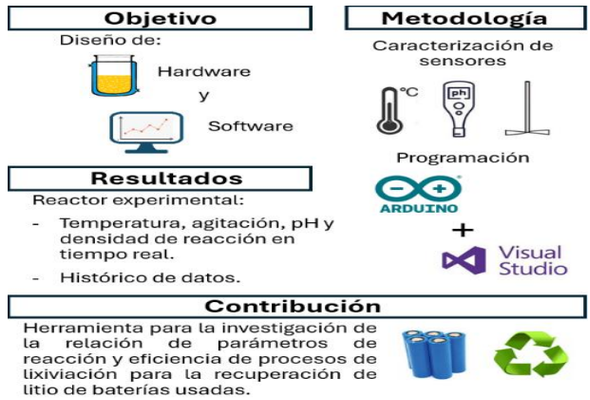


**Reactor, Lixiviación, Litio, Eficiencia, Hardware, Softwar**

**Area**: Development of strategic leading-edge technologies and open innovation for social transformation

**Citation:** Herrera-Gutiérrez, Hugo, Cisneros-Villalobos, Luis, Torres-Islas, Álvaro and Saldarriaga-Noreña, Hugo Albeiro. [2025]. Design of an experimental reactor for the selective and efficient recovery of lithium from waste battery cathode leaching processes. Journal of Technology and Innovation. 12[30]1-6: e41230106.

## Introduction

One of the greatest challenges facing the scientific community today in its various fields is approaching research from a sustainable development perspective [ONU, 2025], where essentially, the solution to a specific need does not compromise the ability to meet the potential needs of future generations [*Sostenibilidad, 2025*]. Globally, halting or even slowing climate change is one of the greatest needs of our time, and the energy transition is emerging as the most promising strategy for achieving this. However, in this context, significant global demand for lithium is expected [John D. Graham et al., 2021] as a key element in energy storage devices [P.E. Marín et al., 2021], with the environmental impact of meeting this demand solely through mining being evident.

A sustainable solution to the anticipated high demand for lithium is to recover this strategic mineral by recycling batteries that have reached the end of their useful life [Chunwei Liu et al., 2019; Min Yu et al., 2019; Jingbo Yang et al., 2021; Urias, P. M. et al., 2020; Fei Meng et al., 2020].

Recent research methods, such as leaching processes, have demonstrated high percentages of selective lithium recovery [Weiguang Lv et al., 2020]; however, testing has been limited mainly to modifying the initial experimental conditions and maintaining them throughout the test period [Qian Cheng et al., 2019], which excludes the possibility of evaluating the effects of variable conditions during the process on recovery efficiency.

This work promises to meet that expectation by monitoring leaching processes for selective lithium recovery in real time, evaluating efficiency under different experimental conditions.

## Methodology

The hardware is the central element where the leaching process for selective lithium recovery takes place, and is designed on the basis of a 250 ml double-layer reaction bottle. As can be seen in Figure 1, the double layer is useful for circulating a fluid at a controlled temperature without coming into direct contact with the reaction solution, transferring heat to it, while the opening necks allow the entry of temperature and pH sensors, as well as reagents.

## Box 1

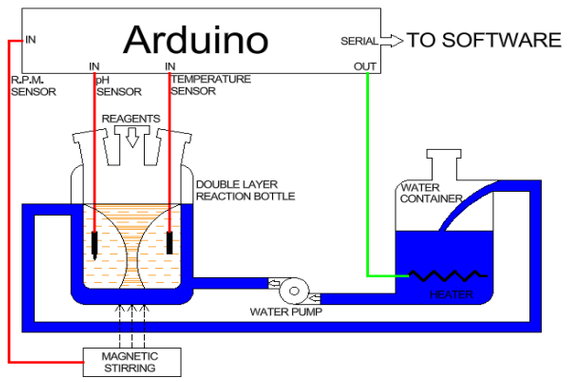


**Figure 1**

Schematic diagram of the hardware.

*Source: Own elaboration.*

A variable-speed magnetic stirring module has been designed to be placed under the reaction bottle. Temperature control and monitoring, as well as pH and stirring speed monitoring, are performed using an Arduino board.

The desired temperature is programmed into the Arduino code and measured using a sensor inserted through one of the opening necks of the reaction bottle, in direct contact with the solution. When the measured temperature is lower than the temperature programmed into the Arduino code, one of its outputs turns on the heater and turns off when the measured temperature is equal to the programmed temperature.

During the characterization of the temperature sensor, a commercial laser thermometer was used to perform the necessary calibration, as shown in Figure 2. The temperature is sent to the Arduino serial port within a character string, in the variable defined as “temp.”

## Box 2


**Figure 2**

Calibration of the temperature sensor.

ISSN: 2410-3993.
RENIECYT: 1702902


Herrera-Gutiérrez, Hugo, Cisneros-Villalobos, Luis, Torres-Islas, Álvaro and Saldarriaga-Noreña, Hugo Albeiro. [2025]. Design of an experimental reactor for the selective and efficient recovery of lithium from waste battery cathode leaching processes. Journal of Technology and Innovation. 12[30]1-6: e41230106
https://doi.org/10.35429/JTI.2025.12.30.4.1.6

The pH monitoring is carried out using a sensor inserted through another open neck of the reaction bottle, which was previously characterized using pH standards and test strips for proper signal processing within the Arduino code, as shown in Figure 3.

This parameter will be determined by the amount and concentration of the acidic and oxidizing agents introduced into the process, which must be done manually in this first version of the reactor. Once the corresponding pH value has been calculated, this signal is also sent to the serial port character string, in the variable defined as "pH.".

As for monitoring the agitation, the magnetic stirrer controller was previously characterized by measuring the speed as a function of the position of the control potentiometer, and the Arduino code calculates the revolutions per minute, which is also sent to the serial port character string, in the variable defined as "rpm."

In the Arduino code, the variable "status" has also been defined to be sent within the character string; this variable indicates the status of the heater and is used in the software to turn the corresponding indicator on and off.

## Box 3

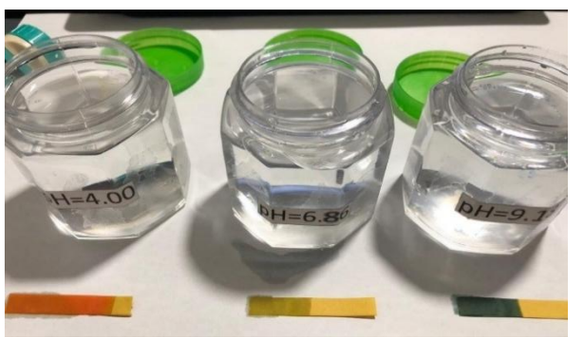


**Figure 3**

Standard solutions and reagent strips used during the characterization of the pH sensor.

*Source: Own elaboration.*

The software was developed in the Visual Studio C# programming environment, using the Windows Forms interface framework.

The objective of this development is to receive, graphically represent, and tabulate the information sent by Arduino through the serial port at a sampling frequency of 1 data string per second, as shown in Figure 4.

## Box 4

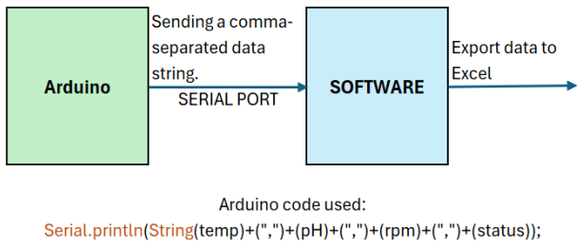


**Figure 4**

Serial communication between hardware and software.

The software separates the data from the received information string and processes it within the code for graphical representation and tabulation. The reaction time parameters and solution density are calculated within the software code.

## Results

Figure 5 shows the hardware assembly, where the reaction bottle has been secured to an aluminum support using a clamp. A black container with an internal heater adapted to it can also be seen. From this container, and through a pump, the fluid circulates through the outer layer of the reaction bottle at a programmed temperature.

The temperature and pH sensors are placed inside the inner layer of the bottle, and at the rear, a metal cabinet can be seen housing the Arduino board along with all the circuits necessary to power each hardware component.

## Box 5

**Figure 5**

Hardware assembly

ISSN: 2410-3993.
RENIECYT: 1702902


Herrera-Gutiérrez, Hugo, Cisneros-Villalobos, Luis, Torres-Islas, Álvaro and Saldarriaga-Noreña, Hugo Albeiro. [2025]. Design of an experimental reactor for the selective and efficient recovery of lithium from waste battery cathode leaching processes. Journal of Technology and Innovation. 12[30]1-6: e41230106
https://doi.org/10.35429/JTI.2025.12.30.4.1.6

Figure 6 shows the section of the software developed where the quantity and type of reagents added to the reaction bottle are entered, the main data being the quantity in grams of NMC cathode material to be leached.

The software allows for the registration of any addition of reagent that is desired to be made after the start of the test, indicating the corresponding amount and pressing the "Add" button for each action. In Figure 7, a graph of the data exported to Excel from a simulation is shown, where 15 grams of NMC Cathode material are added to 50 ml of deionized water 10 seconds after the process begins, showing how the calculated density changes from 0 g/l to 300 g/l; subsequently, when 5 grams of a solid reagent are added 10 seconds after the first action, the density is recalculated to 400 g/l; on the contrary, if liquid reagents are added, the density decreases, as observed in the graph in Figure 8, where the addition of 10 ml of a liquid reagent is simulated 31 seconds after the process starts.

## Box 6

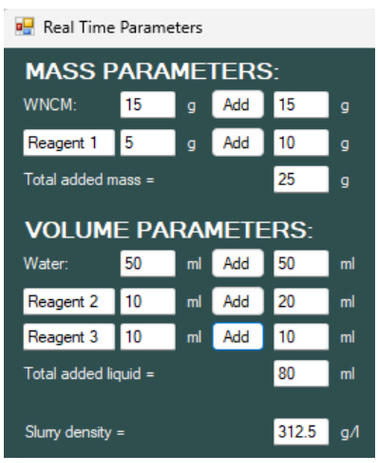


**Figure 6**

Reagent data section of the software.

## Box 7

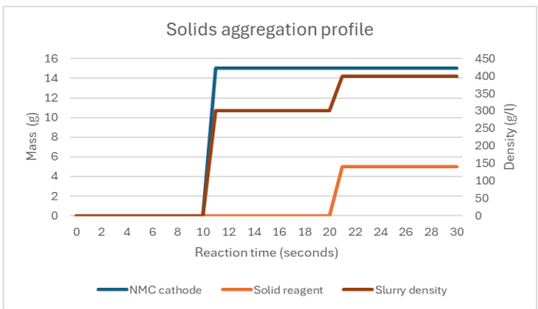


**Figure 7**

Graph of solid reactants aggregation profile.

## Box 8

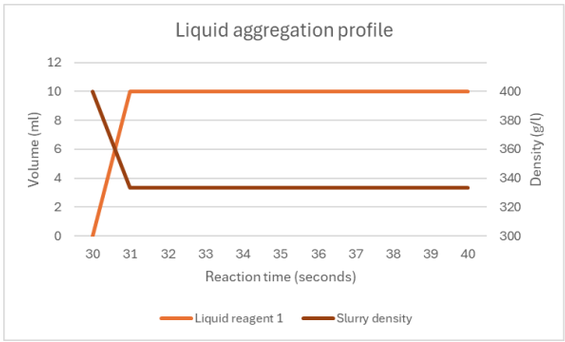


**Figure 8**

Profile graph of liquid reagent aggregation.

Finally, Figure 9 shows the complete software window, displaying the temperature and pH graphs throughout the reaction time, as well as the table with historical data for all parameters involved in the selective lithium leaching processes described in the literature

## Box 9


**Figure 9**

Software window of the experimental reactor

## Conclusions

This article presents the design, construction, and performance testing of an experimental reactor based on hardware and software, which promises to be a valuable tool for studying the efficiency of methods for recovering lithium from cathode materials in used batteries through leaching processes.

It was confirmed that the experimental reactor developed can monitor in real time each and every one of the parameters involved in the leaching processes described in the literature, allowing a future version to modify the experimental conditions with actuators that dose the reagents to control the pH and density of the solution, as well as vary the temperature and agitation with specific reaction profiles, etc.

ISSN: 2410-3993.
RENIECYT: 1702902


Herrera-Gutiérrez, Hugo, Cisneros-Villalobos, Luis, Torres-Islas, Álvaro and Saldarriaga-Noreña, Hugo Albeiro. [2025]. Design of an experimental reactor for the selective and efficient recovery of lithium from waste battery cathode leaching processes. Journal of Technology and Innovation. 12[30]1-6: e41230106
https://doi.org/10.35429/JTI.2025.12.30.4.1.6

This can be done after using the experimental reactor in its first phase of development to investigate the relationship between changes in experimental parameters during the process and lithium recovery efficiency, moving towards the development of a reactor that is intelligent in every sense of the word.

## Declaracions

### Conflict of interest

The authors declare no interest conflict. They have no known competing financial interests or personal relationships that could have appeared to influence the article reported in this article.

### Author contribution

*Herrera-Gutiérrez, Hugo*: Development of hardware and software, writing [review and editing].

*Cisneros-Villalobos, Luis*: Conceptualization, methodology, and supervision.

*Torres-Islas, Álvaro*: Formal analysis and research.

*Saldarriaga-Noreña, Hugo Albeiro*: Formal analysis and research.

### Availability of data and materials

The original contributions presented in this study are included in the article. For more information, please contact the corresponding author.

### Funding

This research did not receive any funding.

### Abbreviations

| | |
|---|---|
| ml | Milliliter |
| NMC | Nickel-Manganese-Cobalt |
| Ph | Hydrogen Potential |
| g | Gram |
| g/l | Gram per liter |

## References

### Basics

ONU. [2025]. Naciones Unidas. Paz, dignidad e igualdad en un planeta sano.

Sostenibilidad. [2025]. Pacto Mundial Red España.

### Antecedents

John D. Graham, John A. Rupp & Eva Brungard. [2021]. Lithium in the Green Energy Transition: The Quest for Both Sustainability and Security. *Sustainability*, *13[20]*.

P.E. Marín, Y. Milian, S. Ushak, L.F. Cabeza, M. Grágeda & G.S.F. Shire. [2021] Lithium compounds for thermochemical energy storage: A state-of-the-art review and future trends. *Renewable and Sustainable Energy Reviews*, *149*.

### Supports

Chunwei Liu, Jiao Lin, Hongbin Cao, Yi Zhang & Zhi Sun. [2019]. Recycling of spent lithium-ion batteries in view of lithium recovery: A critical review. *Journal of Cleaner Production*, *228*, 801-813.

Min Yu, Zehui Zhang, Feng Xue, Bin Yang, Guanghui Guo & Jianghua Qiu. [2019]. A more simple and efficient process for recovery of cobalt and lithium from spent lithium-ion batteries with citric acid. *Separation and Purification Technology*, *215*, 398-402.

Jingbo Yang, Ersha Fan, Jiao Lin, Faiza Arshad, Xiaodong Zhang, Hanyong Wang, Feng Wu, Renjie Chen & Li Li. [2021]. Recovery and Reuse of Anode Graphite from Spent Lithium-Ion Batteries via Citric Acid Leaching. *ACS Applied Energy Materials, 4[6]*.

Urias, P. M., dos Reis Menêzes, L. H., Cardoso, V. L., de Resende, M. M., & de Souza Ferreira, J. [2020]. Leaching with mixed organic acids and sulfuric acid to recover cobalt and lithium from lithium ion batteries. *Environmental Technology*, *42*[25], 4027–4037.

Fei Meng, Qingcai Liu, Rina Kim, Jingxiu Wang, Gui Liu & Ahmad Ghahreman. [2020]. Selective recovery of valuable metals from industrial waste lithium-ion batteries using citric acid under reductive conditions: Leaching optimization and kinetic analysis. *Hydrometallurgy*, *191*.

ISSN: 2410-3993.
RENIECYT: 1702902


Herrera-Gutiérrez, Hugo, Cisneros-Villalobos, Luis, Torres-Islas, Álvaro and Saldarriaga-Noreña, Hugo Albeiro. [2025]. Design of an experimental reactor for the selective and efficient recovery of lithium from waste battery cathode leaching processes. Journal of Technology and Innovation. 12[30]1-6: e41230106
https://doi.org/10.35429/JTI.2025.12.30.4.1.6

Weiguang Lv, Zhonghang Wang, Xiaohong Zheng, Hongbin Cao, Mingming He, Yi Zhang, Haijun Yu & Zhi Sun. [2020]. Selective Recovery of Lithium from Spent Lithium-Ion Batteries by Coupling Advanced Oxidation Processes and Chemical Leaching Processes. *ACS Sustainable Chemistry & Engineering*, *8[25]*.

Qian Cheng, William M. Chirdon, Meiduan Lin, Kuber Mishra & Xiaodong Zhou. [2019]. Characterization, modeling, and optimization of a single-step process for leaching metallic ions from $LiNi_{1/3}Co_{1/3}Mn_{1/3}O_2$ cathodes for the recycling of spent lithium-ion batteries. *Hydrometallurgy*, *185*, 1-11.

ISSN: 2410-3993.
RENIECYT: 1702902


Herrera-Gutiérrez, Hugo, Cisneros-Villalobos, Luis, Torres-Islas, Álvaro and Saldarriaga-Noreña, Hugo Albeiro. [2025]. Design of an experimental reactor for the selective and efficient recovery of lithium from waste battery cathode leaching processes. Journal of Technology and Innovation. 12[30]1-6: e41230106
https://doi.org/10.35429/JTI.2025.12.30.4.1.6

**Journal of Technology and Innovation** 12[30]1-8: e51230108
Article

# Drone-based Multi sensor System for Air Quality Monitoring

# Sistema multi sensor para el monitoreo de la calidad del aire utilizando un dron

Sánchez-Reyes, Javier Ángel* [a], Sánchez-Medel, Luis Humberto [b], Sánchez-Sosol, Silvia [c] and Piña-Martínez, Ana Laura [d]

[a] Tecnológico Nacional de México - Instituto Tecnológico Superior de Huatusco• LFT-5899-2024 0009-0009-8349-9313 • 1322490
[b] Tecnológico Nacional de México - Instituto Tecnológico Superior de Huatusco • KWU-8720-2024 • 0000-0002-6783-585X• 655387
[c] Tecnológico Nacional de México - Instituto Tecnológico Superior de Huatusco • 0000-0001-9028-2782• 999012
[d] Tecnológico Nacional de México - Instituto Tecnológico Superior de Huatusco• LTF-1541-2024• 0000-0003-4137-63068319 • 478063

**Classification:**

Area: Engineering
Field: Engineering
Discipline: Chemical engineering
Subdiscipline: Atmospheric pollution

https://doi.org/10.35429/JTI.2025.12.30.5.1.8
**History of the article:**
Received: September 07, 2025
Accepted: November 30, 2025

* ✉ [javier.angelsanrey@gmail.com]

**Abstract**

Air pollution represents a global environmental and health challenge. This study addresses the issue of air quality in the central area of Huatusco, Veracruz, through the implementation of a monitoring system based on low-cost sensors and the SparkFun platform. Strategic sampling points were selected based on population density and pollutant emission sources, using data from INEGI. The study focused on measuring criterion pollutants by conducting vertical soundings to obtain a detailed profile of their atmospheric concentration.

| Drone-based Multisensor System for Air Quality Monitoring | | |
|---|---|---|
| Objetives | Methodology | Contribution |
| Develop a multi-sensor intelligent system for remote air quality monitoring using a Drone. | 1) Determine the pollutants to be included in the study scope.<br>2) Identify the suitable microcontroller/sensors for the project's needs.<br>3) Acquire air quality measurements in designated áreas. | It will enable us to more effectively identify pollution sources, assess the effectiveness of mitigation measures, and make informed decisions to improve air quality and protect public health. |

**Drone monitoring, air quality, low-cost sensors.**

**Resumen**

La contaminación atmosférica representa un desafío ambiental y de salud a nivel global. En este trabajo, se aborda la problemática de la calidad del aire en la zona centro de Huatusco, Veracruz, mediante la implementación de un sistema de monitoreo con sensores de bajo costo y la plataforma SPARKFUN. Se seleccionaron puntos de muestreo estratégicos, considerando la densidad poblacional y las fuentes de emisión de contaminantes, a partir de información proporcionada por el INEGI. El estudio se enfocó en la medición de contaminantes criterio, realizando sondeos verticales para obtener un perfil detallado de su concentración en la atmósfera.

| Sistema multi sensor para el monitoreo de la calidad del aire utilizando un dron | | |
|---|---|---|
| Objetivos | Metodología | Contribución |
| Desarrollar un sistema inteligente multi sensor destinado al monitoreo remoto de la calidad del aire, empleando un dron. | 1) Determinar los contaminantes a incluir en el alcance del estudio.<br>2) Identificar el microcontrolador/sensores adecuados para las necesidades del proyecto.<br>3) Adquirir mediciones de calidad del aire en las áreas designadas. | Nos permitirá identificar de manera más efectiva las fuentes de contaminación, evaluar la eficacia de las medidas de mitigación y tomar decisiones informadas para mejorar la calidad del aire y proteger la salud pública. |

**Monitoreo con Drones, calidad del aire, sensores de bajo costo.**

**Area**: Development of strategic leading-edge technologies and open innovation for social transformation

**Citation:** Sánchez-Reyes, Javier Ángel, Sánchez-Medel, Luis Humberto, Sánchez-Sosol, Silvia and Piña-Martínez, Ana Laura. [2025]. Drone-based Multi sensor System for Air Quality Monitoring. Journal of Technology and Innovation. 12[30]1-8: e51230108.

## Introduction

Air pollution poses a serious threat to global health, causing millions of premature deaths and a substantial loss of healthy life years annually. Its health impact is comparable to that of other well-known risk factors, such as unhealthy diets and tobacco use. Indeed, atmospheric pollution has been identified as the leading environmental risk to human health globally [17].

In Mexico, the Secretariat of Environment and Natural Resources [SEMARNAT], through the National Institute of Ecology and Climate Change [INECC], established the National Air Monitoring Program [PNMA]. Furthermore, SEMARNAT issued an Official Mexican Standard [Norma Oficial Mexicana, NOM] that stipulates the minimum requirements for the establishment and operation of systems for air quality monitoring and atmospheric pollutant sampling [14].

Previous research includes a field experiment where air quality was measured using a drone [DR-TAPM] equipped with sensors for carbon monoxide [CO], ozone [O3], nitrogen dioxide [NO2], particulate matter [PM2.5 and PM10], and sulfur dioxide [SO2].

The measurements were conducted in a controlled open-burn scenario simulating typical pollution in agricultural areas. The experimental design involved varying the drone's altitude [5 and 10 meters] and distance from the emission source [1 to 20 meters] to capture the spatial variability of pollutants [8].

Another precedent in the country involved testing a UAV-based system across different sites in Mexico, selected based on their pollution levels and geographical features. The UAV collected data at various altitudes [10, 30, 50, and 100 meters] for periods ranging from 16 to 26 minutes, storing the data on a micro SD card and transmitting it in real-time via LoRaWAN and ThingSpeak networks [5].

On a regional level, studies in the cities of Xalapa and Veracruz have applied drones and sonars for vertical atmospheric sounding. These works describe the equipment, procedures, and analysis of vertical profiles for temperature, relative humidity, and wind.

Data were analyzed using graphical and statistical methods, compared to reference data, and the limitations of the techniques were evaluated [1].

The application of Unmanned Aerial Vehicles [UAVs] is rapidly expanding beyond established fields into specialized urban and environmental management tasks. Recent research highlights the versatility of these platforms in addressing complex challenges within Latin American contexts. For instance, studies in Mexico have explored the use of data-driven technologies like IoT and drone-based sensors to optimize resource management in critical sectors such as agriculture [13].

In Colombia, the viability of drones for urban logistics has been analyzed, identifying the key regulatory and social barriers to successful implementation [11]. Furthermore, the methodological frontier is being pushed by combining UAVs with advanced artificial intelligence. High-resolution projects have successfully used deep learning models to detect specific objects like floating plastic debris or to estimate agricultural yields, proving the superiority of this approach over satellite-based methods for detailed tasks [7].

Other developments have focused on creating autonomous drone systems for security and surveillance applications, such as tracking individuals in outdoor environments [2]. This growing body of work demonstrates a clear trend: the integration of customized sensor technology on drone platforms is a powerful and adaptable solution for a wide range of monitoring and operational challenges.

This paper presents the development of a low-cost air quality monitoring system for the central area of Huatusco, Veracruz. The study is structured as follows: first, the methodology is detailed, including the identification of the criterion pollutants of interest, the selection and acquisition of specific sensors, and the choice of an unmanned aerial vehicle [UAV] as the measurement platform. Subsequently, the numerical results from monitoring these pollutants at strategic sampling points are presented.

Finally, the implications of these findings are discussed, and conclusions are drawn regarding the feasibility of the implemented system.

ISSN: 2410-3993
RENIECYT: 1702902


Sánchez-Reyes, Javier Ángel, Sánchez-Medel, Luis Humberto, Sánchez-Sosol, Silvia and Piña-Martínez, Ana Laura. [2025]. Drone-based Multi sensor System for Air Quality Monitoring. Journal of Technology and Innovation. 12[30]1-8: e51230108.
https://doi.org/10.35429/JTI.2025.12.30.5.1.8

## Methodology

### 1.1 Identification of Pollutants of Interest

Numerous studies have been conducted in diverse settings, including schools [16], urban environments such as parks [3] and city centers [15], suburban and rural areas [18], and locations known for high pollutant concentrations, such as landfills [12], wastewater treatment plants [4], and coal-fired power plants [6]. The primary variables of interest in these investigations included particulate matter, ozone, carbon dioxide, and atmospheric variables. In Mexico, the National Air Quality Information System [SINAICA] identifies six criterion pollutants for measuring air quality: particulate matter [PM10 and PM2.5], Ozone [O3], Sulfur Dioxide [SO2], Nitrogen Dioxide [NO2], Carbon Monoxide [CO], and Lead [Pb]. Based on the objectives of this project, this study focuses on particulate matter PM10 and PM2.5, and the pollutant gases O3, SO2, NO2, and CO.

Furthermore, meteorological variables specifically pressure, temperature, and humidity were also included, as they can significantly influence the distribution and characterization of these pollutants.

Table 1 details the key characteristics of each target pollutant as defined by the official standard NOM-172-SEMARNAT-2019. This includes the permissible limit values concentrations that do not pose a health risk their corresponding measurement unit, and the specific guidelines within the standard that establish these limits.

### 1.2 Sensor Selection and Acquisition

**Box 1**

**Table 1**

Specifications for Criteria Pollutants

| Pollutant | Average concentration | Limit value | NOM |
|---|---|---|---|
| PM10 | 24 hrs | 70 µg/m3 | NOM-025-SSA1-2021 |
| PM 2.5 | 24 hrs | 41 µg/m3 | NOM-025-SSA1-2021 |
| O3 | 1 hrs | 0.09 PPM | NOM-020-SSA1-2022 |
| NO2 | 1 hrs | 0.106 PPM | NOM-023-SSA1-2023 |
| CO | 8 hrs | 9 PPM | NOM-021-SSA1-2024 |
| SO2 | 24 hrs | 0.11 PPM | NOM-022-SSA1-2025 |

*Source: sinaica.inecc.gob.mx/scica/#*

A review of the literature identified sensors with operational principles similar to those employed in this study. Among the examples found, some sensors [e.g., SPS30, SEN0470] are factory-calibrated, whereas for others [e.g., MQ131, MICS 6814], calibration procedures are specified in their respective datasheets. The selection of all sensors was guided by the pollutant specifications detailed in Table 1.

The sensors selected for this study are presented in Table 2.

**Box 2**

**Table 2**

Selected Sensors for the Study and Their Characteristics.

| Sensor Name | Parameter | Resolution |
|---|---|---|
| SPS30 | PM 2.5 y PM 10 | 1 µg/m$^3$, 2,5 µg/m$^3$, 4 µg/m$^3$ y 10 µg/m$^3$. |
| SEN0470 | SO2 | 0.1 PPM |
| MICS 6814 | CO | 1 PPM |
| | NO2 | 0.1 PPM |
| MQ131 | O3 | 10 PPB |

The microcontroller used to process the signals from each sensor is the SparkFun IoT RedBoard development board. The components that constitute the multi sensor module are shown in Figure 1.

**Box 3**

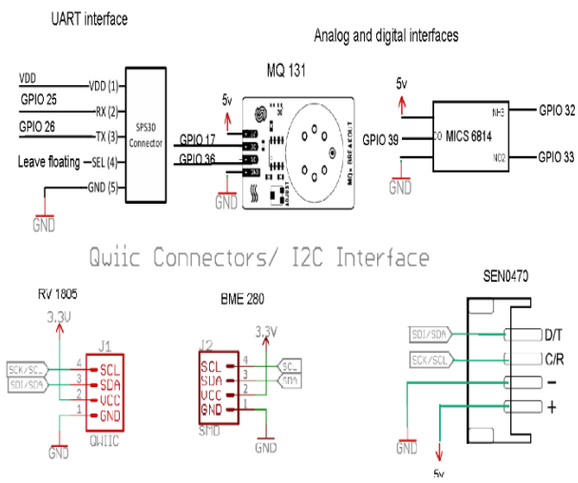


**Figure 1**

Design of the multi-sensor module for retrieving criteria pollutant parameters.

.

ISSN: 2410-3993
RENIECYT: 1702902


Sánchez-Reyes, Javier Ángel, Sánchez-Medel, Luis Humberto, Sánchez-Sosol, Silvia and Piña-Martínez, Ana Laura. [2025]. Drone-based Multi sensor System for Air Quality Monitoring. Journal of Technology and Innovation. 12[30]1-8: e51230108.
https://doi.org/10.35429/JTI.2025.12.30.5.1.8

1.3 Drone Selection and Acquisition

The selection of a suitable drone platform for this project was based on fundamental technical criteria: sufficient payload capacity to accommodate the developed multi sensor system, adequate flight autonomy for the planned sampling missions, structural robustness, reliable control and navigation systems, and modularity to facilitate integration and future adaptations [10]. Based on these criteria, the Holybro X650 development kit was selected. The most significant features of the drone are summarized in Table 3.

**Box 4**

**Table 3**

Notable Features of the X650 Kit.

| Feature | Description/Specification |
|---|---|
| Frame Material | High-quality carbon fiber, articulated arms with aluminum connectors, and reinforced landing gear. |
| Payload | Up to 3.1 KG [with 10,000 mAh battery]. |
| Sistema de control y navegación | Controladora de vuelo PIXHAWK 6X, GPS M10, telemetría radio SIK Plug & Play |
| Advantage | Simplifies the integration of custom payloads, streamlines setup and maintenance. |

*Source: holybro.com/collections/x650 kits/products/x650-development-kit?variant=43004805447869*

The methodological framework adopted in this study, which integrates a custom-built sensor module with a low-cost UAV platform for remote monitoring, aligns with a proven architectural approach for specialized urban applications. A similar configuration, employing an ESP32-based sensor module with Wi-Fi data transmission mounted on a drone, was successfully implemented for the detection of inactive aerial cabling in an urban setting [9].

This precedent validates the technical feasibility of our chosen components for infrastructure inspection. Furthermore, the core principle of using drone-mounted systems to detect and quantify specific environmental targets is well-established.

For example, the work in [7] effectively used a YOLO-based AI model to identify and classify different types of physical objects [plastic debris] from UAV imagery, demonstrating the robustness of this general methodology for environmental characterization.

**Results**

The study area was defined by three zones in the city center of Huatusco: Ignacio Zaragoza Park [19°09'00.5"N, 96°57'38.1"W], the Emiliano Zapata Esplanade [19°08'48.8"N, 96°58'04.0"W], and Agustín Chicuéllar Alameda [19°09'08.5"N, 96°58'23.5"W], as shown in Figure 2.

**Box 5**

**Figure 2**

Designated Study Areas

Data collection began on April 11, continued from April 14 to 18, and concluded during the week of April 22 to 25. For particulate matter [PM2.5], the average concentrations measured were 34.29 µg/m³ at the park, 32.26 µg/m³ at the Emiliano Zapata Esplanade, and 34.69 µg/m³ at the Agustín Chicuéllar Alameda. Figure 3 illustrates the temporal behavior of these concentrations and shows their proximity to the permissible limits established by the standard NOM-025-SSA1-2021.

**Box 6**

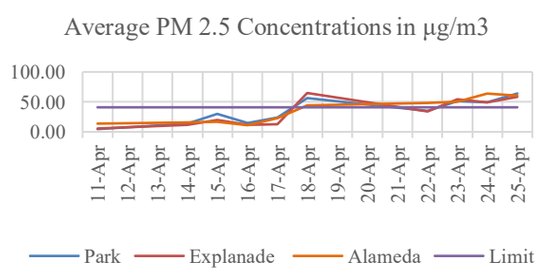


**Figure 3**

Distribution of PM 2.5 particulate matter with respect to the limit established in NOM-025-SSA1-2021

ISSN: 2410-3993
RENIECYT: 1702902


Sánchez-Reyes, Javier Ángel, Sánchez-Medel, Luis Humberto, Sánchez-Sosol, Silvia and Piña-Martínez, Ana Laura. [2025]. Drone-based Multi sensor System for Air Quality Monitoring. Journal of Technology and Innovation. 12[30]1-8: e51230108.
https://doi.org/10.35429/JTI.2025.12.30.5.1.8

For particulate matter PM10, the weekly average concentrations recorded were 34.95 µg/m³ at the park, 32.21 µg/m³ at the Esplanade, and 35.33 µg/m³ at the Alameda. Although the distribution of PM10 was similar to that of PM2.5, the concentrations for this pollutant did not exceed the limit established by the standard. The distribution of PM10 throughout the study days is presented in Figure 4.

**Box 7**

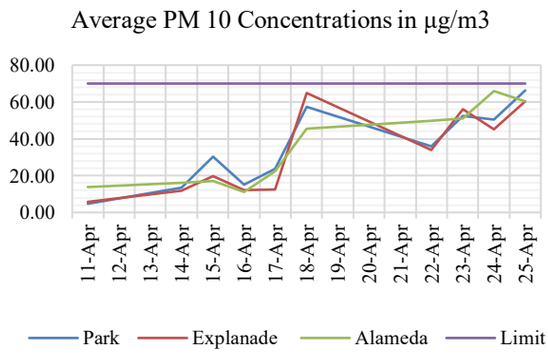


**Figure 4**

Distribution of PM 10 particulate matter with respect to the limits established in NOM-025-SSA1-2021. .

Regarding the pollutant parameters for Ozone [O3], Nitrogen Dioxide [NO2], Carbon Monoxide [CO], and Sulfur Dioxide [SO2], no significant variations were observed during the entire week of measurements. This could be attributed to two potential factors: either the pollution levels in the monitored areas were not substantially high, or the pollutant concentrations were below the minimum detection limit of the sensors, as illustrated in Figure 5.

**Box 8**

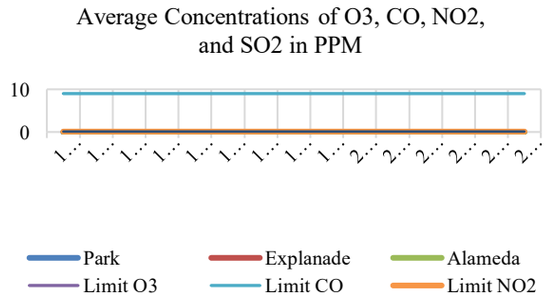


**Figure 5**

Distribution of Ozone, Carbon Monoxide, Nitrogen Dioxide, and Sulfur Dioxide with respect to the limits established in NOM-020-SSA1-2022, NOM-021-SSA1-2024, NOM-023-SSA1-2023, and NOM-022-SSA1-2025, respectively.

The average meteorological variables recorded during the study were as follows. For relative humidity, the values were 53.95% at the park, 46.89% at the Esplanade, and 47.20% at the Alameda. The atmospheric pressure averaged 876.48 hPa at the park, 875.85 hPa at the Esplanade, and 871.88 hPa at the Alameda.

**Box 9**

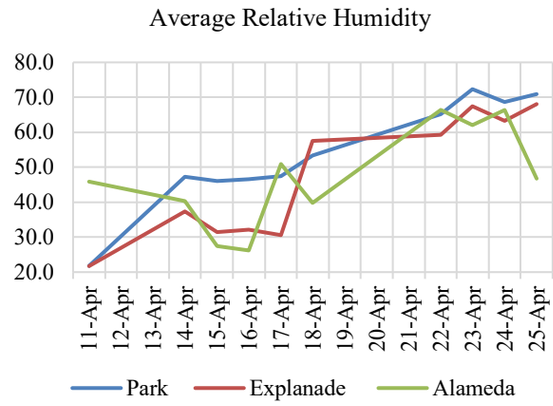


**Figure 6**

Distribution of relative humidity during the study in the areas of interest.

Finally, the average temperatures were 21.74 °C at the park, 24.64 °C at the Esplanade, and 26.58 °C at the Alameda.

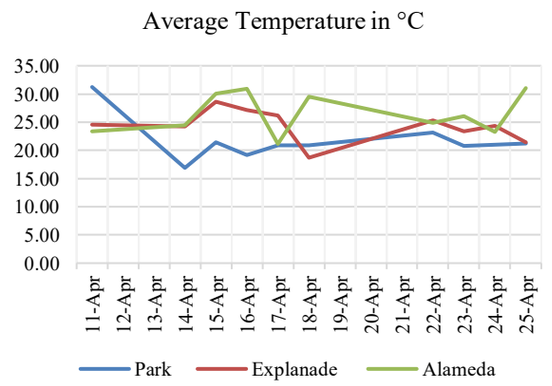


**Figure 7**

Changes in temperature recorded through the collection of air quality parameters.
*Source: Own elaboration.*

## Conclusions

Based on the analysis of the data collected between April 11 and 25 at the Park, Esplanade, and Alameda locations, the following conclusions are drawn:

ISSN: 2410-3993
RENIECYT: 1702902


Sánchez-Reyes, Javier Ángel, Sánchez-Medel, Luis Humberto, Sánchez-Sosol, Silvia and Piña-Martínez, Ana Laura. [2025]. Drone-based Multi sensor System for Air Quality Monitoring. Journal of Technology and Innovation. 12[30]1-8: e51230108.
https://doi.org/10.35429/JTI.2025.12.30.5.1.8

PM2.5 Concentrations: Daily and inter-site variations were observed in the average PM2.5 concentrations. Exceedances of the regulatory limit of 41 µg/m³ were recorded at all three locations on several days: specifically, on April 18, 23, 24, and 25 at the Park and Esplanade, and on April 18, 22, 23, 24, and 25 at the Alameda. The highest values were concentrated towards the end of the monitoring period.

PM10 Concentrations: Average daily PM10 concentrations remained below the established limit of 70 µg/m³ across all measurements taken during the study period. Although no exceedances occurred, a trend towards higher values was observed during the final days of the period [April 22-25].

Gas Concentrations [O3, CO, NO2, SO2]: The data indicate that the average daily concentrations for Ozone [O3], Carbon Monoxide [CO], Nitrogen Dioxide [NO2], and Sulfur Dioxide [SO2] were 0 ppm at all three locations throughout the evaluation period. Consequently, these values remained well below their respective regulatory limits [90 ppm for O3, 9 ppm for CO, 0.106 ppm for NO2, and 0.11 ppm for SO2].

Relative Humidity [RH%]: The Park station consistently recorded the highest RH% values, while the Alameda station generally showed the lowest values.

Atmospheric Pressure [hPa]: A consistent pattern was observed: The Park station recorded the highest-pressure values, followed by the Esplanade, and finally the Alameda with the lowest values.

Temperature [°C]: The Alameda station tended to record the highest average temperatures, while the Park station consistently recorded the lowest among the three locations.

While the results confirm the technical feasibility of our prototype, its transition from a controlled experiment to a large-scale urban deployment requires consideration of broader challenges. The work on drone logistics in Colombia highlights that the primary hurdles for urban UAV adoption are often not technological, but regulatory and social, including public concerns over privacy, noise, and safety [12].

A successful implementation of our air quality system would therefore necessitate a clear operational framework that addresses these issues. Furthermore, the accuracy of any sensor-based system is highly dependent on its calibration within the specific operational context. This is underscored by the findings in [2], which demonstrated that a state-of-the-art object detection model required retraining with simulation-specific data to perform effectively, proving that general models often fail in specialized environments.

This suggests that future work on our system should include rigorous field calibration to account for the unique atmospheric and pollutant characteristics of Huatusco. Finally, the emphasis on developing a low-cost solution aligns with the challenges of technological adoption in Mexico, where economic barriers can hinder the implementation of high-cost systems, as noted in studies of the agricultural sector [13].

## Declarations

### Conflict of interest

The authors declare no interest conflict. They have no known competing financial interests or personal relationships that could have appeared to influence the article reported in this article.

### Author contribution

*Sánchez-Reyes, Javier Ángel*: Conceptualization, Methodology, Software, Validation, Formal Analysis, Investigation, Data Curation, Writing – Original Draft, Writing – Review & Editing, Visualization, Project Administration.

*Sánchez-Medel, Luis Humberto*: Conceptualization, Methodology, Resources, Data Analysis, Supervision, Writing – Review & Editing.

*Sánchez-Sosol, Silvia*: Investigation, Formal Analysis, Writing – Review & Editing.

*Piña-Martínez, Ana Laura*: Methodology, Investigation, Visualization.

### Availability of data and materials

The datasets generated during and/or analyzed during the current study are available from the corresponding author on reasonable request.

ISSN: 2410-3993
RENIECYT: 1702902


Sánchez-Reyes, Javier Ángel, Sánchez-Medel, Luis Humberto, Sánchez-Sosol, Silvia and Piña-Martínez, Ana Laura. [2025]. Drone-based Multi sensor System for Air Quality Monitoring. Journal of Technology and Innovation. 12[30]1-8: e51230108.
https://doi.org/10.35429/JTI.2025.12.30.5.1.8

**Funding**

This research was supported by the Consejo Nacional de Humanidades, Ciencias y Tecnologías [CONAHCYT] through the master's scholarship granted to the first author [1322490].

**Acknowledgements**

To the Higher Technological Institute of Huatusco and its Research and Postgraduate Subdirectorate.

**Abbreviations**

AI: Artificial Intelligence
CO: Carbon Monoxide
CONAHCYT: National Council of Humanities, Sciences and Technologies [Consejo Nacional de Humanidades, Ciencias y Tecnologías]
hPa: Hectopascal
INECC: National Institute of Ecology and Climate Change [Instituto Nacional de Ecología y Cambio Climático]
INEGI: National Institute of Statistics and Geography [Instituto Nacional de Estadística y Geografía]
IoT: Internet of Things
NOM: Official Mexican Standard [Norma Oficial Mexicana]
NO2: Nitrogen Dioxide
O3: Ozone
Pb: Lead [Plomo]
PM: Particulate Matter
PM2.5: Particulate Matter with a diameter of 2.5 micrometers or less
PM10: Particulate Matter with a diameter of 10 micrometers or less
PNMA: National Air Monitoring Program [Programa Nacional de Monitoreo Atmosférico]
RH: Relative Humidity
SEMARNAT: Secretariat of Environment and Natural Resources [Secretaría de Medio Ambiente y Recursos Naturales]
SINAICA: National Air Quality Information System [Sistema Nacional de Información de la Calidad del Aire]
SO2: Sulfur Dioxide
UAV: Unmanned Aerial Vehicle
WHO: World Health Organization
YOLO: You Only Look Once

**References**

**Basic**

Álvarez-Pérez, J. A., Quiroz-Amoroso, N., & Tejeda-Martínez, A. [2023]. Algunas técnicas de sondeo vertical de la atmósfera urbana [Some vertical sounding techniques for the urban atmosphere]. *Geos*, 42[2], 1-15.

Alonso Rodríguez, A. [2025]. *Utilización de drones para detección y seguimiento de personas y objetos en entornos de exteriores* [Use of drones for detection and tracking of people and objects in outdoor environments].

Baglioli, F., & Godoi, R. H. M. [2023]. Sniffing Drones: A Promising Solution for Measuring Railroad Emissions in Urban Environments. *Atmosphere*, 14[5], 865.

Burgués, J., Esclapez, M. D., Doñate, S., Pastor, L., & Marco, S. [2021]. Aerial Mapping of Odorous Gases in a Wastewater Treatment Plant Using a Small Drone. *Remote Sensing*, 13[9], 1757.

Camarillo Escobedo, R., Flores, J. L., Marín Montoya, P., García Torales, G., & Camarillo Escobedo, J. M. [2022]. Smart multi-sensor system for remote air quality monitoring using unmanned aerial vehicle and LoRaWAN. *Sensors*, 22[5], 1706.

Chen, Y., Wang, J., Chang, C., Chuang, M., Chou, C. C., Pan, X., Ho, Y., Ou-Yang, C., Liu, W., & Chang, C. [2023]. Using drone soundings to study the impacts and compositions of plumes from a gigantic coal-fired power plant. *The Science of The Total Environment*, 893, 164709.

Codes Alcaraz, A. M. [2025]. *Teledetección con vehículos aéreos no tripulados y técnicas de aprendizaje profundo para la gestión agrícola. Aplicación a dos casos de estudio en la provincia de Alicante* [Remote sensing with unmanned aerial vehicles and deep learning techniques for agricultural management. Application to two case studies in the province of Alicante].

Duangsuwan, S., Prapruetdee, P., Subongkod, M., & Klubsuwan, K. [2022]. 3D AQI mapping data assessment of low-altitude drone real-time air pollution monitoring. *Drones*, 6[8], 191.

García Fernández, E. D., & Guerra Zevallos, D.

ISSN: 2410-3993
RENIECYT: 1702902

S. [2025]. *Implementación de un sensor remoto de campo electromagnético con tecnología Wi-Fi...* [Implementation of a remote electromagnetic field sensor with Wi-Fi technology...].

Jońca, J., Pawnuk, M., Bezyk, Y., Arsen, A., & Sówka, I. [2022]. Drone-Assisted Monitoring of Atmospheric Pollution—A Comprehensive Review. *Sustainability*, 14[18], 11516.

Navarro Zúñiga, W. R., Hidalgo Urrea, J. E., & Candil Parra, L. M. [2025]. *Propuesta para la implementación de drones en las entregas de última milla en áreas urbanas de Colombia* [Proposal for the implementation of drones in last-mile deliveries in urban areas of Colombia].

Olaguer, E., Jeltema, S., Gauthier, T., et al. [2022]. Landfill Emissions of Methane Inferred from Unmanned Aerial Vehicle and Mobile Ground Measurements. *Atmosphere*, 13[6], 983.

Ortiz, S. Y. C., Cabrera, J. C. F., Castillo, M. Á. A., Pichardo, C. D. C., & Castillo, A. Á. A. [2025]. Optimización del sector agrícola mediante el análisis de datos para una gestión eficiente de los recursos naturales: Una perspectiva para México [Optimization of the agricultural sector through data analysis for efficient resource management: A perspective for Mexico]. *Ciencia Latina: Revista Multidisciplinar*, 9[2], 241-257.

SEMARNAT. [2020]. *Monitoreo y evaluación de la Calidad del Aire* [Monitoring and Evaluation of Air Quality].

Simo, A., Dzitac, S., Dzitac, I., Frigura-Iliasa, M., & Frigura-Iliasa, F. M. [2021]. Air quality assessment system based on self-driven drone and LoRaWAN network. *Computer Communications*, 175, 13-24.

Thalman, R. [2024]. Development and Testing of a Rocket-Based Sensor for Atmospheric Sensing Using an Unmanned Aerial System. *Sensors*, 24[6], 1768.

World Health Organization. [2021]. *Global air quality guidelines: particulate matter* [PM2.5 and PM10], ozone, nitrogen dioxide, sulfur dioxide and carbon monoxide.

Zhao, T., Yang, D., Liu, Y., et al. [2022]. Development of an Integrated Lightweight Multi-Rotor UAV Payload for Atmospheric Carbon Dioxide Mole Fraction Measurements. *Atmosphere*, 13[6], 855.

ISSN: 2410-3993
RENIECYT: 1702902


Sánchez-Reyes, Javier Ángel, Sánchez-Medel, Luis Humberto, Sánchez-Sosol, Silvia and Piña-Martínez, Ana Laura. [2025]. Drone-based Multi sensor System for Air Quality Monitoring. Journal of Technology and Innovation. 12[30]1-8: e51230108.
https://doi.org/10.35429/JTI.2025.12.30.5.1.8

**Journal of Technology and Innovation** 12[30]1-5: e61230105
Article

# Analysis and methodological design for the implementation of a home electrical energy loss detection system

# Análisis y diseño metodológico para la implementación de un sistema de detección de pérdidas de energía eléctrica en el hogar

Duran-Belman, Israel * [a], García-Guzmán, José Miguel [b], Perez, Gerardo Daniel [c] and Gallardo-Alvarez, Dennise Ivonne [d]

[a] Tecnológico Nacional de México/ITS de Irapuato • V-7806-2019 • 0000-0002-1394-0486 • 691483
[b] Tecnológico Nacional de México/ITS de Irapuato• NQE-8170-2025 • 0000-0003-4904-6213 • 470152
[c] Tecnológico Nacional de México/ITS de Irapuato• NQE-7292-2025 • 0009-0007-5168-8123 • 869877
[d] Tecnológico Nacional de México/ITS de Irapuato• S-4921-2018• 0000-0002-9197-6425• 691690

**Classification:**
Area: Engineering
Field: Telematics and Intelligent Networks
Discipline: Information and Control Systems
Sub-discipline: Internet of Things [IoT] for home energy monitoring

https://doi.org/10.35429/JTI.2025.12.30.6.1.5
**History of the article:**
Received: September 09, 2025
Accepted: November 30, 2025

* ✉ [Israel.db@irapuato.tecnm.mx]

**Abstract**

The project "Home Energy Loss Monitoring and Detection System [SMDPED]" aims to document the technical and structural planning required for its future implementation. This work outlines the organized structure of activities necessary to initiate the development of the energy monitoring project. Five key components were defined: needs analysis, conceptual design, component selection, functional integration, and preliminary validation. Each was designed to ensure consistency between the stated objectives and the technological decisions made, prioritizing accessibility, low cost, and practical application in residential settings. The selection of tools such as the ESP32 microcontroller, electrical sensors, SQL Server databases, and a platform built in ASP.NET Core MVC was based on compatibility, scalability, and simplicity. This article demonstrates that a well-structured planning process is essential to transform a technical need into a functional, replicable solution aligned with the current challenges of energy efficiency in the home.

**Resumen**

El proyecto “Sistema de Monitoreo y Detección de Pérdidas Energéticas Domésticas [SMDPED]” tiene como objetivo principal documentar la planificación técnica y estructural necesaria para lograr su implementación. Este trabajo describe la estructura organizada de actividades necesarias para dar inicio al desarrollo del proyecto de monitoreo energético. Se definieron cinco etapas: análisis de necesidades, diseño conceptual, selección de componentes, integración funcional y validación preliminar. Cada una fue diseñada para asegurar coherencia entre los objetivos planteados y las decisiones tecnológicas adoptadas, priorizando accesibilidad, bajo costo y aplicación práctica en entornos residenciales. La elección de herramientas como el microcontrolador ESP32, sensores eléctricos, bases de datos SQL Server y una plataforma en ASP.NET Core MVC responde a criterios de compatibilidad, escalabilidad y simplicidad. Este artículo demuestra que una planeación bien estructurada es clave para convertir una necesidad técnica en una solución funcional, replicable y alineada con los retos actuales de eficiencia energética en el hogar.

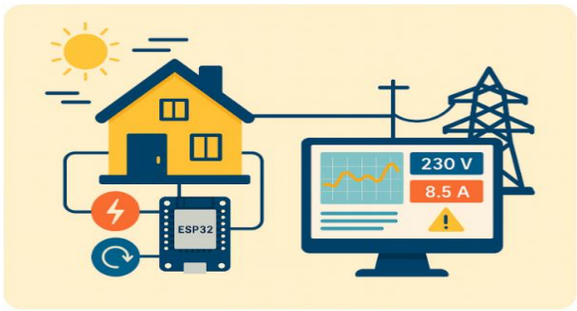


**Home energy monitoring, Energy efficiency, ESP32 microcontroller, SQL Server, ASP.NET Core MVC, System planning**

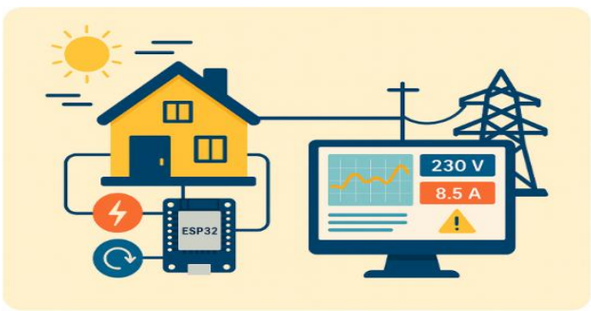


**Monitoreo energético doméstico, Eficiencia energética, Microcontrolador ESP32, SQL Server, ASP.NET Core MVC, Planificación de sistemas.**

**Area**: Development of strategic leading-edge technologies and open innovation for social transformation

**Citation:** Duran-Belman, Israel, García-Guzmán, José Miguel, Perez, Gerardo Daniel and Gallardo-Alvarez, Dennise Ivonne. [2025]. Analysis and methodological design for the implementation of a home electrical energy loss detection system. Journal of Technology and Innovation. 12[30]1-5: e61230105.

## Introduction

The constant increase in residential electricity consumption and the lack of awareness about efficient energy use have created a need to develop accessible solutions that enable families to identify and correct energy losses in their homes. Often, energy waste is not obvious to users, whether due to installation faults, equipment in poor condition, or inefficient habits. In this context, the project called the Domestic Energy Loss Monitoring and Detection System [SMDPED] has emerged as a proposal to lay the foundations for a technological solution that facilitates the identification of these situations.

In recent years, households have become one of the main sources of energy consumption worldwide. According to data from the International Energy Agency [IEA], the residential sector accounts for about 30% of total final energy consumption, with electricity being one of the main resources used for lighting, air conditioning, appliances, and electronic systems. This trend has increased due to population growth, the rise in the number of connected devices, and changes in consumption habits, especially following the rise of working and studying from home.

Historically, the management of electricity consumption in the home has been passive, limited to the periodic payment of bills and, at best, the use of low-consumption appliances. However, advances in technology, especially the development of microcontrollers, smart sensors and web interfaces, have opened up the possibility of creating active solutions that measure consumption in real time, detect anomalies and present understandable information to the end user. This digital transformation in the home has given rise to new approaches that not only save money but also raise awareness about the rational use of energy. The transition to more efficient technologies is not only a technical necessity but also an environmental goal. Energy waste has a direct impact on the increase in greenhouse gas emissions, especially in countries where the energy matrix depends on fossil fuels. From this perspective, every initiative that contributes to improving energy use in the home becomes a significant action within the framework of the Sustainable Development Goals [SDGs], particularly SDG 7 [affordable and clean energy] and SDG 13 [climate action].

This article does not address the physical construction of the system or experimental testing, but focuses exclusively on the technical planning, methodological structuring and selection of technological tools necessary for its future implementation. Documenting this initial phase ensures that decisions are based on criteria of feasibility, functionality and accessibility, establishing a solid framework that minimises risks in the following stages.

To this end, five key stages were defined: needs analysis, conceptual design, component selection, functional integration, and preliminary validation. These phases allow the work to be organised, facilitate decision-making, and ensure that the project is aligned with its central purpose: to build a functional, replicable, and useful tool to promote energy savings in domestic environments.

The choice of technologies such as the ESP32 microcontroller, voltage and current sensors, SQL Server databases and an ASP.NET Core MVC visualisation platform responds to a strategy that prioritises low cost, compatibility and ease of use. These decisions are aimed at facilitating its future implementation in real homes, without requiring advanced technical knowledge or large investments, enabling its application as an educational tool, for family monitoring or institutional support.

In summary, this article presents a methodological approach that seeks to lay the foundations for the development of a technological solution focused on domestic energy monitoring. Through clear and structured planning, it demonstrates that it is possible to transform a technical need into a viable, scalable project with a positive impact on both the economy and the environment.

## Methodology

From its initial conception, the SMDPED project was aimed at building a solid foundation to guide its future development. Instead of focusing on the immediate construction of the system, a reflective phase was chosen, centred on understanding the problem, structuring its components and establishing a clear and well-founded work plan.

ISSN: 2410-3993
RENIECYT: 1702902


Duran-Belman, Israel, García-Guzmán, José Miguel, Perez, Gerardo Daniel and Gallardo-Alvarez, Dennise Ivonne. [2025]. Analysis and methodological design for the implementation of a home electrical energy loss detection system. Journal of Technology and Innovation. 12[30]1-5: e61230105.
https://doi.org/10.35429/JTI.2025.12.30.6.1.5

This stage was conceived as a strategic planning exercise, in which the priority was to define the process precisely, rather than to obtain a functional prototype or carry out experimental tests. Thus, the project advanced as a methodological proposal that seeks to shape a technical solution based on analysis and systematic organisation of development.

It all began with an analysis of the problem, which made it possible to precisely define the scope of the project. The lack of accessible domestic tools for monitoring electricity consumption and detecting energy losses was identified. Based on this diagnosis, the objectives were defined, the criteria for success were established, and technical feasibility was prioritised over complexity, ensuring that the project could be developed within the available resources.

With the objectives clearly defined, a work plan was drawn up, divided into blocks of activities. Estimated times were assigned, dependencies between tasks were identified, and a progressive execution line was constructed. This organisation facilitated the visualisation of the workflow, allowed informed decisions to be made at each stage, and served as a guide to maintain the direction of the project.

Subsequently, a technical review was carried out to choose the most suitable components and tools. The ESP32 microcontroller was chosen for its versatility, along with accessible electrical sensors [ACS712 and ZMPT101B], an SQL Server database for data storage, and an ASP.NET Core MVC web platform for data visualisation. This selection was based on both functional criteria and ease of integration.

The first conceptual diagrams of the system were then drawn up, defining the flow of information from measurement to visual representation. This initial design made it possible to anticipate potential limitations, establish validation points, and predict the expected behaviour of the system before any practical implementation.

During the development of the documentation, each step forward was recorded in technical logs, where decisions, adjustments, setbacks and solutions applied were noted.

This practice made it possible to maintain control of the process, evaluate the completion of activities and facilitate a retrospective analysis useful for future implementations.

**Box 1**


**Figure 1**

Conceptualisation of the Project Development Process

All technological decisions were evaluated and validated theoretically, but without making physical connections or testing on actual devices.

The proposed integration—between hardware, software, and database—was approached as a structural simulation that would serve as a framework for a future phase of physical development.

Finally, all the information generated was consolidated into a comprehensive technical report, including plans, diagrams, code snippets, database structures, and functional diagrams of the platform. This compendium not only demonstrates the validity of the methodological process, but also serves as a guide for its replication, improvement, or future expansion.

Through this structured process, the project demonstrated that clear and well-documented planning is essential for turning a technical idea into a functional, replicable solution aligned with real energy efficiency objectives.

ISSN: 2410-3993
RENIECYT: 1702902


Duran-Belman, Israel, García-Guzmán, José Miguel, Perez, Gerardo Daniel and Gallardo-Alvarez, Dennise Ivonne. [2025]. Analysis and methodological design for the implementation of a home electrical energy loss detection system. Journal of Technology and Innovation. 12[30]1-5: e61230105.
https://doi.org/10.35429/JTI.2025.12.30.6.1.5

The methodological approach allowed us to build a solid foundation that supports not only the final product, but also the entire journey to get there.

## Results

### Evaluation of the Planning Process

1. Control of the Development Process

The project development was expected to follow a predefined schedule for each work block [analysis, planning, component selection, assembly and integration, functional testing].

This monitoring would allow for an evaluation of whether the technical planning was realistic and whether the team could meet the established deadlines.

In general, the first activities [analysis and planning] were completed as scheduled. However, activities related to component selection and system assembly experienced slight delays due to adjustments in the choice of sensors and errors during initial integration.

Testing also took longer than originally estimated, mainly due to code adjustments and data collection under real conditions.

**Box 2**

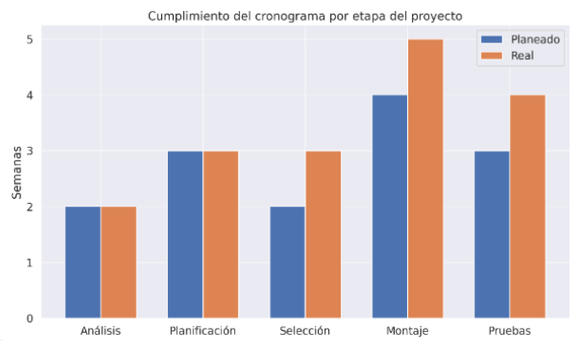


**Figure 2**

1. Distribution of Technical Effort during the Process

During the development of the project, a balanced distribution of time between the different activities was anticipated, especially between the technical part [assembly and programming] and the analytical part [research, documentation and testing]. The idea was not to overload any one area of work in order to ensure a sustainable and well-documented progress.

The time analysis shows that the most demanding tasks were electronic assembly and programming, each accounting for about a quarter of the total time. Technical research and testing occupied similar slots, while documentation - although necessary - was executed with less time burden due to its progressive integration during the project.

**Box 3**

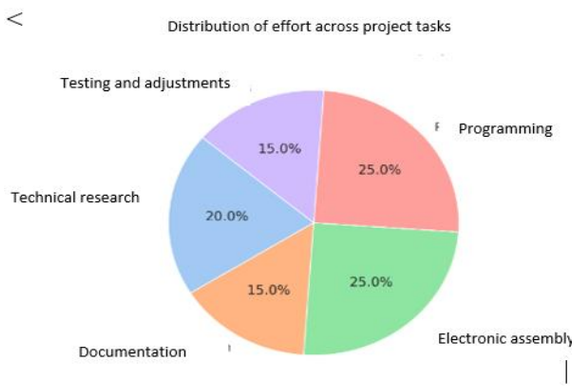


**Figure 3**

2. Weekly Progress Monitoring

A key part of the project process was to keep a continuous record of progress on a weekly basis. This not only facilitated short-term decision making, but also allowed for assessment of the pace of work, identification of possible delays and reinforced accountability.

Weekly monitoring showed a steady progression in the execution of tasks, with slight variations depending on the complexity of the activities in progress. There were weeks with lower productivity - associated with research or integration - and others with a higher concentration of deliverables, such as in the testing and documentation stages.

**Box 4**

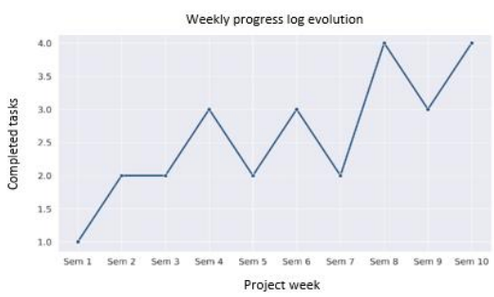


**Figure 4**

ISSN: 2410-3993
RENIECYT: 1702902


Duran-Belman, Israel, García-Guzmán, José Miguel, Perez, Gerardo Daniel and Gallardo-Alvarez, Dennise Ivonne. [2025]. Analysis and methodological design for the implementation of a home electrical energy loss detection system. Journal of Technology and Innovation. 12[30]1-5: e61230105.
https://doi.org/10.35429/JTI.2025.12.30.6.1.5

3. Current status of the project according to its structural process.

The main objective of this work was to lay the methodological and technical foundations for the future construction of the SMDPED project. Through documentation, architecture design, component selection and schematic elaboration, the necessary foundations were laid to start the implementation of the project.

This result clearly shows how far advanced the project preparation is.

To have a solid, complete and validated process structure in place so that, in later phases, the team can start development without the need to redesign or redefine the technical objectives.

**Box 5**

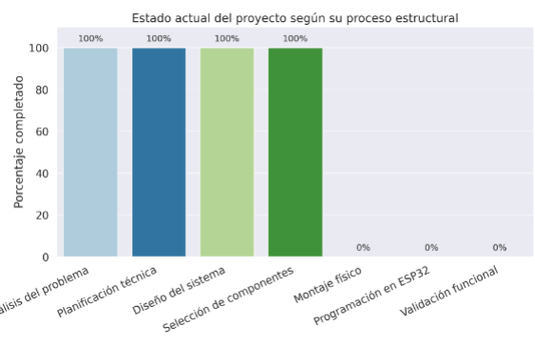


**Figure 5**

## Conclusions

El proyecto “Sistema de Monitoreo y Detección Domestic Energy Losses" has achieved its main objective at this stage: to establish a technical and methodological process that will serve as the basis for its subsequent implementation. Through a structured analysis of the problem, the definition of clear objectives, and the careful selection of technological components, a development roadmap was designed that will allow future construction to begin with a solid frame of reference.

No physical prototype was developed, nor were any functional field tests carried out, as this stage focused exclusively on planning, organising activities, selecting tools and technical documentation. This approach made it possible to anticipate requirements, foresee possible limitations and reduce uncertainty ahead of the next phase.

One of the main achievements was the consistency between what was planned and what was structured. The technical decisions made at this stage remain valid and appropriate, which is a significant advantage in ensuring that, once physical development begins, unnecessary rework and detours are avoided.

In summary, the project is at a transition point: it has successfully completed its preparation phase and has the necessary elements—both technical and methodological—to move forward with its construction. The clarity of the designed process is one of the most important assets of this stage and will serve as a guide for those carrying out the next phase of implementation.

## References

### Background

International Energy Agency [IEA]. [2021]. *Energy Efficiency 2021 Report. [Aporta datos previos sobre tendencias globales de consumo y eficiencia energética, sirve de marco de referencia para contextualizar el problema].*

### Basics

Microsoft Learn. [2023]. *ASP.NET Core MVC Overview. [Base conceptual y técnica del framework utilizado para la aplicación web].*

Arduino Community. [2023]. *ESP32 Energy Monitoring Examples. [Fuente práctica sobre integración de sensores con ESP32, base técnica para el desarrollo].*

### Support

Mishra, S., Sharma, R., & Tripathi, M. [2020]. *IoT-Based Energy Monitoring and Management Systems: A Comprehensive Review.* IEEE Access, 8, 134904–134924. *[Apoya la investigación al presentar trabajos similares en monitoreo energético mediante IoT y validando la importancia del enfoque adoptado].*

ISSN: 2410-3993
RENIECYT: 1702902


Duran-Belman, Israel, García-Guzmán, José Miguel, Perez, Gerardo Daniel and Gallardo-Alvarez, Dennise Ivonne. [2025]. Analysis and methodological design for the implementation of a home electrical energy loss detection system. Journal of Technology and Innovation. 12[30]1-5: e61230105.
https://doi.org/10.35429/JTI.2025.12.30.6.1.5

**Journal of Technology and Innovation** 12[30]1-15: e71230115
Article

# Evaluation of LED Systems for controlled spectral lighting in indoor hydroponic cultivation

# Evaluación de Sistemas LED para iluminación espectral controlada en cultivos hidropónicos de interior

Juárez-Balderas, Mario Alberto [a], Daniel-Eufracio, América Abigail [b], Araiz-Aguilar, Gustavo Rafael [c] and Villaseñor-Aguilar, Marcos Jesús [d]

[a] Tecnológico Nacional de México/Campus Irapuato • S-8744-2018 • 0000-0002-5756-5403 • 99207
[b] Tecnológico Nacional de México/Campus Irapuato • 0009-0003-3141-6017
[c] Tecnológico Nacional de México/Campus Irapuato
[d] Tecnológico Nacional de México/Campus Irapuato • 0009-0003-0598-8145 • 294911 |

**Classification:**

Area: Engineering
Field: Engineering
Discipline: System enginner
Subdiscipline: Electronics

https://doi.org/10.35429/JTI.2025.12.30.7.1.15
**History of the article:**
Received: September 30, 2025
Accepted: December 30, 2025

* ✉ [mario.jb@irapuato.tecnm.mx ]

## Abstract

Indoor farming is emerging as a practical solution to challenges such as urbanization, limited arable land, and climate change, enabling sustainable, efficient, and localized food production. LED lighting has taken on a key role in hydroponic systems by allowing precise spectral control that enhances photosynthesis, morphological development, and the nutritional quality of crops. This article examines how LED spectral design influences the growth of lettuce [Lactuca sativa], emphasizing its benefits in terms of energy efficiency and resource optimization. Additionally, the integration of emerging technologies like artificial intelligence [AI] and the Internet of Things [IoT] is explored. These technologies enable real-time adjustment of critical variables such as light intensity, pH, electrical conductivity, and temperature through predictive algorithms including deep neural networks, fuzzy logic, and LSTM models. Such tools not only boost operational efficiency but also help reduce water, fertilizer, and electricity consumption. Furthermore, the use of computer vision systems has proven effective in monitoring the physiological state of plants and detecting potential deficiencies or anomalies without the need for manual intervention.

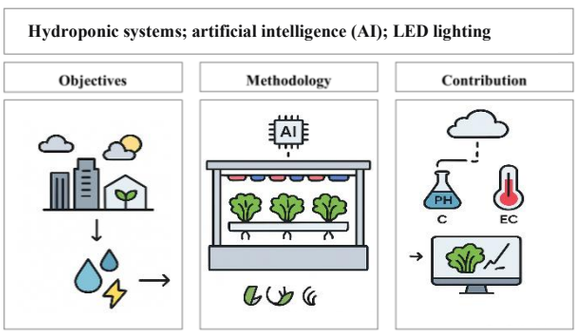


**Hydroponic systems; artificial intelligence [AI]; LED lighting**

## Resumen

La agricultura interior se posiciona como una solución viable frente a desafíos como la urbanización, la escasez de suelo cultivable y el cambio climático, al permitir una producción sostenible, eficiente y localizada, la iluminación LED ha adquirido un papel estratégico en sistemas hidropónicos, al posibilitar un control espectral preciso que mejora la fotosíntesis, el desarrollo morfológico y la calidad nutricional de los cultivos. Este artículo analiza la influencia del diseño espectral LED sobre el crecimiento de lechuga [Lactuca sativa], destacando sus ventajas en términos de eficiencia energética y optimización de recursos .Asimismo, se explora la integración de tecnologías emergentes como la inteligencia artificial [IA] y el Internet de las Cosas [IoT], que permiten ajustar en tiempo real variables críticas como la intensidad de luz, el pH, la conductividad eléctrica y la temperatura, mediante algoritmos predictivos como redes neuronales profundas, lógica difusa y modelos LSTM. Estas herramientas no solo aumentan la eficiencia operativa, sino que también reducen el consumo de agua, fertilizantes y electricidad. Además, el uso de sistemas de visión computacional ha demostrado ser eficaz para monitorear el estado fisiológico de las plantas y anticipar posibles deficiencias o anomalías sin intervención manual.

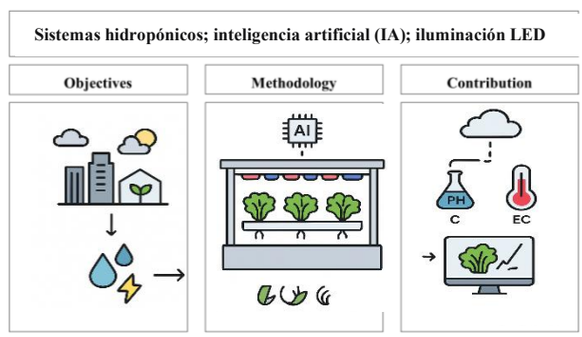


**Sistemas hidropónicos; inteligencia artificial [IA]; iluminación LED**

**Area**: Development of strategic leading-edge technologies and open innovation for social transformation

**Citation:** Juárez-Balderas, Mario Alberto, Daniel-Eufracio, América Abigail, Araiz-Aguilar, Gustavo Rafael and Villaseñor-Aguilar, Marcos Jesús. [2025]. Evaluation of LED Systems for controlled spectral lighting in indoor hydroponic cultivation. Journal of Technology and Innovation. 12[30]1-15: e71230115.

## Introduction

Indoor agriculture has emerged as a key strategy in response to global challenges such as urbanization, limited arable land, and climate change. It enables sustainable, continuous food production as the urban population is projected to reach 8.6 billion by 2050, with 80% living in cities. This approach offers viable solutions for local food production, reducing transport-related emissions, and optimizing space use [Aydin et al., 2023]. The loss of soil fertility due to urban expansion and the indiscriminate use of agrochemicals has driven the adoption of soilless systems like hydroponics.

This method allows vertical farming using nutrient solutions and can save up to 90% of water compared to traditional methods [Regmi et al., 2024]. These systems are not only climate-resilient, operating in controlled environments that lessen the impact of irregular rainfall or extreme temperatures, but also reduce the use of pesticides and fertilizers due to a closed and monitored setting. This improves crop health and lowers pollutant emissions [Bamidele et al., 2024]. Energy efficiency has improved with the use of low-consumption LED lighting and smart control systems powered by artificial intelligence [AI], which allow dynamic adjustment of light intensity and the integration of alternatives like solar energy [Kuankid et al., 2022].

Technologies like the Internet of Things [IoT] and AI have transformed these systems by automating the monitoring and control of key variables such as pH, temperature, humidity, $CO_2$, and electrical conductivity. Connected sensors and actuators enable precision agriculture, increasing yield, reducing resource waste, and improving traceability [Gutiérrez et al.,2021]. AI is also used to diagnose plant diseases, predict harvests, and optimize operations in automated greenhouses. Indoor agriculture offers an integrated solution to the pressures of a changing world, establishing itself as a resilient, efficient, and future-ready production model.

One of the plants commonly used in indoor hydroponic systems is lettuce [*Lactuca sativa*]. Its compact morphology, fast growth, and high photosynthetic efficiency under controlled conditions make it an ideal crop for testing artificial lighting technologies, nutrient solutions, and soilless production systems.

Lettuce has been widely used as a model crop in artificial lighting research. Studies have shown that variations in the LED spectrum particularly the ratio of red, blue, and far-red light significantly affect leaf elongation, nitrate accumulation, and chlorophyll content, making it a reference plant for studying the relationship between light and nutritional quality.

Multiple studies have documented how specific combinations of red, blue, and far-red light influence leaf development, biomass accumulation, and photosynthesis. Factors such as light intensity [PPFD], photoperiod, and even pulsed lighting directly impact lettuce yield, helping reduce energy consumption without compromising quality. The controlled environment also enables the management of nitrate accumulation and the application of machine learning models, such as CNNs [*Convolutional Neural Networks*] for visual analysis and DNNs [*Deep Neural Networks*] for general predictive modeling from diverse data.

These tools are used to estimate growth, detect diseases, or dynamically adjust lighting and nutrients based on the crop's physiological state. Lettuce serves as an ideal bioindicator for validating smart agriculture technologies in controlled environments. [Budavári et al., 2024].

From an agronomic perspective, lettuce has a short cycle [30–45 days from transplant], tolerates high planting densities, and has low nutrient demands [optimal EC of 0.8–1.2 mS/cm], which is the safe nutrient range in water for proper growth. It is sensitive to light spectrum and duration, making it suitable for studying specific responses to light control. Lettuce prefers moderate temperatures [18–22 °C], a pH range of 5.5–6.5, and a photoperiod of 12–16 hours, which can be efficiently supplied with multispectral LED lighting.

These traits have supported its integration into NFT systems [nutrient film technique], floating rafts, and urban vertical modules, giving it an advantage over other crops.

## Photobiological requirements of plants

Light is essential for plant growth and quality. It acts as an energy source for photosynthesis and as a signal that triggers photomorphogenesis and other physiological, biochemical, and molecular responses [Bantis et al., 2023; Bayat et al., 2018].

ISSN: 2410-3993.
RENIECYT: 1702902


Juárez-Balderas, Mario Alberto, Daniel-Eufracio, América Abigail, Araiz-Aguilar, Gustavo Rafael and Villaseñor-Aguilar, Marcos Jesús. [2025]. Evaluation of LED Systems for controlled spectral lighting in indoor hydroponic cultivation. Journal of Technology and Innovation. 12[30]1-15: e71230115
https://doi.org/10.35429/JTI.2025.12.30.7.1.15

Indoor horticulture uses LEDs to control spectrum, intensity, and duration, optimizing crop performance and plant photobiology. [Bantis et al., 2023; Paradiso et al., 2022; Marondedze et al., 2018], The key photobiological requirements of plants that can be controlled through lighting are:

*Absorption Spectra*

*Chlorophyll A and B*: Chlorophyll molecules are the primary photosynthetic pigments that absorb light photons. Leaves containing chlorophyll show peak absorption around 432 nm [blue] and 670 nm [red] [Tavares et al., 2017]. This absorption is critical for photosynthesis. Light in the red and blue regions of the spectrum is mainly absorbed by photosynthetic pigments, accounting for about 90% of the total leaf absorption [Thi et al., 2019].

*Phytochromes:* These photoreceptors are sensitive to red and far-red light. Far-red light [730 nm], although outside the photosynthetically active range [400–700 nm] [Motogaito et al., 2017], plays a key role in shifting phytochromes into their red-absorbing form [Mena et al., 2018]. Phytochromes regulate processes such as stem elongation, branching, leaf expansion, and reproduction [Paradiso et al., 2022]. It has also been observed that plants require relatively low phytochrome photoequilibrium values to trigger flowering [Mena et al., 2018].

*Cryptochromes and Phototropins:* These photoreceptors are activated by blue light [430–450 nm] and mediate responses such as phototropic curvature, inhibition of elongation growth, chloroplast movement, stomatal opening, and seedling development regulation [Bantis et al., 2023; Paradiso et al., 2022]. Blue light also influences chlorophyll biosynthesis and photosynthetic processes [Paradiso et al., 2022].

*Carotenoids:* These pigments absorb blue light and act as photoprotective agents by rapidly dissipating the excited state of chlorophyll [Thi et al., 2019; Tavares et al., 2017].

Figure 1 shows the relative spectral absorption of plant pigments. The absorption profiles represented are:

- Chlorophyll A [dark green]: peaks at ~430 nm and ~662 nm
- Chlorophyll B [light green]: peaks at ~453 nm and ~642 nm
- β-Carotene [orange]: peak at ~470 nm
- Phytochrome [red]: peaks at ~660 nm and ~730

**Box 1**

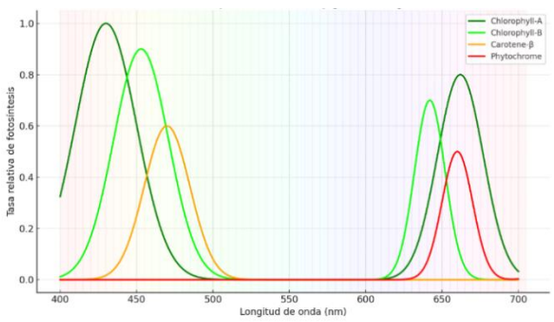


**Figure 1**
Spectral Absorption in Plant Pigments
*Source: Own elaboration*

*Photomorphogenesis and Phototropism*

*Photomorphogenesis* refers to the complex process by which light, through specific signals, regulates plant development, form, and metabolism [Paradiso et al., 2022]. This includes the adjustment of morphological and physiological traits to adapt to different light conditions. Light quality plays a key role in this process.

For example, low radiation intensity can increase specific leaf area [SLA] and plant height to maximize light absorption for photosynthesis, while high radiation intensity can reduce SLA and increase leaf thickness to protect the plant and maintain efficient photosynthesis [Thi et al., 2019].

*Phototropism* is the plant's response to light direction, mediated by photoreceptors activated by blue light [Kozai et al., 2018]. This response is essential for directing plant growth toward an optimal light source.

*PPFD [Photosynthetic Photon Flux Density] and DLI [Daily Light Integral]*

*PPFD [Photosynthetic Photon Flux Density]* is defined as the number of photons within the 400 to 700 nm wavelength range.

ISSN: 2410-3993.
RENIECYT: 1702902


Juárez-Balderas, Mario Alberto, Daniel-Eufracio, América Abigail, Araiz-Aguilar, Gustavo Rafael and Villaseñor-Aguilar, Marcos Jesús. [2025]. Evaluation of LED Systems for controlled spectral lighting in indoor hydroponic cultivation. Journal of Technology and Innovation. 12[30]1-15: e71230115
https://doi.org/10.35429/JTI.2025.12.30.7.1.15

It is a key metric because these photons drive glucose production, which determines the photosynthesis rate [Motogaito et al., 2017]. An average PPFD of 100–300 µmol $m^{-2}$ $s^{-1}$ with a photoperiod of 10–18 hours is suitable for most leafy vegetables grown in plant factories [Kozai et al., 2018]. Studies with spinach have found that a PPFD of 190 µmol $m^{-2}$ $s^{-1}$ may be optimal for growth [Motogaito et al., 2017].

***DLI [Daily Light Integral]*** represents the total amount of photosynthetically active photons a plant receives over the course of a day [Kozai et al., 2018]. Studies have shown that a DLI of 17.3 mol·$m^{-2}$·$d^{-1}$ under LED lighting with a red/blue ratio [R/B] of 6/5—where red light supports biomass accumulation and blue light promotes healthy morphological development—resulted in higher fresh and dry weight in hydroponically grown spinach, along with improved energy efficiency [Semenova et al., 2023].

An adequate DLI ensures that plants receive the total photon input needed to maintain photosynthesis near its maximum rate for most of the day, without reaching levels that cause photoinhibition. Increasing DLI, combined with proper PPFD and photoperiods, is essential for promoting plant growth [Kelly et al., 2020]. DLI is expressed in mol·$m^{-2}$·$d^{-1}$ and can be calculated using the following equation.

$$PPFD \times horas\ de\ luz \left(DLI = PPFD\ \frac{fotoperiodo}{10^6}\right) (1)$$

Where $t$ is the exposure time in seconds per day [for example, 14 hours = 50,400 s], the factor $10^6$ converts micromoles to moles.

This approach allows light intensity and duration to be adjusted for each phenological stage to maximize photosynthetic efficiency. Studies have shown that, for crops like lettuce, a moderate PPFD [100–250 µmol·$m^{-2}$·$s^{-1}$] and an optimized DLI [14–17 mol·$m^{-2}$·$d^{-1}$] under extended light periods [16–20 h/day] promote greater biomass, denser leaves, and better photochemical efficiency [ΦPSII], compared to high-PPFD, short-photoperiod scenarios that reduce efficiency [Palmer et al., 2020]. Additionally, photomorphogenesis which includes responses such as elongation, leaf thickness, chlorophyll development, and stretching is mediated by photoreceptors sensitive to red, blue, and far-red light [phytochromes and cryptochromes].

These receptors regulate key hormonal and genetic pathways related to optimal structure, phenology, defense, and thermoregulation [Li et al., 2023].

g/Wh metric: Indicates the energy efficiency of a crop, expressing how many grams of plant biomass are obtained per watt-hour of electrical energy consumed in the system.

The combined use of PPFD and DLI enables the development of customized "light recipes" for different species, growth stages, and production goals, improving system energy efficiency and crop performance.

## Comparison of Lighting Technologies

*HPS, CFL vs. LED: Spectrum, Energy Use, Heat Dissipation*

Light is a key factor in controlled growing systems, influencing physiological, biochemical, and molecular processes through photomorphogenesis. The selection of artificial lighting sources must consider the emitted spectrum, energy efficiency, and heat dissipation [Chutimanukul et al., 2022].

HPS lamps [High Pressure Sodium] mainly emit in the red-orange range [~580–650 nm], supporting flowering but offering limited effectiveness during vegetative stages. CFLs [compact fluorescent lamps] provide a broader spectrum, though with lower intensity and photon efficiency.

LEDs can emit specific wavelengths [red 660 nm, blue 450 nm, green 510 nm] or full-spectrum light [Chutimanukul et al., 2022; Priya et al., 2023].

This spectral flexibility allows light to be tailored to the physiological needs of different species, such as basil or lettuce, where specific red-to-blue light ratios affect biomass accumulation, secondary metabolite production, and photosynthetic parameters [Shareef et al., 2024].

Figure 2 shows a spectral comparison of lighting technologies used in hydroponic cultivation.

ISSN: 2410-3993.
RENIECYT: 1702902


Juárez-Balderas, Mario Alberto, Daniel-Eufracio, América Abigail, Araiz-Aguilar, Gustavo Rafael and Villaseñor-Aguilar, Marcos Jesús. [2025]. Evaluation of LED Systems for controlled spectral lighting in indoor hydroponic cultivation. Journal of Technology and Innovation. 12[30]1-15: e71230115
https://doi.org/10.35429/JTI.2025.12.30.7.1.15

## Box 2

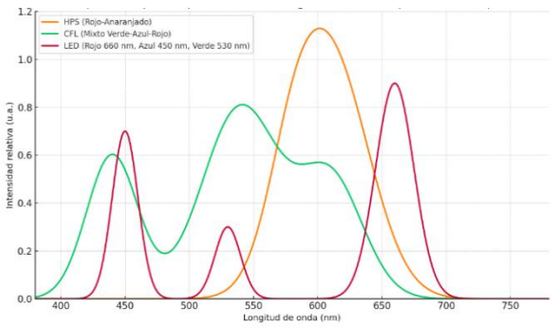


**Figure 2**

Spectral Comparison of Lighting Technologies in Hydroponic Cultivation

From an energy standpoint, LEDs offer efficiencies above 2.0 µmol/J, compared to 1.0–1.7 µmol/J for HPS and 0.5–1.0 µmol/J for CFLs [Chutimanukul et al., 2022; Shareef et al., 2024; Naim et al., 2020]. This efficiency, combined with lower ventilation needs, significantly reduces total electricity consumption. In LEDs, heat dissipation is concentrated at the heat sink, allowing for localized thermal management, unlike the radiated heat from HPS lamps, which can alter the crop microclimate.

### *Types of LEDs used in horticulture*

Among the available technologies, light-emitting diodes [LEDs] stand out for their ability to emit specific spectra with high energy efficiency and low heat dissipation, which has driven their adoption in precision horticulture [Chutimanukul et al., 2022; Shareef et al., 2024]. LED lighting systems used in hydroponic horticulture are mainly divided into:

Monochromatic LEDs: Emit specific wavelengths [e.g., red 660 nm, blue 450 nm, far-red 730 nm]. Used in controlled spectrum studies.

Extended [Full-Spectrum] LEDs: Mimic sunlight with a balanced mix of red, green, blue, and far-red light. Ideal for full-cycle crops.

Narrow-Band Tuned LEDs: Engineered to target specific photosystems [PSI and PSII] or regulate phytochromes and cryptochromes.

## Box 3

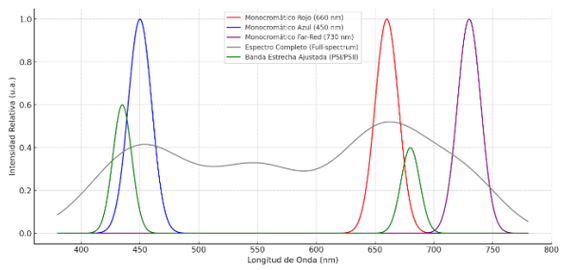


**Figure 3**

Comparison of LED Spectra in Indoor Horticulture

LED light intensity can be controlled through pulse-width modulation [PWM], enabling dynamic photoperiods and adjustment of daily light integral [DLI]. Automated management using microcontrollers and light sensors helps maintain consistent and reproducible environmental conditions [Putra et al., 2024; Stevens et al., 2023].

With modular design, precise spectral control, and PWM regulation, LEDs are a versatile tool for optimizing crops in smart hydroponic systems [Catota-Ocapana et al., 2024]. These technologies improve not only energy-use efficiency but also the quality of secondary metabolites and morphological uniformity [Mohamed et al., 2021; Pennisi et al., 2019].

### *Technical advantages of LED*

LEDs allow for the adjustment of both light intensity and spectral profile. This feature enables the use of specific wavelengths red [~660 nm], blue [400–500 nm], and green [~510 nm] individually or in combination, as well as full-spectrum lighting. Red light is associated with biomass accumulation and storage compounds [sugars, starches], especially in crops like basil under 3R:1B ratios.

Blue light, on the other hand, regulates stomatal opening and can promote leaf compactness and the synthesis of antioxidants and phenolic compounds, particularly effective at higher blue ratios [1R:3B] [Chutimanukul et al., 2022].

Green light has been linked to increased vitamin C and polyphenol synthesis, and can support biomass production in certain ratios [e.g., 2R:1G:2B] [Shareef et al., 2024].

ISSN: 2410-3993.
RENIECYT: 1702902


Juárez-Balderas, Mario Alberto, Daniel-Eufracio, América Abigail, Araiz-Aguilar, Gustavo Rafael and Villaseñor-Aguilar, Marcos Jesús. [2025]. Evaluation of LED Systems for controlled spectral lighting in indoor hydroponic cultivation. Journal of Technology and Innovation. 12[30]1-15: e71230115
https://doi.org/10.35429/JTI.2025.12.30.7.1.15

These spectral configurations can be tailored to the phenological and physiological needs of specific crops like lettuce or basil, maintaining optimal PPFD levels [~200 $\mu mol \cdot m^{-2} \cdot s^{-1}$] and improving the efficiency of light energy use [Yanes et al., 2022].

### *Types of light treatments*

Light treatment design in hydroponic systems considers key variables such as photosynthetic photon flux density [PPFD], energy consumption, and thermal management of LEDs, along with physiological and photosynthetic parameters: net photosynthetic rate [Pn], stomatal conductance [gs], quantum yield of Photosystem II [ΦPSII], and electron transport rate [ETR]. Fresh and dry biomass [FW/DW] provides a direct measure of productivity under different spectral ratios, helping identify optimal configurations specific to each cultivar.

## Box 4

**Table 1**
Effects of Light Spectrum on Lettuce]

| LED spectrum | Effect on yield | Effect on nutritional quality | Energy efficiency [g/Wh or µmol/J] |
|---|---|---|---|
| **Red [R]** | It stimulates stem elongation and leaf expansion; it increases biomass when combined with blue. | It increases sugar accumulation; it reduces nitrate content. | High photosynthetic efficiency when combined with blue; good g/Wh ratio. |
| **Blue [B]** | It promotes plant compactness, increases leaf area, and enhances efficient photosynthesis. | It improves phenolic content and antioxidant capacity; activates the phenylpropanoid pathway. | High quantum efficiency in photosynthetic pigments; moderate energy consumption. |
| **Far-red [FR]** | It promotes leaf expansion and radiation capture; no direct effect on photosynthesis. | It does not directly improve quality but promotes conditions for nutrient accumulation. | Low quantum efficiency; useful in low doses to complement the spectrum. |
| **UV-A [315-400 nm]** | It can induce mild stress, stimulating the production of secondary compounds [phenols, anthocyanins]. | It induces the synthesis of flavonoids and polyphenols through stress; high nutraceutical potential. | Very low photosynthetic efficiency; its use should be limited and controlled. |

LED spectra influence stem elongation, the accumulation of pigments like chlorophyll and carotenoids, and the synthesis of secondary metabolites, as shown in Table 1. These include phenolic compounds, essential oils such as methyl eugenol and caryophyllene, and antioxidants, whose concentrations can be modulated through spectral adjustments. The relationship between light composition and metabolic profiles opens up opportunities to design lighting schemes aimed at improving crop quality [Taha et al., 2022].

## Box 5

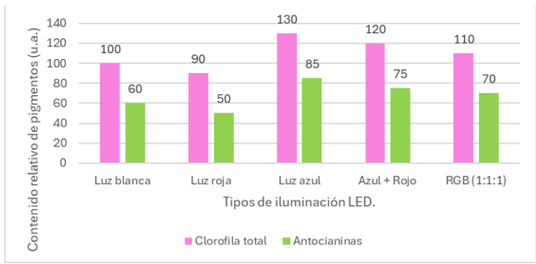


**Figure 4**
Effect of LED light spectrum type on total chlorophyll and anthocyanin accumulation in lettuce.

In Fig. 5, blue light alone produced the highest total chlorophyll [130 relative units] and anthocyanin levels [85 relative units], significantly exceeding other color combinations, such as white light [100 and 60, respectively] or red light [90 and 50]. Mixed schemes, including blue + red or balanced RGB [1:1:1], showed intermediate results but remained below those obtained under pure blue light [Soufi et al., 2023].

Combinations like 2R:1G:2B have been linked to increases in biomass and photosynthetic pigments [Yanes et al., 2022]. Specific spectral treatments using 1R:1B, 3R:1B, 1R:3B, and 2R:1G:2B have been widely tested. Results indicate cultivar-dependent responses affecting biomass, photosynthesis, secondary metabolite accumulation, and pigmentation. While most studies focus on red, blue, and green wavelengths, other ranges such as far-red and ultraviolet [UV] are also recognized for their potential, mainly in optical sensor-based monitoring [Putra et al., 2024].

The most commonly used spectra in Lactuca sativa include:R:B = 3:1: Promueve biomasa y eficiencia en uso del agua [Pennisi et al., 2019].

ISSN: 2410-3993.
RENIECYT: 1702902


Juárez-Balderas, Mario Alberto, Daniel-Eufracio, América Abigail, Araiz-Aguilar, Gustavo Rafael and Villaseñor-Aguilar, Marcos Jesús. [2025]. Evaluation of LED Systems for controlled spectral lighting in indoor hydroponic cultivation. Journal of Technology and Innovation. 12[30]1-15: e71230115
https://doi.org/10.35429/JTI.2025.12.30.7.1.15

R:B = 9:1: Aumenta sacarosa, reduce nitratos [Matysiak et al., 2021].

R:B+FR: Mejora morfología y arquitectura foliar, y puede aumentar área foliar [Legendre & van Iersel, 2021].

In the field of precision horticulture, various LED light treatments have been designed to modulate key physiological processes in crops. Among the most studied spectral combinations are 1R:1B, 3R:1B, 1R:3B, and 2R:1G:2B, which enable targeted control over growth, morphogenesis, secondary metabolite synthesis, and system energy efficiency. The combination of these bands, referred to as a "spectral recipe," is adjusted based on species, cultivar, and phenological stage.

This approach helps optimize photosynthetic performance, plant architecture, and the nutritional content of the crop [Chutimanukul et al., 2022; Shareef et al., 2024]. Adjusting the light spectrum and photoperiod using LEDs is essential in controlled-environment agriculture, as it allows regulation of physiological processes such as photosynthesis, growth, and flowering. Tailoring light duration and intensity to each growth stage improves both crop performance and overall system efficiency [Reyes et al., 2022].

**Photoperiod control**

Photoperiod is defined as the daily duration of light exposure. Plants perceive it through photoreceptors such as phytochromes and cryptochromes, which regulate the transition between phenological stages. In controlled environments, the photoperiod can be adjusted artificially.

There are three types of photoperiodic responses:

Short-day plants: flower when the photoperiod is shorter than a specific threshold.

Long-day plants: require a longer light duration to induce flowering.

Day-neutral plants: flowering is independent of photoperiod length.

Adjusting the photoperiod allows synchronization of flowering and maturation [phenological stages] with production goals, reduces light-induced stress, and helps control biomass accumulation and secondary metabolite synthesis. Additionally, photoperiod control can be combined with dimming [intensity regulation] to avoid overexposure by adjusting light intensity.

Integrated control of light spectrum and photoperiod is a strategic tool to maximize the physiological and biochemical performance of plants. It is considered an essential practice in high-efficiency controlled-environment agriculture [Taha et al., 2022; Yanes et al., 2022; Stevens et al., 2023].

**Spectral characterization and efficiency in lighting systems for smart hydroponics**

In controlled-environment cultivation systems, spectral characterization and photonic efficiency of lighting systems are key variables for optimizing plant growth. The use of LEDs enables precise spectral design and control over light intensity, directly influencing photosynthesis, biomass accumulation, and secondary metabolite synthesis [Chutimanukul et al., 2022; Shareef et al., 2024].

In such systems, photonic efficiency and spectral characterization are critical. LED systems with spectral peaks at 660 nm [red], 450 nm [blue], and 525 nm [green] allow modulation of photosynthesis, morphogenesis, and metabolite biosynthesis.

Their effects have been validated in hydroponic crops such as lettuce, basil, and strawberries. Although the full width at half maximum [FWHM] is not always reported, it is generally estimated to range between 15 and 25 nm in horticultural LEDs.

For environmental monitoring, sensors like the AS7265x offer a spectral resolution of 30 nm, which is useful for assessing lighting conditions, though it does not exactly match the emission profile of the LEDs [Yanes et al., 2022; Taha et al., 2022; Putra et al., 2024].

Photosynthetic photon efficacy [PPE] in commercial LED-based systems—whether white or multi-band-has been reported between 1.8 and 2.7 $\mu mol \cdot J^{-1}$ [Singh et al., 2015].

ISSN: 2410-3993.
RENIECYT: 1702902


Juárez-Balderas, Mario Alberto, Daniel-Eufracio, América Abigail, Araiz-Aguilar, Gustavo Rafael and Villaseñor-Aguilar, Marcos Jesús. [2025]. Evaluation of LED Systems for controlled spectral lighting in indoor hydroponic cultivation. Journal of Technology and Innovation. 12[30]1-15: e71230115
https://doi.org/10.35429/JTI.2025.12.30.7.1.15

The reviewed studies primarily focus on the use of photosynthetic photon flux density [PPFD] as a practical metric, reporting:

200 $\mu mol \cdot m^{-2} \cdot s^{-1}$ for basil and strawberry [Chutimanukul et al., 2022].

150–250 $\mu mol \cdot m^{-2} \cdot s^{-1}$ for lettuce [Stevens et al., 2023].

160–190 $\mu mol \cdot m^{-2} \cdot s^{-1}$ óptimal fos Chinese Cabbage [Taha et al., 2022].

In System like NutriSpec, an average PPFD of 330 $\mu mol \cdot m^{-2} \cdot s^{-1}$ with 12 h/day equivalent a DLI of 14 $mol \cdot m^{-2} \cdot day^{-1}$[Yanes et al., 2022].

Although lux sensors are used in some implementations, this unit—based on human visual perception—does not accurately reflect photosynthetic effectiveness. Estimating PPFD from lux requires knowledge of the light source's spectrum and the application of empirical conversion factors, which limits its accuracy in scientific settings [Singh et al., 2015]. While LEDs emit minimal surface heat, thermal management—either passive or active—is necessary to prevent spectral drift. Maintaining an operating temperature around 25 °C is recommended to ensure spectral stability [Putra et al., 2024].

**Effects of Different Spectra on *Lactuca sativa***

Spectral lighting influences the growth and quality of *Lactuca sativa* in indoor hydroponics. It analyzes how red, blue, green, and combined spectra modulate morphology, nutritional composition, and energy efficiency.

*Morphological performance under different spectra*

Morphological performance under different spectraThe morphological growth efficiency of Lactuca sativa in controlled hydroponic systems largely depends on the applied light spectrum, as well as associated intensity and photoperiod. Various studies have identified an optimal photosynthetic photon flux density [PPFD] range of 150 to 250 µmol·m$^{-2}$·s$^{-1}$ for vegetative development in lettuce [Chen et al., 2021; Shareef et al., 2024].

Specifically, a PPFD of 200 µmol·m$^{-2}$·s$^{-1}$ with a 16-hour photoperiod has been reported to support balanced and sustained growth in leafy crops such as lettuce and basil [Putra et al., 2024].

The application of LED spectra in controlled hydroponic cultivation allows modulation of several physiological processes in Lactuca sativa, including morphogenesis, secondary metabolism, and light energy use efficiency. Spectral adjustment is a key strategy for tailoring lighting to different phenological stages and production goals.

Red light [R], with a peak at 660 nm, promotes the accumulation of carbohydrates such as sucrose and starch, but its exclusive use may induce excessive elongation of hypocotyls and cotyledons, compromising plant structure [Pennisi et al., 2019]. Blue light [B, 400–500 nm] promotes a more compact architecture by influencing stomatal opening, which contributes to transpiration control and leaf thickness [Yanes et al., 2022].

Green light [G, ~510 nm], although traditionally less studied, has shown complementary effects. In combinations such as 2R:1G:2B, improvements have been observed in fresh weight [FW] and shoot elongation, outperforming conventional R:B setups [Chutimanukul et al., 2022; Shareef et al., 2024].

This combination also supports the accumulation of pigments and secondary metabolites such as polyphenols. From an agronomic perspective, smart hydroponic systems show improved biomass and morphological traits compared to traditional systems. Experimental data show differences in plant height [28 cm vs 27.5 cm] and fresh weight [216 g vs 161.2 g] under controlled lighting conditions [Putra et al., 2024].

A PPFD of 330 µmol·m$^{-2}$·s$^{-1}$ for 12 h/day, equivalent to a daily light integral [DLI] of 14 mol·m$^{-2}$·d$^{-1}$, is adequate for maintaining photosynthetic activity in lettuce [Stevens et al., 2023]. Regarding secondary metabolism, blue light has been shown to activate the phenylpropanoid pathway and increase phenolic content in red lettuce. Likewise, the 2R:1G:2B spectrum has been associated with higher levels of polyphenols and vitamin C, suggesting a positive interaction between G and B in the biosynthesis of functional compounds [Shareef et al., 2024].

ISSN: 2410-3993.
RENIECYT: 1702902


Juárez-Balderas, Mario Alberto, Daniel-Eufracio, América Abigail, Araiz-Aguilar, Gustavo Rafael and Villaseñor-Aguilar, Marcos Jesús. [2025]. Evaluation of LED Systems for controlled spectral lighting in indoor hydroponic cultivation. Journal of Technology and Innovation. 12[30]1-15: e71230115
https://doi.org/10.35429/JTI.2025.12.30.7.1.15

Spectroscopic studies have shown that reflectance in visible bands decreases with increasing macronutrient [N, P, K] levels, while near-infrared reflectance [720–1300 nm] increases, indicating greater leaf area and water content [Taha et al., 2022].

In terms of energy efficiency, R:B ratios such as 90:10 have been shown to optimize sucrose accumulation and reduce nitrate content, improving the biomass-to-energy ratio [Pennisi et al., 2019].

Configurations such as R:B=3:1 have been effective for maximizing growth without compromising nutritional quality. Additionally, [Palmer and van Iersel [2020]] found that extending the photoperiod while keeping the DLI constant reduces the required PPFD, increasing system lighting efficiency.

Far-red light [FR] has been proposed as a complementary spectrum to enhance radiation capture and light use efficiency [RUE]. FR has been shown to increase leaf area and photon absorption without significantly increasing energy consumption [Legendre & van Iersel, 2021].

Full-spectrum white light, while less efficient in terms of biomass per watt, offers operational and ergonomic advantages. This limitation can be addressed through intelligent control systems such as diffuse lighting or Random Forest-based models, which have demonstrated 70–90% reductions in water and energy use in NFT/DWC systems [Budavári et al., 2024; Gutierrez Leon et al., 2019].

A comparative summary of studies on LED lighting in hydroponic lettuce [Lactuca sativa] includes details on light spectra, PPFD, photoperiod, LED type, and main physiological responses observed in the plant.

**Box 6**

**Table 2**

Comparison between LED configurations and responses in *Lactuca sativa*

| LED Spectrum | PPFD [µmol/m²/s] | Photoperiod [h/day] | Tipo de LED | Physiological Response | APA Reference |
|---|---|---|---|---|---|
| **R:B:G = 70:18:12** | 160 | 16 | Multispectral RGB | Higher biomass with 70:18:12; no effect on nitrates. | Matysiak et al. [2021] |
| **R+B [435+663 nm], ±G** | 60–270 | 16 | Combined Monochromatic | ↑ Photosynthesis with B435 + R663; B/R = 1.25:1, ↑ Phenolics | Mohamed et al. [2021] |
| **R:B = 60:40 ± FR** | 200 + FR 50 | 18 | Mixed + FR | More blue = ↑ nutrients; FR = ↑ biomass, but ↓ phenolics | Van Brenk et al. [2024] |
| **White, R+B, R+B+FR+G, ±UV-B** | 250 | 16 | Varied Multispectral | White = ↑ yield; R + B = ↑ phenolics; FR = bolting | Alrajhi et al. [2023] |
| **R:B = 3:1** | 215 | 16 | Combined Monochromatic | R:B = 3:1 optimizes biomass and water use | Pennisi et al. [2019] |
| **R:B = 90:10** | 200 | 16 | Combined Monochromatic | R:B = 90:10 = ↑ sucrose, ↓ nitrates, good efficiency | Chen et al. [2021] |
| **R+B base ± FR [700–800 nm]** | 207 + FR | 16 | Mixed + FR | FR = ↑ leaf area, ↑ biomass per photon | Legendre & van Iersel [2021] |
| **Continuous R + B ± Green** | CL [24h] | 24 [continuous] | R+B vs. R+B+G | Green reduces CL stress, ↑ photosynthesis | Bian et al. [2018] |
| **R, B, R+B [4:1], FL** | ~100 | 16 | Monochromatic vs. Combined vs. FL | B and R + B improve seedlings, resulting in more robust plants after transplanting | Johkan et al. [2010] |
| **Pure Red vs. R + B** | 150 [est.] | 14–16 | Monochromatic vs. Combined | Adding blue = ↑ chlorophyll, antioxidants, and biomass | Naznin et al. [2019] |

*Source [Own elaboration]*

## Emerging technological aspects: IoT, dynamic spectral control, PWM, and DLI automation

Modern hydroponic cultivation systems increasingly rely on the integration of advanced technologies to optimize both plant growth and energy efficiency.

ISSN: 2410-3993.
RENIECYT: 1702902


Juárez-Balderas, Mario Alberto, Daniel-Eufracio, América Abigail, Araiz-Aguilar, Gustavo Rafael and Villaseñor-Aguilar, Marcos Jesús. [2025]. Evaluation of LED Systems for controlled spectral lighting in indoor hydroponic cultivation. Journal of Technology and Innovation. 12[30]1-15: e71230115
https://doi.org/10.35429/JTI.2025.12.30.7.1.15

Internet of Things [IoT]: Microcontroller-based platforms such as ESP32, Arduino, and Raspberry Pi are used for remote and automated monitoring of key parameters including pH, electrical conductivity [EC], temperature, and light intensity, with data transmitted to cloud platforms such as Azure IoT Hub and ThingSpeak [Hadj et al., 2023; Fisher et al., 2022].

Some implementations report the use of 6LoWPAN architectures with master-slave control schemes for efficient remote lighting management.

Dynamic spectral control: Although still emerging, this approach appears in studies combining spectral data from nutrient solutions with AI models—such as MH-cDCGAN—to dynamically adjust lighting conditions [intensity, spectrum, and photoperiod] in real time. A spectroscopic IoT system has also been developed to monitor nitrogen content in hydrogels, laying the groundwork for comparable spectral control strategies.

PWM [Pulse-Width Modulation]: This technique is already used to regulate actuators [pumps, motors, mobile sensors] in Arduino-controlled hydroponic systems and is directly applicable to LED intensity control, enabling precise and energy-efficient light modulation.

DLI Automation [Daily Light Integral]: While explicit DLI control is not yet widely adopted, advanced IoT systems integrate light sensors and predictive algorithms to optimize daily light duration and intensity. A recent study on lettuce cultivation reported a 20% improvement in energy efficiency and a 15% yield increase through dynamic light adjustments based on plant growth stage [Nezha Kharraz et al., 2025].

**Neural networks for modeling plant growth based on LED spectrum**

Convolutional Neural Networks [CNNs] have proven to be highly effective tools for image analysis, particularly in contexts requiring automated extraction of complex visual features. In hydroponic agriculture, their application has gained relevance by enabling accurate assessment of plant growth and physiological status through real-time image capture [Priya et al., 2023].

One of the key capabilities of CNNs is their ability to analyze leaf color, size, shape, and texture with a level of detail that allows these features to be directly correlated with the type and intensity of LED light applied in the cultivation environment. This not only supports continuous visual monitoring of plant development but also provides valuable insights into plant responses to specific spectral variations [Alrajhi et al., 2023; Chen et al., 2021].

**Visual detection and assessment of plant status**

CNNs process plant images to recognize visual patterns that reflect plant health status. This capability has been successfully applied in the early detection of diseases, water stress, nutrient deficiencies, and chemical imbalances. Recent studies report that these models can achieve over 95% accuracy in identifying pests and diseases, and up to 98.5% accuracy in diagnosing nutrient deficiencies including nitrogen, phosphorus, potassium, iron, calcium, and zinc based on visible symptoms on leaves [Priya et al., 2023].

In hydroponically grown lettuce, for example, RGB image analysis using architectures such as VGG16 and VGG19 has been applied to estimate nutrient concentrations. These models have demonstrated accuracies ranging from 87.5% to 100%, depending on the cultivar and image quality, making them reliable tools for agronomic monitoring [Budavári et al., 2024].

**Integration with lighting and sensor data**

The true value of CNNs in these systems lies in their ability to correlate plant visual features with lighting conditions. By integrating visual data with sensor inputs collected via IoT platforms such as temperature, humidity, electrical conductivity [EC], pH, and light intensity it is possible to establish direct relationships between plant physiological responses and the applied LED spectral configurations [Chen et al., 2021].

This combined approach helps identify how specific wavelengths or intensity levels affect leaf color, morphology, or texture. Based on these correlations, lighting can be dynamically adjusted to optimize plant development, contributing to improved energy efficiency and more effective crop cycle planning.

ISSN: 2410-3993.
RENIECYT: 1702902


Juárez-Balderas, Mario Alberto, Daniel-Eufracio, América Abigail, Araiz-Aguilar, Gustavo Rafael and Villaseñor-Aguilar, Marcos Jesús. [2025]. Evaluation of LED Systems for controlled spectral lighting in indoor hydroponic cultivation. Journal of Technology and Innovation. 12[30]1-15: e71230115
https://doi.org/10.35429/JTI.2025.12.30.7.1.15

**Real-time intelligent spectral control using recurrent neural networks**

While Convolutional Neural Networks [CNNs] have proven effective for visual analysis of plant development, Recurrent Neural Networks [RNNs] and Long Short-Term Memory [LSTM] models offer a different approach focused on temporal prediction. These algorithms process sequential data from environmental sensors and historical crop records, enabling the anticipation of changes in light demand before they impact plant physiology [Putra et al., 2024; Kharraz et al., 2025].

The key innovation lies in the ability of RNNs/LSTMs to detect evolving patterns not immediately apparent. For example, they can identify microfluctuations in leaf growth rate associated with slight spectral mismatches and project their cumulative effect on biomass and lettuce quality over the following days [Chen et al., 2021; Kelly, Choe, Meng, & Runkle, 2020].

This enables preemptive LED spectrum adjustments to avoid suboptimal lighting periods that could impair photosynthesis or alter morphology.

Another distinctive feature is the capacity to correlate multiple dynamic variables such as air temperature, relative humidity, root zone temperature, and variations in actual photoperiod simultaneously [Gutierrez Leon, et al., 2023].

Using this data, LSTM models generate predictive profiles of physiological response, identifying which combinations of wavelengths and light intensities are likely to be most efficient in the next crop stage [Kuankid & Aurasapon, 2022]. This approach does not rely on fixed rules but evolves progressively with the plant, minimizing both energy consumption and unnecessary exposure to non-beneficial spectra.

RNNs also support zonal lighting strategies within greenhouses by recognizing that different areas may experience microclimatic variations. Rather than applying a uniform light spectrum across the entire crop, the system customizes light intensity and spectral ratio for each zone based on historical data and projected growth [Catota-Ocapana, el at , 2024].

This level of control is still underexplored in the literature and represents a promising direction for energy optimization.

When integrated with embedded controllers, these recurrent networks enable spectral micro-adjustments at minute-level intervals, allowing synchronization of artificial lighting with finer physiological rhythms such as stomatal opening pulses or activation of specific metabolic pathways [Kharraz et al., 2025; Hadj et al., 2023].

This transforms LED lighting into a dynamic, adaptive component capable of modulating not only structural growth but also nutritional quality parameters such as antioxidant or phenolic compound accumulation [Mohamed, Latif, & Ali, 2021]. The use of RNN/LSTM models goes beyond basic automation, constituting a predictive control system where each lighting decision is based on the crop's temporal evolution rather than isolated instantaneous values [Putra et al., 2024; Kharraz et al., 2025].

As such, this approach—still largely unexplored in commercial systems—points toward self-regulating greenhouses that optimize yield, energy efficiency, and product quality simultaneously.

**Conclusions**

Indoor agriculture is emerging as a resilient and sustainable solution to global challenges such as climate change, urbanization, and the loss of arable land. The integration of hydroponic systems with automated environmental control enables not only the efficient use of water and nutrients but also improves crop quality and traceability while reducing emissions and minimizing agrochemical use.

Technologies such as IoT and machine learning enhance productivity by enabling precision agriculture in urban environments, with lettuce serving as an ideal bioindicator for evaluating plant responses to light spectra, nutrient availability, and controlled conditions. Light management is one of the critical factors for optimizing productivity in controlled environments. Photomorphogenesis and phototropism—regulated by photoreceptors such as phytochromes, cryptochromes, and phototropins—explain how plants perceive and respond to light quality, intensity, and direction.

ISSN: 2410-3993.
RENIECYT: 1702902


Juárez-Balderas, Mario Alberto, Daniel-Eufracio, América Abigail, Araiz-Aguilar, Gustavo Rafael and Villaseñor-Aguilar, Marcos Jesús. [2025]. Evaluation of LED Systems for controlled spectral lighting in indoor hydroponic cultivation. Journal of Technology and Innovation. 12[30]1-15: e71230115
https://doi.org/10.35429/JTI.2025.12.30.7.1.15

This knowledge, applied through metrics such as PPFD and DLI, supports the development of tailored light recipes that maximize photosynthetic efficiency and crop quality. For instance, moderate PPFD levels [100–250 $\mu mol \times m^{-2} \times s^{-1}$] and optimized DLIs [14–17 $mol \times m^{-2} \times d^{-1}$] have been shown to promote higher biomass and photochemical yield in lettuce while reducing energy consumption.

The differential spectral response of pigments such as chlorophyll A and B, carotenoids, and phytochromes reinforces the need for adjustable spectra that combine red, blue, and far-red wavelengths to drive leaf elongation, biomass accumulation, or flowering control.

The implementation of predictive models based on recurrent neural networks [RNN/LSTM] introduces an additional layer of optimization by forecasting lighting needs from historical growth, temperature, and DLI data.

This enables real-time synchronization of spectral quality, light intensity, and photoperiod with the plant's circadian and phenological rhythms. Such predictive capabilities not only improve growth and energy efficiency but also support adaptive self-regulation of the system, reducing manual intervention and dynamically adjusting light exposure to optimize photosynthesis and yield.

In terms of lighting technology, LEDs have become the most versatile and efficient alternative compared to HPS and CFL systems. Their ability to emit specific wavelengths [e.g., red 660 nm, blue 450 nm, far-red 730 nm] and full-spectrum light with low heat dissipation makes them ideal for controlled environments. When combined with predictive algorithms and IoT systems, dynamic lighting recipes can be implemented that respond to current conditions and anticipate future metabolic demands, optimizing yield [g/Wh] and crop nutritional quality.

The synergy between plant physiological knowledge [photomorphogenesis, phototropism, and photobiology], lighting metrics [PPFD and DLI], predictive models [RNN/LSTM], and multispectral LED technology establishes a new paradigm in indoor agriculture.

This integrated model transforms lighting into a dynamic, responsive input capable of inducing specific morphophysiological responses, maximizing energy efficiency, and supporting a scalable, adaptive, and sustainable production system.

Lettuce, as a model crop, demonstrates the potential for these strategies to be applied to more complex species, pointing toward the development of intelligent, self-regulating greenhouses that simultaneously optimize growth, quality, and resource use.

## References

### Basic

Alrajhi, A., Assiri, R., & Alzahrani, S. [2023]. Effects of different LED spectra and UV-B exposure on growth and phytochemical accumulation in red and green lettuce cultivars. Plants, 12[3], 463.

Aydin, R. [2023]. Hydroponics and urban agriculture: Redefining food production in cities. African Journal of Food Science and Technology, 14[12].

Bamidele Ogunlade, C., & Ebenehi Enemaku, L. [s.f.]. Hydroponic farming: A panacea for climate change impacts on food security in Nigeria. The Federal Polytechnic.

Bantis, F., & Koukounaras, A. [2023]. Impact of Light on Horticultural Crops. Agriculture, 13[828].

Bayat, Leyla & Arab, Mostafa & Aliniaeifard, Sasan & Seif, Mehdi & Lastochkina, Oksana & Li, Tao. [2018]. Effects of growth under different light spectra on the subsequent high light tolerance in rose plants. AoB PLANTS. 10.

Bian, Zhonghua, Cheng, Ruifeng, Wang, Yu, Yang, Qichang, Lu, Chungui, Effect of green light on nitrate reduction and edible quality of hydroponically grown lettuce [Lactuca sativa L.] under short-term continuous light from red and blue light-emitting diodes. Environmental and Experimental Botany

Budavári, N., Pék, Z., Helyes, L., Takács, S., & Nemeskéri, E. [2024]. An overview on the use of artificial lighting for sustainable lettuce and microgreens production in an indoor vertical farming system. Horticulturae, 10[9], 938.

ISSN: 2410-3993.
RENIECYT: 1702902


Juárez-Balderas, Mario Alberto, Daniel-Eufracio, América Abigail, Araiz-Aguilar, Gustavo Rafael and Villaseñor-Aguilar, Marcos Jesús. [2025]. Evaluation of LED Systems for controlled spectral lighting in indoor hydroponic cultivation. Journal of Technology and Innovation. 12[30]1-15: e71230115
https://doi.org/10.35429/JTI.2025.12.30.7.1.15

Catota-Ocapana, P., Minaya-Andino, C., Astudillo, P., & Pichoasamin, D. [2024]. Smart control models used for nutrient management in hydroponic crops: a systematic review. IEEE Access

Chen, X., Guo, W., Xue, X., Wang, L., & Qiao, X. [2021]. Light quality regulates plant architecture, biomass accumulation, and energy-use efficiency in hydroponic lettuce. Scientific Reports, 11, 8374.

Chutimanukul, P., Wanichananan, P. Janta, S. et al. [2022]. The influence of different light spectra on physiological responses, antioxidant capacity and chemical compositions in two holy basil cultivars. Scientific Reports.

Fisher, P. [2022, noviembre 21]. Fixed vs. dynamic lighting for indoor hydroponic lettuce. Greenhouse Management.

Gutiérrez León, E., Montiel Arguijo, J. E., Carreto Arellano, C., & Menchaca García, F. R. [2019]. Propuesta de sistema de gestión inteligente basado en IoT para hidroponia. Research in Computing Science, 148[10], 219–233

Hadj Abdelkader, Oussama & Bouzebiba, Hadjer & Pena, Danilo & Aguiar, A. Pedro. [2023]. Energy-Efficient IoT-Based Light Control System in Smart Indoor Agriculture. Sensors. 23.

Johkan, M., Shoji, K., Goto, F., Hashida, S. N., & Yoshihara, T. [2010]. Blue light-emitting diode light irradiation of seedlings improves seedling quality and growth after transplanting in Lactuca sativa L. HortScience, 45[12], 1809–1814.

Kharraz, N., Revoly, A., & Szabó, I. [2025]. IoT-Based Adaptive Lighting Framework for Optimizing Energy Efficiency and Crop Yield in Indoor Farming. *Journal of Sensor and Actuator Networks*, *14*[3], 59.

Kelly, Nathan & Choe, Daegeun & Meng, Qingwu & Runkle, Erik. [2020]. Promotion of lettuce growth under an increasing daily light integral depends on the combination of the photosynthetic photon flux density and photoperiod. Scientia Horticulturae. 272.

Kozai, T. [2018]. Smart Plant Factory the Next Generation Indoor Vertical Farms: The Next Generation Indoor Vertical Farms.

Kuankid, S., & Aurasapon, A. [2022]. The effect of LED lighting on lettuce growth in a vertical IoT based indoor hydroponic system. International Journal of Online Engineering, 18[7], Artículo 25467.

Lee, M. J., Park, S. Y., & Oh, M. M. [2015]. Growth and cell division of lettuce plants under various ratios of red to far-red light-emitting diodes. Horticulture Environment and Biotechnology, 56[2], 186–194.

Legendre, J. M., & van Iersel, M. W. [2021]. Far-red light enhances growth of lettuce by increasing radiation capture efficiency. Plants, 10[1], 166.

Li, Y., Xin, G., Shi, Q., Yang, F., & Wei, M. [2023]. Response of photomorphogenesis and photosynthetic properties of sweet pepper seedlings exposed to mixed red and blue light. Frontiers in Plant Science, 13, Artículo 984051.

Marondedze, Claudius & Liu, Xinyun & Huang, Shihui & Wong, Cynthia & Zhou, Xuan & Pan, Xutong & An, Huiting & Xu, Nuo & Tian, Xuechen & Wong, Aloysius. [2018]. Towards a tailored indoor horticulture: a functional genomics guided phenotypic approach. Horticulture Research. 5. 68. 10.1038/s41438-018-0065-7.

Matysiak, B., Kowalska, I., & Janas, R. [2021]. The impact of different light spectra on the growth and nutritional quality of lettuce [Lactuca sativa L.] in hydroponic cultivation. Agriculture, 11[11], 1133.

Mena Amado, D. J. [s.f. 2018]. Sistema IoT para el monitoreo y control de fuentes de luz artificial aplicado a la agricultura de precisión [Proyecto de grado, Universidad Distrital Francisco José de Caldas]. Facultad de Ingeniería, Proyecto Curricular de Ingeniería Electrónica.

Mohamed, A. H., Latif, H. H. A., & Ali, A. M. [2021]. Impact of spectral composition of LED light on antioxidant properties and growth of Lactuca sativa. Plants, 10[10], 2162.

Motogaito, A., Hashimoto, N., Hiramatsu, K. and Murakami, K. [2017] Study of Plant Cultivation Using a Light-Emitting Diode Illumination System to Control the Spectral Irradiance Distribution. Optics and Photonics Journal, 7, 101-108.

ISSN: 2410-3993.
RENIECYT: 1702902


Juárez-Balderas, Mario Alberto, Daniel-Eufracio, América Abigail, Araiz-Aguilar, Gustavo Rafael and Villaseñor-Aguilar, Marcos Jesús. [2025]. Evaluation of LED Systems for controlled spectral lighting in indoor hydroponic cultivation. Journal of Technology and Innovation. 12[30]1-15: e71230115
https://doi.org/10.35429/JTI.2025.12.30.7.1.15

Naim Khalid, S. M. [2020]. Crop production manual: a guide to fruit and vegetable production in the Federated States of Micronesia.

Naznin, M. T., Lefsrud, M., Gravel, V., & Azad, M. O. K. [2019]. Blue light added with red LEDs enhance growth characteristics and total phenolic content of lettuce [Lactuca sativa L.]. Plants, 8[4], 93.

Oh, J. M., Kang, H. J., & Yang, B. D. [2015]. A PWM phase-shift circuit using an RC delay for multiple LED driver ICs. Journal of Semiconductor Technology and Science, 15[4], 484–492.

Palmer, S., & van Iersel, M. W. [2020]. Increasing growth of lettuce and mizuna under sole-source LED lighting using longer photoperiods with the same daily light integral. Agronomy, 10[11], 1722.

Paradiso, Roberta & Proietti, Simona. [2022]. Light-Quality Manipulation to Control Plant Growth and Photomorphogenesis in Greenhouse Horticulture: The State of the Art and the Opportunities of Modern LED Systems. Journal of Plant Growth Regulation. 41.

Pennisi, G., Takagaki, M., & van Iersel, M. W. [2019]. Optimal red:blue ratio in LED lighting for plant growth and energy use efficiency in lettuce. Scientific Reports, 9, 14127.

Priya, G. Lakshmi & Baskar, Chanthini & Deshmane, Sanket & Adithya, C & Das, Souranil. [2023]. Revolutionizing Holy-Basil Cultivation With AI-Enabled Hydroponics System. IEEE Access. PP. 1-1..

Putra, S. D., Heriansyah, E. F. C., Anggriani, K., & Jaya, M. H. I. S. [2024]. Development of smart hydroponics system using AI-based sensing. Journal Infotel, 16[3], 1–12

Regmi, A., Rueda-Kunz, D., Liu, H., Trevino, J., Kathi, S., & Simpson, C. [2024]. Comparing resource use efficiencies in hydroponic and aeroponic production systems. Technology in Horticulture, 4[1], Artículo 0002.

Reyes Yanes, Abraham & Abbasi, Rabiya & Martínez, Pablo & Ahmad, Dr Rafiq. [2022]. Digital Twinning of Hydroponic Grow Beds in Intelligent Aquaponic Systems. Sensors. 22.

Semenova, Natalya & Proshkin, Yuri & Smirnov, Alexander & Dorokhov, Alexey & Ivanitskikh, Alina & Burynin, Dmitry & Dorokhov, Artem & Uyutova, Nadezhda & Chilingaryan, Narek. [2023]. The Influence of the Spectral Composition and Light Intensity on the Morphological and Biochemical Parameters of Spinach [Spinacia oleracea L.] in Vertical Farming. Horticulturae. 9. 1130.

Shareef, Umar & Rehman, Ateeq & Ahmad, Dr Rafiq. [2024]. A Systematic Literature Review on Parameters Optimization for Smart Hydroponic Systems. AI. 5. 1517-1533.

Singh, D., Basu, C., Meinhardt-Wollweber, M., & Roth, B. [2015]. LEDs for energy efficient greenhouse lighting. Renewable and Sustainable Energy Reviews, 49, 139–147.

Soufi, H. R., Roosta, H. R., & Hamidpour, M. [2023]. The plant growth, water and electricity consumption, and nutrients uptake are influenced by different light spectra and nutrition of lettuce. Scientific Reports, 13, Artículo 48284.

Stevens, J. D., Murray, D., Diepeveen, D., & Toohey, D. [2023]. Development and Testing of an IoT Spectroscopic Nutrient Monitoring System for Use in Micro Indoor Smart Hydroponics. Horticulturae, 9[2], 185.

Taha, M. F., ElManawy, A. I., Alshallash, K. S., ElMasry, G., Alharbi, K., Zhou, L., ... & Qiu, Z. [2022]. Using Machine Learning for Nutrient Content Detection of Aquaponics-Grown Plants Based on Spectral Data. Sustainability, 14[19], 12318

Tavares, P. & Guimaraes, I. & Braga, Henrique & Bender, V. C. & Almeida, Pedro. [2017]. LED system with independent red and blue channels employing radiant flux estimation and indirect flux control for greenhouse hop cultivation. 1-9.

Teo, E. P., Chan, K. Y., Mokhtar, S. M., & Lee, C. L. [2024]. Effect of LED wavelength and power on the hydroponic indoor vegetable farming. Universal Journal of Agricultural Research, 12[1], 41–50.

ISSN: 2410-3993.
RENIECYT: 1702902


Juárez-Balderas, Mario Alberto, Daniel-Eufracio, América Abigail, Araiz-Aguilar, Gustavo Rafael and Villaseñor-Aguilar, Marcos Jesús. [2025]. Evaluation of LED Systems for controlled spectral lighting in indoor hydroponic cultivation. Journal of Technology and Innovation. 12[30]1-15: e71230115
https://doi.org/10.35429/JTI.2025.12.30.7.1.15

Thi Phuong Dung, Nguyen & Tran, T.T.H. & Nguyen, Q.T.. [2019]. Effects of light intensity on the growth, photosynthesis and leaf microstructure of hydroponic cultivated spinach [Spinacia oleracea L.] under a combination of red and blue LEDs in house. International Journal of Agricultural Technology. 15. 75-90.

Tiago Queiroz, A., Lopes, R. S., Fortes, M. Z., Tomaz, R. C., Ferreira Beaklini, A. C., Marcos, A., Pereira, E., Soares Moreira, B., Borba, C., & Cavalcanti Tomáz, R. [2019]. Efficiency evaluation in public lighting by using LED and HPS technologies. International Journal of Energy Science and Engineering, 5[1], 12–21.

Van Brenk, Courbier S, Kleijweg CL, Verdonk JC, Marcelis LFM. Paradise by the far-red light: Far-red and red:blue ratios independently affect yield, pigments, and carbohydrate production in lettuce, Lactuca sativa. Front Plant Sci. 2024

ISSN: 2410-3993.
RENIECYT: 1702902


Juárez-Balderas, Mario Alberto, Daniel-Eufracio, América Abigail, Araiz-Aguilar, Gustavo Rafael and Villaseñor-Aguilar, Marcos Jesús. [2025]. Evaluation of LED Systems for controlled spectral lighting in indoor hydroponic cultivation. Journal of Technology and Innovation. 12[30]1-15: e71230115
https://doi.org/10.35429/JTI.2025.12.30.7.1.15

# [[Title in TNRoman and Bold No. 14 in English and Spanish]

Surname, Name 1st Author*[a], Surname, Name 1st Co-author[b], Surname, Name 2nd Co-author[c] and Surname, Name 3rd Co-author[d] [No.12 TNRoman]

[a] Affiliation institution, Researcher ID, ORC ID, SNI-SECIHTI ID or CVU PNPC [No.10 TNRoman]
[b] Affiliation institution, Researcher ID, ORC ID, SNI-SECIHTI ID or CVU PNPC [No.10 TNRoman]
[c] Affiliation institution, Researcher ID, ORC ID, SNI-SECIHTI ID or CVU PNPC [No.10 TNRoman]
[d] Affiliation institution, Researcher ID, ORC ID, SNI-SECIHTI ID or CVU PNPC [No.10 TNRoman]

All ROR-Clarivate-ORCID and SECIHTI profiles must be hyperlinked to your website.
Prot- University of South Australia • 7038-2013• 0000-0001-6442-4409 • 416112

**SECIHTI classification:**
https://marvid.org/research_areas.php [No.10 TNRoman]
Area:
Field:
Discipline:
Subdiscipline:

**DOI:** https://doi.org/
**Article History:**
Received: [Use Only ECORFAN]
Accepted: [Use Only ECORFAN]
Contact e-mail address:
* ✉ [example@example.org]

**Abstract [In English]**
Must contain up to 150 words
**Graphical abstract [In English]**

| Your title goes here | | |
|---|---|---|
| **Objectives** | **Methodology** | **Contribution** |
| | | |

Authors must provide an original image that clearly represents the article described in the article. Graphical abstracts should be submitted as a separate file. Please note that, as well as each article must be unique. File type: the file types are MS Office files.No additional text, outline or synopsis should be included. Any text or captions must be part of the image file. Do not use unnecessary white space or a "graphic abstract" header within the image file.

**Keywords [In English]**
Indicate 3 keywords in TNRoman and Bold No. 10

**Abstract [In Spanish]**
Must contain up to 150 words
**Graphical abstract [In Spanish]**

| Your title goes here | | |
|---|---|---|
| **Objectives** | **Methodology** | **Contribution** |
| | | |

Authors must provide an original image that clearly represents the article described in the article. Graphical abstracts should be submitted as a separate file. Please note that, as well as each article must be unique. File type: the file types are MS Office files.No additional text, outline or synopsis should be included. Any text or captions must be part of the image file. Do not use unnecessary white space or a "graphic abstract" header within the image file.

**Keywords [In Spanish]**
Indicate 3 keywords in TNRoman and Bold No. 10

**Citation:** Surname, Name 1st Author, Surname, Name 1st Co-author, Surname, Name 2nd Co-author and Surname, Name 3rd Co-author. Article Title. Journal of Technology and Innovation. Year. V-N: Pages [TN Roman No.10].

## Introduction

Text in TNRoman No.12, single space.

General explanation of the subject and explain why it is important.

What is your added value with respect to other techniques?

Clearly focus each of its features.

Clearly explain the problem to be solved and the central hypothesis.

Explanation of sections Article.

## Development of headings and subheadings of the article with subsequent numbers

[Title No.12 in TNRoman, single spaced and bold]

Products in development No.12 TNRoman, single spaced.

## Including figures and tables-Editable

In the article content any table and figure should be editable formats that can change size, type and number of letter, for the purposes of edition, these must be high quality, not pixelated and should be noticeable even reducing image scale.

[Indicating the title at the bottom with No.10 and Times New Roman Bold]

**Box**

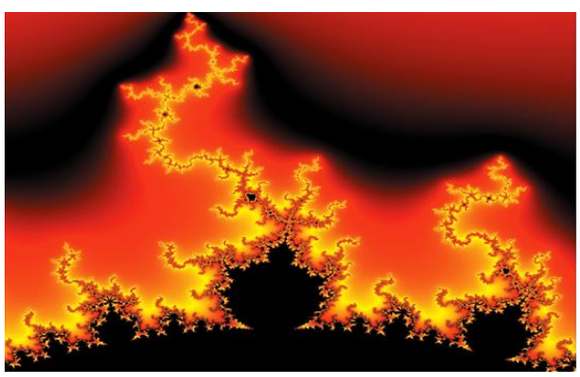

**Figure 1**

Title [Should not be images-everything must be editable]

*Source [in italic]*

**Box**

**Table 1**

Title [Should not be images-everything must be editable]

| | | | |
|---|---|---|---|
| | | | |

*Source [in italic]*

**The maximum number of Boxes is 10 items**

**For the use of equations, noted as follows:**

$$Y_{ij} = \alpha + \sum_{h=1}^{r} \beta_h X_{hij} + u_j + e_{ij} \qquad [1]$$

Must be editable and number aligned on the right side.

## Methodology

Develop give the meaning of the variables in linear writing and important is the comparison of the used criteria.

## Results

The results shall be by section of the article.

## Conclusions

Clearly explain the results and possibilities of improvement.

## Annexes

Tables and adequate sources.

**The international standard is 7 pages minimum and 14 pages maximum.**

## Declarations

## Conflict of interest

The authors declare no interest conflict. They have no known competing financial interests or personal relationships that could have appeared to influence the article reported in this article.

ISSN 2444-4979

**Author contribution**

Specify the contribution of each researcher in each of the points developed in this research.

Prot-
*Benoit-Pauleter, Gerard*: Contributed to the project idea, research method and technique.

**Availability of data and materials**

Indicate the availability of the data obtained in this research.

**Funding**

Indicate if the research received some financing.

**Acknowledgements**

Indicate if they were financed by any institution, University or company.

**Abbreviations**

List abbreviations in alphabetical order.

Prot-

| | |
|---|---|
| ANN | Artificial Neural Network |

**References**

Use APA system. Should not be numbered, nor with bullets, however if necessary numbering will be because reference or mention is made somewhere in the Article.

Use the Roman alphabet, all references you have used should be in Roman alphabet, even if you have cited an article, book in any of the official languages of the United Nations [English, French, German, Chinese, Russian, Portuguese, Italian, Spanish, Arabic], you should write the reference in Roman alphabet and not in any of the official languages.

Citations are classified the following categories:

**Antecedents.** The citation is due to previously published research and orients the citing document within a particular scholarly area.

**Basics.** The citation is intended to report data sets, methods, concepts and ideas on which the authors of the citing document base their work.

**Supports.** The citing article reports similar results. It may also refer to similarities in methodology or, in some cases, to the reproduction of results.

**Differences.** The citing document reports by means of a citation that it has obtained different results to those obtained in the cited document. This may also refer to differences in methodology or differences in sample sizes that affect the results.

**Discussions.** The citing article cites another study because it is providing a more detailed discussion of the subject matter.

The URL of the resource is activated in the DOI or in the title of the resource.

Prot-
Mandelbrot, B. B. [2020]. Negative dimensions and Hölders, multifractals and their Hölder spectra, and the role of lateral preasymptotics in science. Journal of Fourier Analysis and Applications Special. 409-432.

**Intellectual Property Requirements for editing:**

- Authentic Signature in Color of Originality Format Author and Coauthors.
- Authentic Signature in Color of the Acceptance Format of Author and Coauthors.
- Authentic Signature in blue color of the Conflict of Interest Format of Author and Co-authors.

ISSN 2444-4979

**Reservation to Editorial Policy**

Journal of Technology and Innovation reserves the right to make editorial changes required to adapt the Articles to the Editorial Policy of the Journal. Once the Article is accepted in its final version, the Journal will send the author the proofs for review. ECORFAN® will only accept the correction of errata and errors or omissions arising from the editing process of the Journal, reserving in full the copyrights and content dissemination. No deletions, substitutions or additions that alter the formation of the Article will be accepted.

**Code of Ethics - Good Practices and Declaration of Solution to Editorial Conflicts**

**Declaration of Originality and unpublished character of the Article, of Authors, on the obtaining of data and interpretation of results, Acknowledgments, Conflict of interests, Assignment of rights and Distribution**

The ECORFAN-Mexico, S.C Management claims to Authors of Articles that its content must be original, unpublished and of Scientific, Technological and Innovation content to be submitted for evaluation.

The Authors signing the Article must be the same that have contributed to its conception, realization and development, as well as obtaining the data, interpreting the results, drafting and reviewing it. The Corresponding Author of the proposed Article will request the form that follows.

Article title:

- The sending of an Article to Journal of Technology and Innovation emanates the commitment of the author not to submit it simultaneously to the consideration of other series publications for it must complement the Format of Originality for its Article, unless it is rejected by the Arbitration Committee, it may be withdrawn.

- -None of the data presented in this article has been plagiarized or invented. The original data are clearly distinguished from those already published. And it is known of the test in PLAGSCAN if a level of plagiarism is detected Positive will not proceed to arbitrate.

- References are cited on which the information contained in the Article is based, as well as theories and data from other previously published Articles.

- The authors sign the Format of Authorization for their Article to be disseminated by means that ECORFAN-Mexico, S.C. In its Holding Bolivia considers pertinent for disclosure and diffusion of its Article its Rights of Work.

- Consent has been obtained from those who have contributed unpublished data obtained through verbal or written communication, and such communication and Authorship are adequately identified.

- The Author and Co-Authors who sign this work have participated in its planning, design and execution, as well as in the interpretation of the results. They also critically reviewed the paper, approved its final version and agreed with its publication.

- No signature responsible for the work has been omitted and the criteria of Scientific Authorization are satisfied.

- The results of this Article have been interpreted objectively. Any results contrary to the point of view of those who sign are exposed and discussed in the Article.

**Copyright and Access**

The publication of this Article supposes the transfer of the copyright to ECORFAN-Mexico, SC in its Holding Bolivia for it Journal of Technology and Innovation, which reserves the right to distribute on the Web the published version of the Article and the making available of the Article in This format supposes for its Authors the fulfilment of what is established in the Law of Science and Technology of the United Mexican States, regarding the obligation to allow access to the results of Scientific Research.

Article Title:

| Name and Surnames of the Contact Author and the Coauthors | Signature |
|---|---|
| 1. | |
| 2. | |
| 3. | |
| 4. | |

**Principles of Ethics and Declaration of Solution to Editorial**

**Conflicts Editor Responsibilities**

The Publisher undertakes to guarantee the confidentiality of the evaluation process, it may not disclose to the Arbitrators the identity of the Authors, nor may it reveal the identity of the Arbitrators at any time.

The Editor assumes the responsibility to properly inform the Author of the stage of the editorial process in which the text is sent, as well as the resolutions of Double-Blind Review.

The Editor should evaluate manuscripts and their intellectual content without distinction of race, gender, sexual orientation, religious beliefs, ethnicity, nationality, or the political philosophy of the Authors.

The Editor and his editing team of ECORFAN® Holdings will not disclose any information about Articles submitted to anyone other than the corresponding Author.

The Editor should make fair and impartial decisions and ensure a fair Double-Blind Review.

**Responsibilities of the Editorial Board**

The description of the peer review processes is made known by the Editorial Board in order that the Authors know what the evaluation criteria are and will always be willing to justify any controversy in the evaluation process. In case of Plagiarism Detection to the Article the Committee notifies the Authors for Violation to the Right of Scientific, Technological and Innovation Authorization.

**Responsibilities of the Arbitration Committee**

The Arbitrators undertake to notify about any unethical conduct by the Authors and to indicate all the information that may be reason to reject the publication of the Articles. In addition, they must undertake to keep confidential information related to the Articles they evaluate.

Any manuscript received for your arbitration must be treated as confidential, should not be displayed or discussed with other experts, except with the permission of the Editor.

The Arbitrators must be conducted objectively, any personal criticism of the Author is inappropriate.

The Arbitrators must express their points of view with clarity and with valid arguments that contribute to the Scientific, Technological and Innovation of the Author.

The Arbitrators should not evaluate manuscripts in which they have conflicts of interest and have been notified to the Editor before submitting the Article for Double-Blind Review.

**Responsibilities of the Authors**

Authors must guarantee that their articles are the product of their original work and that the data has been obtained ethically.

Authors must ensure that they have not been previously published or that they are not considered in another serial publication.

Authors must strictly follow the rules for the publication of Defined Articles by the Editorial Board.

The authors have requested that the text in all its forms be an unethical editorial behavior and is unacceptable, consequently, any manuscript that incurs in plagiarism is eliminated and not considered for publication.

Authors should cite publications that have been influential in the nature of the Article submitted to arbitration.

**Information services**

**Indexation - Bases and Repositories**

LATINDEX (Scientific Journals of Latin America, Spain and Portugal)
RESEARCH GATE (Germany)
REBIUN (Network of Spanish University Libraries, Spain)
ROAD (Directory of Open Access scholarly Resources)
GOOGLE SCHOLAR (Citation indices-Google)
REDIB (Ibero-American Network of Innovation and Scientific Knowledge- CSIC)
MENDELEY (Bibliographic References Manager)

**Publishing Services**

Citation and Index Identification H
Management of Originality Format and Authorization
Testing Article with PLAGSCAN
Article Evaluation
Certificate of Double-Blind
Review Article Edition
Web layout
Indexing and
Repository
ArticleTranslation
Article Publication
Certificate of Article
Service Billing

**Editorial Policy and Management**

21 Santa Lucía, CP-5220. Libertadores -Sucre–Bolivia. Phones: +52 1 55 6159 2296, +52 1 55 1260 0355, +52 1 55 6034 9181; Email: contact@ecorfan.org www.ecorfan.org

# Journal of Technology and Innovation




2410 3993
ISSN 2410 - 3993


www.ecorfan.org